



HAL
open science

Volcanic and Tectonic Constraints on the Evolution of Venus

Richard Ghail, Suzanne Smrekar, Thomas Widemann, Paul Byrne, Anna Gülcher, Joseph O’rourke, Madison Borrelli, Martha Gilmore, Robert Herrick, Mikhail Ivanov, et al.

► **To cite this version:**

Richard Ghail, Suzanne Smrekar, Thomas Widemann, Paul Byrne, Anna Gülcher, et al.. Volcanic and Tectonic Constraints on the Evolution of Venus. *Space Science Reviews*, 2024, 220 (4), pp.36. 10.1007/s11214-024-01065-2 . hal-04589829

HAL Id: hal-04589829

<https://u-paris.hal.science/hal-04589829>

Submitted on 27 May 2024

HAL is a multi-disciplinary open access archive for the deposit and dissemination of scientific research documents, whether they are published or not. The documents may come from teaching and research institutions in France or abroad, or from public or private research centers.

L’archive ouverte pluridisciplinaire **HAL**, est destinée au dépôt et à la diffusion de documents scientifiques de niveau recherche, publiés ou non, émanant des établissements d’enseignement et de recherche français ou étrangers, des laboratoires publics ou privés.



Distributed under a Creative Commons Attribution 4.0 International License



Volcanic and Tectonic Constraints on the Evolution of Venus

Richard C. Ghail¹ · Suzanne E. Smrekar² · Thomas Widemann^{3,4} · Paul K. Byrne⁵ · Anna J.P. Gülcher² · Joseph G. O'Rourke⁶ · Madison E. Borrelli⁶ · Martha S. Gilmore⁷ · Robert R. Herrick⁸ · Mikhail A. Ivanov⁹ · Ana-Catalina Plesa¹⁰ · Tobias Rolf¹¹ · Leah Sabbeth² · Joe W. Schools¹² · J. Gregory Shellnutt¹³

Received: 6 March 2023 / Accepted: 27 March 2024
© The Author(s) 2024

Abstract

Surface geologic features form a detailed record of Venus' evolution. Venus displays a profusion of volcanic and tectonics features, including both familiar and exotic forms. One challenge to assessing the role of these features in Venus' evolution is that there are too few impact craters to permit age dates for specific features or regions. Similarly, without surface water, erosion is limited and cannot be used to evaluate age. These same observations indicate Venus has, on average, a very young surface (150–1000 Ma), with the most recent surface deformation and volcanism largely preserved on the surface except where covered by limited impact ejecta. In contrast, most geologic activity on Mars, the Moon, and Mercury occurred in the 1st billion years. Earth's geologic processes are almost all a result of plate tectonics. Venus' lacks such a network of connected, large scale plates, leaving the nature of Venus' dominant geodynamic process up for debate. In this review article, we describe Venus' key volcanic and tectonic features, models for their origin, and possible links to evolution. We also present current knowledge of the composition and thickness of the crust, lithospheric thickness, and heat flow given their critical role in shaping surface geology and interior evolution. Given Venus' hot lithosphere, abundant activity and potential analogues of continents, roll-back subduction, and microplates, it may provide insights into early Earth, prior to the onset of true plate tectonics. We explore similarities and differences between Venus and the Proterozoic or Archean Earth. Finally, we describe the future measurements needed to advance our understanding of volcanism, tectonism, and the evolution of Venus.

Keywords Venus · Formation of volcanic and tectonic features · Mantle dynamics · Subduction and plate tectonics · Topography · Hotspot volcanism · Plume-induced subduction · Crust and surface composition · Lithospheric thickness · Coronae · Lava channels · Venus resurfacing history

Venus: Evolution Through Time
Edited by Colin F. Wilson, Doris Breuer, Cédric Gillmann, Suzanne E. Smrekar, Tilman Spohn and Thomas Widemann

Extended author information available on the last page of the article

1 Introduction

This article describes current thinking on Venus' tectonic and volcanic processes, which provide essential insights on Venus' evolution through time. Given the often-noted gross similarities between Earth and Venus, an essential comparative planetology question is to know which processes differ or are the same between the two planets, and why? As the role of plate tectonics in Earth's long-term habitability becomes more evident, many exoplanet models have focussed on predicting the likelihood of this process. As the only other Earth-sized planet in the Solar System, Venus is the logical planet to explore this question (see Rolf et al. 2022 and many references therein). Venera measurements of radiogenic elements in Venus' crust show Earth-like concentrations, implying a similar internal heat budget. However, plate tectonics has not always been the dominant process on Earth either. Exactly when plate tectonics started and continents formed is debated, but certainly processes in the Archean (much of the first half of Earth's history) appear to have been very different to the modern Earth. The high surface temperature on Venus creates lithospheric temperatures similar to the elevated heat flow in the Archean (e.g., Van Kranendonk, 2010; Harris and Bédard 2014, 2015; Gerya et al. 2015), although with a transition to eclogite at a shallower depth than in Earth's present-day crust (e.g., Namiki and Solomon 1993). Much of Earth's early record has been erased by both plate tectonics and erosion. Tectonic and volcanic processes on Venus today may therefore inform our understanding of Archean Earth and vice versa. Some features on Venus appear consistent with localized subduction of the lithosphere (e.g., Schubert and Sandwell 1995; Harris and Bédard 2014, 2015). As subduction is believed to be the first step in creating a plate tectonic system, understanding the conditions necessary to permit this process to occur, is the absence of a plate tectonic framework. Other key issues include the formation of Venus' tesserae and whether or not Earth's Archean cratons formed in an analogous manner.

A key constraint on interpreting geologic processes on another planet is the size and spatial distribution of impact craters. Venus has only ~1000 impact craters and their distribution cannot be distinguished from a random one. The average surface age is very young, relative to other terrestrial planets, but poorly constrained (estimates span at least ~0.15–1 Ga). The processes that removed older terrains thereby removing craters are controversial (Herrick et al. 2023, this collection). The absence of large regions of conspicuously different ages on Venus has been used to infer a very different tectonic style from Earth (e.g., Herrick et al. 2023, this collection). Furthermore, only ~10% of the craters are widely regarded as modified by subsequent geologic activity. However, many more craters might have suffered modification by sedimentary (Carter et al. 2023, this collection) and/or volcanic processes (e.g., Herrick and Rumpf 2011; Herrick et al. 2023, this collection). The random spatial distribution and ambiguous modification state of the impact craters has led to competing interpretations of Venus' impact record. In the "catastrophic resurfacing" model, the entire surface was wiped clean of impact craters, either by burial under a thick layer of lavas (e.g., Schaber et al. 1992; Head et al. 1994; Strom et al. 1994) and/or by recycling of the surface via overturn of the lithosphere (e.g., Parmentier and Hess 1992). Subsequently, geologic activity declined, allowing the surface to accumulate impact craters at random. The globally ancient surfaces of Mars, Mercury, and the Moon are in a stagnant lid convective regime, with interior heat lost primarily through conduction across a thick, immobile lithosphere. However, for Venus, a fully stagnant lid does not provide sufficient heat loss, leading to the idea that Venus has cycled between a stagnant lid regime today and a past plate tectonic regime, allowing for greater heat loss over time (Turcotte et al. 1999), consistent with the inference of a past catastrophic resurfacing event.

The opposite end-member is the ‘equilibrium resurfacing’ hypothesis (e.g., Phillips et al. 1992). Under this scenario, impact craters are removed at a roughly constant rate by geologic activity that has no spatial organization, in contrast to Earth. Perhaps more likely is an intermediate hypothesis of ‘regional equilibrium resurfacing’ that allows for spatial and temporal variability of regions less than ~ 1000 km in diameter, consistent with the impact crater distribution (e.g., Phillips et al. 1992). Herrick et al. (2023, this collection) provides a thorough discussion of these models and their implications. We introduce these interpretations here because of the fundamental role that both the mean surface age and local variability play in framing the geologic evolution of Venus and the interpretation of interior and atmospheric processes (e.g., Rolf et al. 2022, this collection). Recently, the concept of a partially mobile ‘squishy’ lid regime has been proposed, in which intrusive volcanism allows for plate-tectonic-like levels of heat loss (Lourenço et al. 2020). Below, we discuss a range of geologic features observed on Venus, along with implications for lithospheric structure and convective regime.

In parallel with the notion of ‘episodic vs. equilibrium’ resurfacing is the concept of ‘directional vs non-directional’ geologic history (Guest and Stofan 1999). Does the variety of geologic features observed on Venus occur in a specific sequence everywhere, consistent with an episodic (or ‘catastrophic’) resurfacing event? Ivanov and Head (2011) mapped the whole Venus surface at 1:10 million scale and identified a global stratigraphic sequence with 13 distinct members, with tesserae identified everywhere as the oldest unit, then various deformed plains, ‘groove’ (extensional) and mountain (compressional) belts, through undeformed plains, to ‘lobate’ (lava flow) plains and rift zones. The authors argued that since this sequence is never found next to, and offset from, an adjacent sequence, the sequence must represent a global change through time, i.e., a directional geologic history. Arguments against this sequence (Guest and Stofan 1999) take two principal forms: first, that the stratigraphic methods and interpretation of some authors (e.g., Ivanov and Head 2011) mix material (rock) units with tectonic (structural) events; and second, that radar is sensitive to surface texture and relatively insensitive to rock type. For example, the regional plains, which cover a third of the planet, may have very different ages but appear texturally the same, and hence cannot be used as a stratigraphic marker. A further problem for interpretation is that since radar is very sensitive to surface roughness near the radar wavelength, apparent boundaries and onlap relationships, such as the ‘flooding’ of tesserae by regional plains, may be a result of gradational downslope grain size changes, indicating the opposite age relationship (Carter et al. 2023, this collection, and references therein). Further, others argue that this sequence is not observed everywhere and that in places, tesserae may be younger than the plains (e.g., Ghail 2002; Ivanov and Head 1996; Gilmore and Head 2000). The scarcity of impact craters and the lack of any other independent dating technique hamper a resolution to this question.

Our understanding of current processes and conditions effectively provide boundary conditions for extrapolation backward into Venus’ geologic and convective history (see Rolf et al. 2022, this collection). The size, type, distribution, and (where available) chemistry of volcanic features offers a window into interior processes such as upwelling/downwelling, decompression melting and mantle temperature. Venus hosts a wide array of volcanic features, from those seen on Earth including volcanic edifices and lava flows, to those unique (at least in abundance) to Venus, such as novae and coronae (e.g. Glaze et al. 2002; Krassilnikov and Head 2003). The overlap between volcanoes, coronae, and novae is an interesting puzzle, as discussed below. Tectonic features provide constraints on the rheology and thickness of the lithosphere and the origin and magnitude of driving stress fields. Gravity data provide further information on the thickness of the crust, the lithosphere, and subsurface density variations due to processes such as mantle upwellings. The low resolution of current datasets often results in multiple interpretations of a given feature or process. The goal

here is not to provide a single view, but to represent a range of possible interpretations, the constraints available from current data, and to outline specific needs for future datasets.

A rocky body's crustal layer provides a complex archive for the planet's evolution. The crust may be primary, a direct consequence of a magma ocean freezing, secondary, a result of active magmatism and volcanism in the solidified interior, or tertiary, which invokes remelting of primary and/or secondary crust (e.g., like the Earth's continental crust). In the case of Venus, crustal composition is dominantly basaltic (Hess and Head 1990) and its young surface age dictates that most of its volume is likely secondary crust. Tessera terrains may represent tertiary crust (see Gilmore et al., 2023, this collection). The formation of eclogite from basalt may play a key role on Venus in terms of both mantle dynamics and the formation of specific volcanic and tectonic features. Delamination driven by eclogite formation has been proposed to drive the formation of both coronae (e.g., Piskorz et al. 2014; Gülcher et al. 2023) and tessera plateaus (e.g., Bindschadler and Parmentier 1990). Delamination would also result in the formation of secondary or tertiary crust (Elkins-Tanton et al. 2007). Whether or not delamination leads to mobilisation of an otherwise stagnant lid depends on the details of the mantle convection models (e.g., Armann and Tackley 2012; Rolf et al. 2018; Adams et al. 2022, see Rolf et al. 2022, this collection). Mantle convection models are useful tools to simulate the growth history of Venus' crust through its long-term evolution and how this relates to the planet's thermal state and geodynamic regime. A stagnant-lid scenario may lead to a relatively hot mantle, promoting magmatism and crustal growth. In contrast, episodically or partially mobile (plutonic squishy lid) lithosphere may reset crustal thickness and therefore limit its effective thickness (see Rolf et al. 2022, this collection, for details).

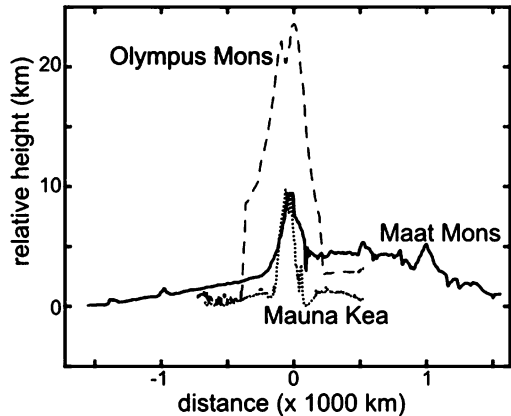
2 Overview of Volcanic Features

The surface of Venus is replete with volcanoes—that is, discrete edifices, although there is evidence for non-constructional volcanoes such as fissure vents, too. Early post-Magellan surveys (e.g., Head et al. 1992) reported on the positional details of almost 1,700 volcanic edifices across the planet, finding that roughly half the large volcanoes on Venus are located in the Beta, Atla, and Themis region, which covers less than a quarter of the surface (Crumpler et al. 1993). The largest volcanoes are well in excess of 100 km across: some, such as Maat (Fig. 1), Sif, and Tepev Montes, are several hundred kilometres in diameter (e.g., Janle et al. 1988; Senske et al. 1992), and lava flows as long as ~500–1000 km are observed (Head et al. 1992). Indeed, vast lava flows are a common feature of the largest volcanoes on Venus, which are typically located atop topographic rises (e.g., Ivanov and Head 2013). These edifices are classic shield volcanoes, being far broader than they are tall; generally, Venus' largest volcanoes are up to 9 km tall, comparable to the largest volcanoes on Earth (Fig. 1).

Venus also exhibits ~200 large flow fields, with areal extents of ~39,000 to 744,000 km² (e.g., Magee and Head 2001). The majority of these flow fields emanate from either central volcanos or coronae, and are thus covered under the discussion of these features below. In addition, another ~40 large flow fields occur in association with chasmata or fracture zones (e.g., Magee and Head 2001; Lancaster et al. 1995). These tectonic features are discussed below as well.

Volcanoes less than 100 km in diameter are distributed widely across the planet and are often characterized by radial lava flows and conical or shield-like shapes; some have flat-topped summits (Head et al. 1992). By far the greatest number of individual edifices are

Fig. 1 Maat Mons and Mauna Kea (Hawaii) both reach ~ 9 km of prominence, but Maat Mons is several hundred km across. For comparison, Olympus Mons (Mars) reaches ~ 24 km of prominence, but still is narrower than Maat Mons



those less than 20 km in diameter (e.g., Crumpler et al. 1997; Grindrod et al. 2010), with recent mapping suggesting that there are at least tens of thousands of volcanoes < 5 km across (Hahn and Byrne, 2022). Crumpler et al. (1997), classified volcanic edifices as “large”, “intermediate” and “small” on the basis of Venera 15 and 16 results; large volcanoes are those equal to or larger than 100 km, intermediate volcanoes are those ≥ 20 km and < 100 km, and small volcanoes are those < 20 km in diameter, regardless of their geologic significance. Establishing the exact shape of these small edifices is difficult with the limited topographic resolution of Magellan and so determining whether they are conical or truly shield-like in appearance requires new data from future missions. Given their prevalence, volcanic processes likely have a key role in forming the young surface through the burial of impact craters and other old terrains (see Herrick et al. 2023, this collection). As on Earth, some volcanism can be linked directly to decompression melting above mantle plumes, while other features may be associated with lithospheric extension, delamination or dripping, or other processes (e.g. Head et al. 1992; Martin et al. 2007). The features that can most clearly be linked to mantle plumes are the ten or so volcanic rises, which share many key characteristics with Hawaii and other terrestrial hotspots (Stofan and Smrekar 2005).

The ~ 500 enigmatic coronae (mean diameter ~ 250 km) are widely distributed across the surface (e.g., Stofan et al. 1992), although $\sim 62\%$ occur in association with rifts or fracture belts (e.g., Glaze et al. 2002). These features likely have multiple formation mechanisms, but many probably formed above small-scale mantle plumes (e.g., Gülcher et al. 2020). Some proposed mechanisms have terrestrial analogues, such as large igneous provinces (LIPs) and plume-induced subduction. However, these processes are not active on Earth today. Two key questions for the formation of coronae are: (i) why do coronae form on Venus but not on present-day Earth, and (ii) why does Venus appear to have two largely distinct scales of mantle upwellings? For the latter question, one hypothesis is that different volcanic features, such as volcanic rises and coronae, formed at different times in Venus’ evolution; another is that layered (or otherwise variable scales of) mantle convection generates different features (see Rolf et al. 2022, this collection).

2.1 Spatial Distribution of Volcanism

Given the seeming lack of obvious fluvial or aeolian sedimentary processes (although see Carter et al. 2023, this collection), volcanism is the major contributor to the formation of surface material on Venus (Head 1990) at least during its observable part of geologic history.

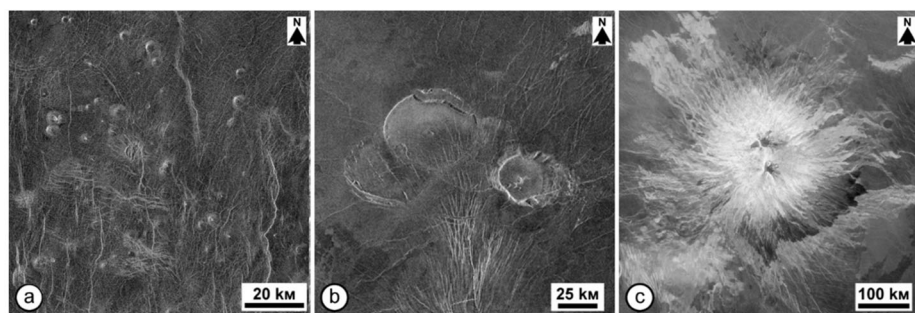


Fig. 2 - Examples of volcanic edifices on Venus: (a) a cluster of small edifices (< 20 km in diameter) that populate an exposure of shield plains; (b) a cluster of steep-sided domes that represent the intermediate volcanoes (from Crumpler and Aubele 2000); (c) a large volcano (> 100 km) of Sapas Mons (from Crumpler and Aubele 2000)

Indeed, Venus is a “volcanic” planet on which volcanic materials compose $\sim 92\%$ of the surface (e.g., Ivanov and Head 2011). The remaining surface consists of tessera (as discussed below in Sect. 3.1).

The most areally extensive volcanic landforms on Venus are volcanic plains, some of which are as large as a few million square kilometres (e.g., Ivanov and Head 2011, 2013).

Small edifices (Fig. 2a) populate the surface of shield plains and are the most abundant volcanic form (Addington 2001; Crumpler et al. 1993; Hahn and Byrne, 2022). The exact number of these volcanoes is unknown but it may exceed the tens of thousands. These edifices are relatively small with the decile diameter range (central 80% of the population) from ~ 2.5 to ~ 5.5 km (Hahn and Byrne, 2022). In an early global catalogue of volcanic landforms of Venus (Head et al. 1992), the sub-population of small volcanoes on the shield plains were assigned to a class of “shield fields,” which may represent isolated outcrops of shield plains embayed by younger materials (e.g., Ivanov and Head 2004).

A recently compiled, new global volcano catalogue for Venus indicates the presence of more than 85,000 edifices, the vast majority of which ($\sim 52,000$) are barely resolvable with available Magellan radar image data (Hahn and Byrne, 2022) (Fig. 3a). Of those volcanoes that are more readily identifiable, $\sim 32,500$ are < 5 km in diameter, 729 are 5–100 km in diameter, and 118 have diameters greater than 100 km. Previous studies had further grouped volcanoes into “fields” (e.g., Grosfils et al. 2000; Pavri et al. 1992); Hahn and Byrne (2022) found that (for specific criteria, including 25 edifices as a minimum number) the global volcano population could be grouped into 566 fields comprising about 65% of all mapped volcanoes; the remainder did not fall within clusters of ≥ 25 edifices.

The spatial distribution of volcanoes on Venus (Fig. 3a) appears to be drastically different from that on Earth, where the active volcanoes are mostly occurring within zones along convergent and divergent boundaries and along hotspot tracks (Fig. 3b) (Byrne and Krishnamoorthy 2022), although it should be noted that the distribution of (presumably) active volcanoes on Venus is currently unknown. Even so, the difference in spatial distribution suggests that Venus possesses a mechanism of the internal heat leakage which is dissimilar to terrestrial plate tectonics (e.g., Solomon and Head 1982; Solomon et al. 1992; Stofan and Saunders 1990). Grossly speaking, volcanoes on Venus show slightly greater spatial concentration in the Beta–Atla–Themis region and in a region north of Aphrodite Terra relative to the rest of the planet surface (Hahn & Byrne, 2022) (Fig. 3a).

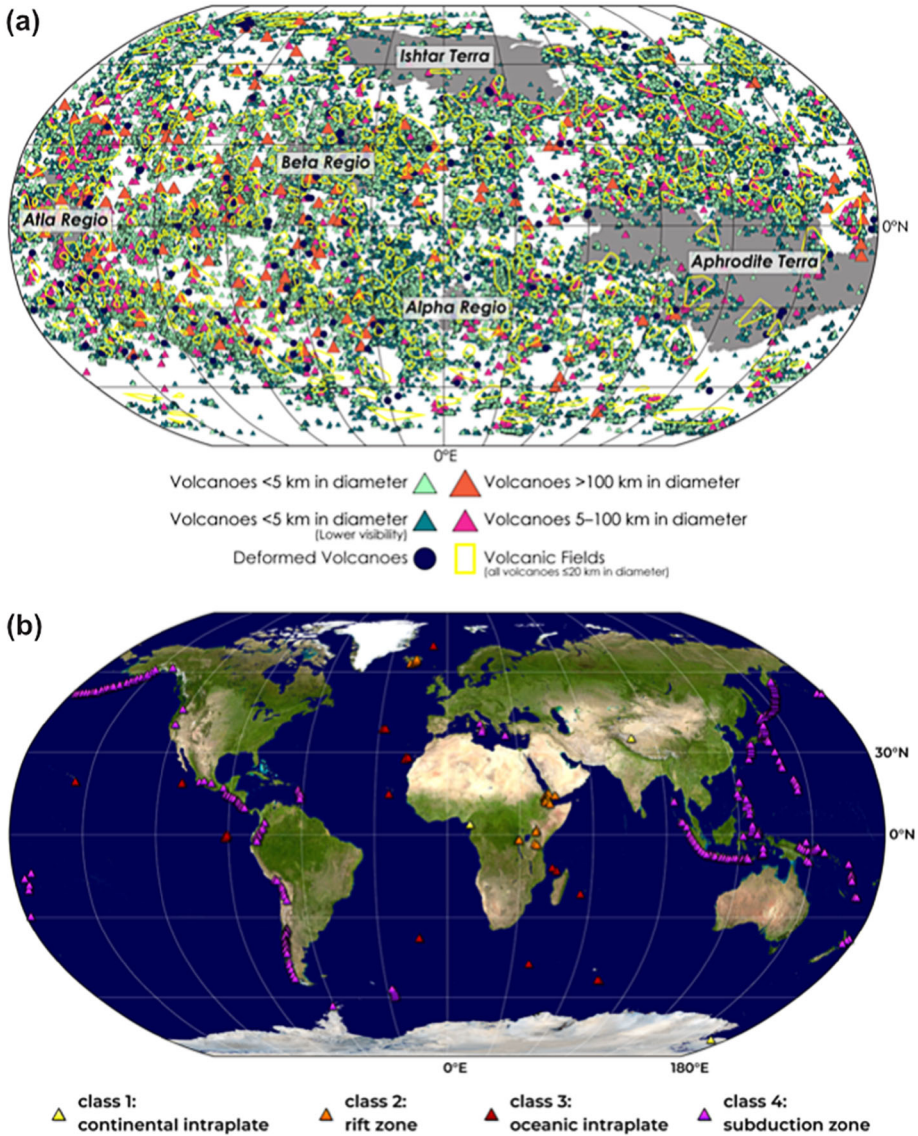


Fig. 3 The spatial distribution of volcanoes on: (a) Venus, and (b) Earth. The databases of Venusian volcanic edifices are from Hahn and Byrne (2022). Terrestrial volcanoes are those that are thought to have been active during the Holocene volcanoes, which are mostly located at plate boundaries (Global Volcanism Program 2023). This database from the Smithsonian also has a list of terrestrial volcanoes that may have been active during the Pleistocene

2.1.1 Lava Channels

Lava channels are widespread on Venus. Almost 200 such features were mapped using Magellan data, divided into six different types (e.g., Komatsu et al. 1993): sinuous rilles; canali; simple channels with associated flow margins; complex channels with flow margins; com-

plex channels without flow margins; and compound channels. Some of these channels resemble features seen on Mars and Earth's Moon. For example, sinuous rilles have large depth-to-width ratios and morphologies similar to those of lunar and Martian rilles (e.g., Komatsu and Baker 1994; Oshigami et al. 2009). Usually, no lateral flow deposits are observed near rilles, but flow deposits are sometimes found at their termini. Channel sources are sometimes unidentifiable, but they are often found to originate in depressions. Mappers have identified ~59 rilles with average lengths of ~10–300 km and widths up to several kilometres (e.g., Baker et al. 1992; Komatsu et al. 1993). More than half of the rilles are associated with coronae or coronae-like features (e.g., arachnoids), while the remainder are almost evenly distributed between the plains and highlands (e.g., Komatsu et al. 1993). Valley networks on Venus are also typically associated with coronae and sinuous rilles—and they seem to be subject to tectonic control than rilles (Komatsu et al. 2001). Overall, both rilles and valley networks appear to have formed via incision into the surrounding terrain. Other types of simple, complex, and compound channels appear shallower and often have flow margins—suggesting a constructional (i.e., volcanic) origin (e.g., Komatsu et al. 1993; Komatsu and Baker 1994; Komatsu et al. 2001).

Canali are long, narrow channels that superficially resemble meandering rivers on Earth. They are typically more than 500 km long, ~1 km wide, and ~24 m deep on average (Baker et al. 1992; Komatsu et al. 1993; Williams-Jones et al. 1998). Baltis Vallis is ~6,800 km long—the longest canali on Venus and the longest channel of any sort so far found in the solar system (e.g., Baker et al. 1992). This extreme length makes Baltis Vallis useful as a stratigraphic marker (e.g., Basilevsky and Head 1996) and as a tool with which to study the evolution of topography (e.g., Conrad and Nimmo 2023). River-like features such as cut-off meander bends, abandoned channel segments, and terminal deposits are often observed at canali. Narrow levees are sometimes seen, but only at the limit of the resolution of the radar imagery. Canali are concentrated on the plains—although identifying their sources and/or termini is often difficult or impossible. Unusual types of lava are often invoked to explain the apparently unique properties of canali (e.g., Kargel et al. 1994). For example, some studies favored carbonatite-rich (or carbonatite-sulphate-rich, with a eutectic composition) lavas that have low viscosity (to explain river-like meanders) and low melting temperatures (to explain the extreme lengths). For example, one carbonatite lava from the Oldoinyo Lengai volcano on Earth was observed to have a liquidus temperature of only 763 K, although ~1000 K is a more typical value of this type of lava (e.g., Dawson et al. 1990; Keller and Krafft 1990). Mafic and ultramafic lavas that are observed on Earth and other rocky planets, such as basalt or komatiite, have relatively high melting temperatures (>1300–1600 K). They could create channels via thermal erosion, but they might tend to solidify after travelling tens (or, at most, hundreds) of km across the surface (e.g., Flynn et al. 2023), rather than the thousands of km needed for some canali (e.g., Head and Wilson 1986).

Speculatively, the formation of canali may be important to models of the evolution of Venus. Carbonatite lavas on Earth typically contain >30–50 volume percent of carbonate minerals (Dawson 1962). Some studies suggest that canali formed with discharge rates >10⁵ m³ s⁻¹ for up to ~100 years (Kargel et al. 1994). Lava that formed each canale seen on the surface today thus could have degassed enough CO₂ to produce a small portion of the modern atmosphere (e.g., Kargel et al. 1994). Such rapid resurfacing with carbon-rich lava may lead to a coupled evolution of the surface and atmosphere—perhaps burying old impact craters (e.g., Komatsu et al. 1993; Strom et al. 1994) and creating a greenhouse effect that drives the global climate from clement to hellish (e.g., Way and Del Genio, 2020; Way et al., 2016). However, many questions about canali and carbonatite volcanism on Venus await answers.

2.1.2 Hotspots and Hotspot Volcanoes

Some of the large volcanoes on Venus can be classified as ‘hotspot’ volcanoes. On Earth, hotspots are defined as the surface manifestation of hot mantle that diapirically rises from the lower mantle or core–mantle boundary, generating volcanoes via pressure-release melting (Griffiths and Campbell 1990; Hoggard et al. 2020; Jellinek and Manga 2004; Morgan 1972). Mantle plumes and their tails are thought to be responsible for flood basalt volcanism and the formation of hotspots (White and McKenzie 1995); specifically, the bulbous head of a mantle plume impinges to the base of the lithosphere and generates mafic and ultramafic melts for a short time. On Earth, plumes have mantle potential temperatures that are 150 K to 350 K above ambient conditions. Seismic data indicates these mantle upwellings are generated at specific regions of the Earth’s lower mantle that are known as Large Low Shear Velocity Provinces (LLSVPs) (Torsvik et al., 2014).

Nine hotspots are inferred to have originated from or near the core–mantle boundary on Venus (McGill 1994; Smrekar et al. 1997). They have been identified on the basis of their great topographic swells (~ 1000 – 2000 km diameter, ~ 1 – 2 km high), large volcanic edifices, gravity anomalies that indicate compensation by low-density material at the base of the lithosphere (the plume head) (e.g., Smrekar and Phillips 1991), and, in some cases, rifts and coronae (Stofan et al. 1995). No hotspot tracks are observed in association with mantle plumes, consistent with a lack of plate tectonics operating at Venus. However, the large interior volcanoes and ring of wrinkle ridges surrounding Laufey Regio were interpreted as evidence of a past plume at that location (Brian et al. 2004). Once that rising mantle plume has cooled, the thermal isostasy from it no longer supports the topographic rise proposed to account for the circumferential wrinkle ridges.

Many coronae likely formed above small plumes but are typically too small to be caused by core–mantle boundary-sourced plumes. Artemis is larger (at ~ 2600 km in diameter) than many of the hotspot features discussed above, and has been proposed to be a site of plume-induced subduction (Davaille et al. 2017; McKenzie et al. 1992; Sandwell and Schubert 1992b). Other large coronae could have formed over deep mantle plumes: despite their relatively low resolution, gravity data at Quetzelpetlatl corona (~ 900 km diameter) are indicative of an active plume (Davaille et al. 2017). Heng-o (~ 1100 km diameter) is another large corona, but neither its topography nor gravity suggests activity today. The nine large volcanic rises (Stofan and Smrekar 2005) on Venus (ten, if Laufey is included) exclude these few very large coronae. This is based on both on the smaller size of all features exclusive of Artemis and the analogy to Earth’s hotspots, which do not have the evidence of plume-induced subduction seen at Quetzelpetlatl and Artemis Coronae (Ivanov and Head, 2011; Davaille et al. 2017). However, plume-induced subduction is proposed to have occurred earlier in Earth’s history (e.g. Whattam and Stern, 2015), and thus excluding Artemis is perhaps artificial. Additionally, the larger features can be resolved in the Magellan gravity data, which provides evidence of an active plume at these features (e.g. Smrekar and Phillips 1991). As discussed below, there are multiple lines of evidence supporting these hotspots as likely active. Other (non-hotspot) volcanoes may also be active, but available data are inadequate to assess this possibility.

The classic volcanic edifices at terrestrial oceanic hotspots (e.g., Hawaii, Iceland) form shield volcanoes that are composed of a thick sequence (sometimes more than 10 km) of many individual lava flows (typically ~ 2 – 20 m thick). These flows in turn form a broad base, on the order of 100 km across, with relatively steep lower slopes ($\sim 10^\circ$) that grade to more gentle upper slopes (2° to 3°). The morphology of oceanic hotspot volcanoes is due to the sequential accumulation of low viscosity lava flows that erupt over a period of 1 million

years; volcanic activity can last up to 200 million years for a single hotspot (Heaman and Kjarsgaard 2000; Kasbohm and Schoene 2018; Wei et al. 2020). The lava compositions are 90 to 95% basaltic, with minor volumes of silicic volcanic rocks (e.g., rhyolite, trachyte, dacite) present within the youngest flow sequences (Jeffery and Gertisser 2018). After the initial effusive flows, the preponderance of subsequent flows during the shield-building stage are tholeiitic basalt, but minor volumes of alkali basalt may erupt during waning or rejuvenation stages (Thordarson and Garcia 2018).

On Venus, many of the hotspots described above have large shield volcanoes (e.g., Stofan et al. 1995), as well as other types of volcanism. Large shield volcanoes occur in many locations and geologic settings across Venus, as is the case on Earth (e.g., Hahn and Byrne, 2022). Without high-resolution geophysical and detailed geochemical data, the deep mantle origin and general eruption history of Venusian hotspot volcanism must be inferred from the geologic setting, gravity and topography, morphology and by analogy with Earth. Moreover, the quality of Magellan-based altimetric and stereo-derived topographic data are not sufficient to fully characterise volcano shape and slopes to the extent possible for Earth (and Mars). Nonetheless, on the basis of Magellan radar imagery, shield volcanoes on Venus appear to have broadly comparable morphologies and, presumably, slope values.

2.1.3 Coronae

Coronae are oblong to circular volcano-tectonic features ranging in diameter from 60 km to up to 2600 km, with a median size on the order of 200 km (Glaze et al. 2002). A ring of closely spaced concentric fractures and/or ridges is the defining characteristic of coronae. Stofan et al. (2001) divided coronae into two categories: Type 1, with $>180^\circ$ of a fracture annulus (Fig. 4c), and Type 2, or stealth coronae (Fig. 4b), with $<180^\circ$ (Stofan et al. 2001). Glaze et al. (2002) identified 406 coronae of Type 1 and 107 of Type 2. Coronae have also been categorized into five classes based on their fracture annuli: concentric, concentric double-ring, radial/concentric, asymmetric, and multiple (Stofan et al. 1992). Coronae often have circumferential rims or trenches that can extend beyond the annulus, which are not necessarily correlated radially or azimuthally with fracture annuli and can be equally incomplete and irregular in shape. They can also have interior domes, plateaus, and depressions. Based on these topographic elements, Smrekar and Stofan (1997) defined nine topographic classes. Three coronae that fall into a common topographic class (3a, rim surrounding interior high) with varying fracture patterns are illustrated in Fig. 4.

Coronae are found in every geologic environment on Venus (e.g., Stofan et al. 1992). The majority (62%) occur along fracture/rift belts (chasmata) (Glaze et al. 2002). Coronae appear randomly located in these extensional environments, suggesting that the detailed locations of coronae are not influenced by rifts and vice versa (Martin et al., 2007). Nonetheless, the concentration of coronae in extension environments implies a genetic relationship with these tectonic structures (e.g., Piskorz et al. 2014), although the remaining coronae occur in the plains (25%), at large topographic rises (11%), and tessera (1%) (Glaze et al. 2002).

Large volcanoes (see below) and smaller coronae overlap in scale. Morphologies can be transitional as well, leading some to propose that (some) coronae form via volcanic construction (Dombard et al. 2007; Lang and López 2015; McGovern et al. 2013). Others have pointed to the similarity between giant radiating dyke swarms on Earth and the radiating lineaments that occur at some coronae (e.g., Ernst et al. 1995).

The margins of some larger coronae, such as Artemis and Quetzalpetlal, have been proposed to be sites of retrograde lithospheric subduction (e.g., McKenzie et al. 1992; Sandwell

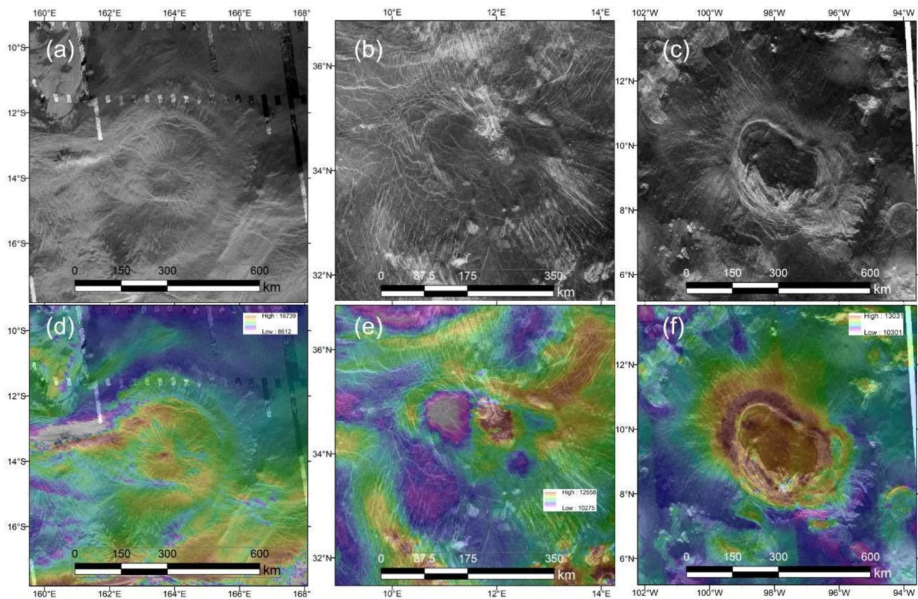


Fig. 4 Magellan left-look SAR images of (a) Miralaidji, (b) Ponnakya, and (c) Aruru coronae, with respective stereo-derived topography (Herrick et al., 2012) in (d) and (e), and Magellan topography (f). Miralaidji Corona, near Latona and Dali Chasma, has radial fractures, and thus a morphology similar to that of novae (Krassilnikov and Head 2003). Ponnakya Corona, a stealth corona, has $<180^\circ$ concentric fractures, with a short NE-SW axis of ~ 175 km and long NW-SE axis of ~ 300 km, and $>180^\circ$ of a topographic rim. The appearance both in SAR and in topography is obscured by regional strain and interior volcanism, and orthogonal fractures obscure its appearance in SAR, in particular. Aruru Corona, a large volcanic centre (Tucker and Dombard 2023), has interior lava flooding, shield fields in the SW, and lava flows to the ESE

and Schubert 1992b; Schubert and Sandwell 1995). These coronae show topographic flexural signatures, beginning in the fracture annulus and extending outward, that resemble flexural signatures caused by retrograde subduction observed on Earth (Johnson and Sandwell 1994; O'Rourke and Smrekar 2018; Sandwell and Schubert 1992b). Moreover, interior extensional features displayed by Artemis corona are reminiscent of back-arc spreading centres (e.g., Brown and Grimm 1995; Sandwell and Schubert 1992b), contributing to the interpretation of retreating lithospheric subduction occurring at the south-eastern margin of the corona (McKenzie et al. 1992; Sandwell and Schubert 1992b), although others suggest Artemis Chasma is a site of convergence (Brown and Grimm 1995; Suppe and Connors 1992).

The diverse morphologies and sizes displayed by coronae may indicate that they form via a range of mechanisms. Modelling studies of the various mechanisms proposed to be responsible for corona formation are elaborated in more detail in Sect. 5.1.4 below. Regardless of the specific processes involved in their formation, coronae likely contribute to heat loss (Smrekar and Stofan 1997; Turcotte 1993). Moreover, coronae offer the opportunity to estimate the elastic lithospheric thickness through flexural modelling (e.g., O'Rourke and Smrekar 2018; Russell and Johnson 2021; Smrekar et al. 2023 and refer to Sect. 3 below and Rolf et al. 2022, this collection). As such, coronae offer important clues on the tectonic and resurfacing history of the planet.

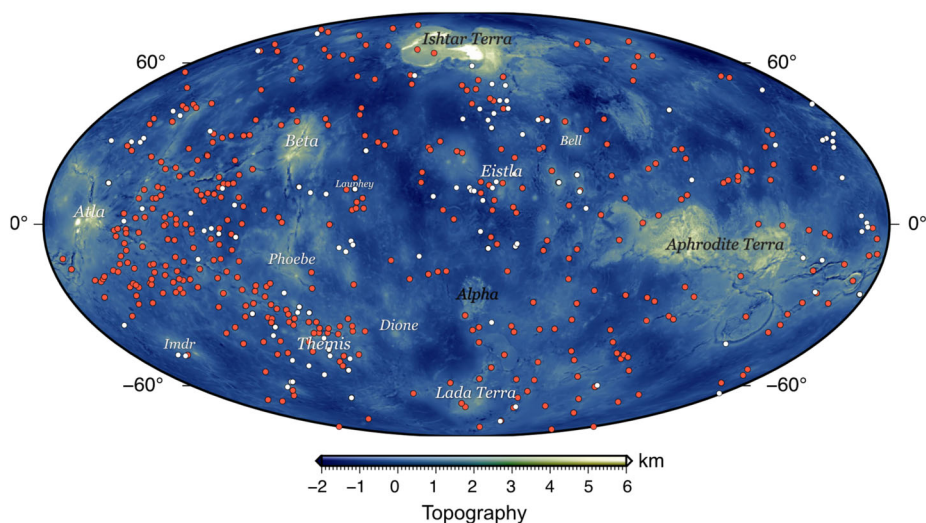


Fig. 5 - Magellan topography data superposed by locations of topographic rises (labelled with white names), major crustal plateaus (labelled with black names), Type 1 coronae (red dots), and Type 2 coronae (white dots). Blues and purple are topographically low regions; yellow and white are topographically high. Coronae locations and classifications from Stofan et al. (2001); Glaze et al. (2002)

2.1.4 Novae

Novae (singular: nova) are structures with prominent, stellate fracture patterns consisting of a mesh of graben centered on a central summit (Head et al. 1992; Krassilnikov and Head 2003). They are usually 100–300 km in diameter, have a prominent upraised topography (refer to Fig. 4a), and are associated with lava flows. Apparently distinct from volcanoes, novae show a dominance of tectonic over volcanic activity. Sixty-four novae have been identified on the Venusian surface (Krassilnikov and Head 2003), mainly located in areas of regional rises and rift zones, with a small number in the lowlands.

It is generally assumed that novae are formed by volcanic updoming and fracturing due to impingement of hot mantle diapirs on the upper part of the lithosphere (Janes et al. 1992; Koch and Manga 1996). Novae have been proposed to be the initial stages of corona development (e.g., Janes et al. 1992), or even perhaps “failed coronae” if the source of dynamic support were retracted early in the formation of what would go on to become a corona. Some studies suggested that novae within coronae represent reactivation of the corona location (Aittola and Kostama 2002), while others pointed out that the lengths of the radial structures often exceed the anticipated distance for diapiric uplift and fracturing, and instead linked novae to radial fracturing caused by dyke emplacement processes from a central magma source (e.g., Parfitt and Head 1993). However, it is important to note that <5% of coronae have radial fractures similar to novae, calling into question the hypothesis that novae are the first stage of corona formation.

2.2 Evidence for Recent Volcanism and Likely Active Features

One of the biggest scientific debates about Venus concerns its style of volcanism throughout its geologic history. As discussed above and in Herrick et al. (2023, this collection),

both catastrophic and regional resurfacing models are viable for Venus. Rolf et al. (2022, this collection) discuss the importance of understanding the history of volcanism for internal evolution models. Over the last ~ 15 years, numerous studies have shown evidence for current volcanic activity, suggesting Venus is likely more active today than previously understood. Many studies have argued for recent volcanism based on signatures of chemical, thermal, atmospheric gas, and surface change. Analysis of geophysical data supports the location of activity at rifts and hotspots.

Chemical signatures of recent volcanism are based on interpreting surface emissivity data as an indication that the weathering of new lava flows has not proceeded to completion. Evidence of 'recent' volcanism was first noted in Magellan emissivity data. The relative youth of Idunn and Maat Montes as well as some coronae is further corroborated by high values of Magellan radar emissivity at their summits, consistent with relatively little weathering (Klose et al. 1992; Robinson and Wood 1993). Brossier et al. (2020) further investigated these and other regions, suggesting additional minerals that could explain these signatures. Measurements made by the Visible and Infrared Thermal Imaging Spectrometer (VIRTIS) instrument aboard Venus Express were used to derive a map of thermal emission at 1.02 microns of much of Venus' southern hemisphere added further evidence of recent volcanism. Higher thermal emissivity displayed by some lava flows were interpreted as the chemical weathering signature of geologically recent lava flows (Smrekar et al. 2010; Stofan et al. 2016; D'Incecco et al. 2017). The presence of volcanic activity was found at Idunn Mons (in Imdr Regio), Hathor and Innini Montes (in Dione Regio), and Mielikki Mons (in Themis Regio). Prior interpretation of gravity and topography data in these areas provided evidence of mantle plumes beneath these regions, providing further evidence of activity in these areas (Smrekar et al. 2010 and references therein). The age of these incompletely weathered flows is debated. Filiberto et al. (2020) suggest that the flows are as young as a few years based on weathering experiments done using terrestrial air. Others argue for much slower weathering (up to $\sim 500,000$ yr) based on kinetic calculations applied to Venus spectral data (Dyar et al. 2020). Much work remains to fully interpret the age of 'recent' flows.

Other studies have provided evidence of a thermal signature of active flows. Transient bright spots in data from the Venus Monitoring Camera (VMC) were suggested to arise from volcanic activity associated with the Ganis Chasma rift zone in the Atla Regio (Shalygin et al. 2015). Some transient features could also be artefacts of cloud motion or instrumental corrections for background temperature. However, the areas with the bright spots also have high radar emissivity associated with relative geologic youthfulness (Brossier et al. 2020). Bondarenko et al. (2010) argued for subsurface thermal anomalies in Bereghinia Planitia using Magellan microwave radiometer data. This area, along with $\sim 50\%$ of the planet, is not covered by VIRTIS data, which cover most of the southern hemisphere. Additionally, the Magellan radar emissivity signatures, which may be due to incomplete weathering, are found only above ~ 0.7 km altitude.

Together with Earth-based radar maps, Campbell et al. (2017) interpreted several radar-bright deposits to reflect the early stage of recently renewed magmatic activity in eastern Eistla, western Eistla, Phoebe, and Dione Regiones. Herrick and Hensley (2023) found a volcanic vent near the summit of Maat Mons that seems to have changed in shape during the Magellan mission, providing the first direct observational evidence for active surface change driven by volcanism. Both studies offer evidence for volcanism using radar imaging in the same areas where Magellan radar and/or VIRTIS thermal emissivity offer evidence of incomplete weathering.

Interpretation of the gravity and topography data (See Sect. 4) is also consistent with the locations of many of these recent and perhaps currently active centers of volcanism

by revealing regions of upwelling and thin lithosphere. The long-wavelength geoid data suggest that both rifts and many areas that exhibit wrinkle ridges are likely supported by dynamic compensation and thermal anomalies at depth (Sandwell et al., 1997). The strong spatial correlation of the transient bright spots with rift zones suggests a correlation between deep and broad thermal upwellings and surface volcanism (Piskorz et al. 2014; Shalygin et al. 2015). Smrekar et al. (2010) provide an overview of several studies pointing to mantle plumes beneath the volcanic centers where emissivity anomalies are located. Other studies estimate elastic thickness from topographic flexure or admittance, and then derive heat flow as discussed in Sect. 3.2. High heat flow is a strong indication of activity, and is found at most coronae and nearby features where flexure is observed, including those coronae concentrated along Parga Chasma (e.g., O'Rourke and Smrekar 2018, Russell and Johnson 2021, Smrekar et al. 2023). Additionally, Gülcher et al. (2020) argued that 37 coronae with outer trench and rise morphology require ongoing suction above downwards-moving lithospheric material and an elevated interior supported by upwelling buoyancy.

Atmospheric data also offer a whiff of recent volcanism at unspecified sites. Varying rates of atmospheric SO₂ were interpreted as evidence of volcanic activity (e.g., Marcq et al. 2013). Analysis of the Soviet VeGa-2 probe (1985) data indicated, in the last few kilometres above the ground level, a lapse rate that would be unstable in the absence of a stabilising chemical gradient, which has been suggested to arise from a vertical gradient in nitrogen caused by density-driven separation of N₂ from CO₂ (Lebonnois and Schubert 2017). Cordier et al. (2019) found that producing a stabilising gradient with only CO₂ released from the Venusian crust would require an unrealistically huge rate of volcanic degassing. See also Wilson et al. (2024, this collection) for a discussion of effects of volcanic eruptions on the modern atmosphere of Venus.

3 Overview of Tectonic Features

3.1 Tessera Terrain

Approximately 8% of the surface of Venus is classified as tessera terrain (Ivanov and Head 1996), defined as having relatively complex patterns of deformation (e.g., Barsukov et al. 1986; Ivanov and Head; 1996). Tesserae are found as large (~1000 s km) plateaus standing ~1–4 km above the mean planetary radius, and as small outcrops (~10 s –100 s km) scattered in the plains (Gilmore et al., 2023, this collection). Global mapping of the tessera shows that most tessera margins are embayed by plains, thus establishing the tessera as the oldest materials in a proposed global stratigraphic column (e.g., Ivanov and Head 2011, 2013). This interpretation is supported by the total crater population of tessera terrain, which with ~80 craters is up to ~1.4 times the global average crater age (Gilmore et al. 1997; Ivanov and Basilevsky 1993), and may be older if deformed craters are recognized with future, higher-resolution imaging and topography data. The crater record, while sparse, does indicate that the observable phases of tessera deformation occurred at the time of, or just before, the global average age, although the rock age of the tesserae is unknown. Some tessera boundaries show interaction with plains units. Margin-parallel tessera structures are observed to uplift and deformed later plains units, e.g., in the southeast part of Thetis Regio (Ghail 2002), the western boundary of Alpha Regio (Gilmore and Head 2000), and the northern margin of Ovda Regio (Romeo and Capote 2011), suggesting that tessera deformation continued in places after the emplacement of marginal plains.

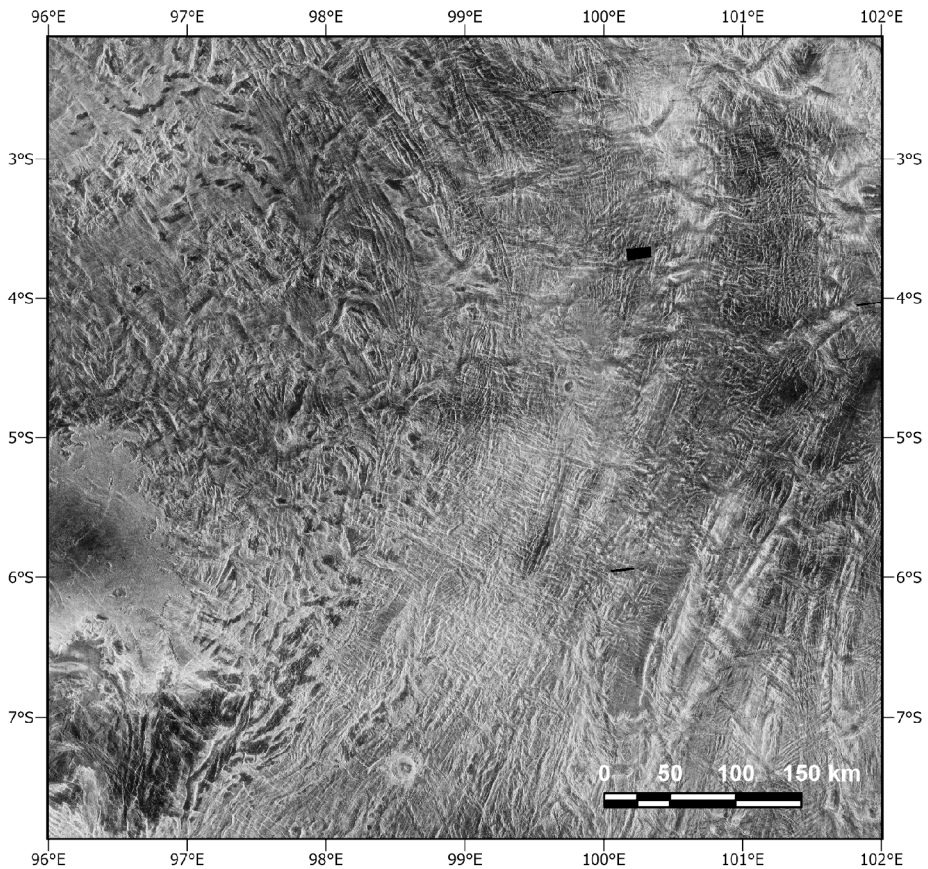


Fig. 6 - Margin-parallel ridge belts adjacent to interior facies of Ovda Regio

Shortening, extensional and transpressional structures are recognized in the tesserae (e.g., Ghent and Hansen 1999; Gilmore et al. 1998; Tuckwell and Ghail 2003). The style of extensional structures affects the interpretation of plateau origin and stratigraphy (i.e., whether their formation started with tectonic compression versus extension). First, these extensional features may be graben resulting from crustal relaxation that deformed older compression structures that, in turn, originated presumably from an earlier compressional, plateau-building phase (e.g., Bindschadler et al. 1992). Second, an alternative interpretation holds that the extensional features are steep ($\sim 90^\circ$), open tensile fractures (called ribbon terrain). This hypothesis requires that they formed during an early extensional phase that precedes later compression and wide graben formation (e.g., Ghent and Tibuleac 2002; Hansen and Willis 1996). These endmember models call for the formation of tessera plateaus during mantle downwelling or upwelling (e.g., Phillips and Hansen 1998; Gilmore et al. 1998; Hansen et al. 2000), respectively, which can be tested with high-resolution images of extensional features. In several large plateaus (e.g., Ovda Regio, Tellus Regio), ridge belts are found parallel to the plateau margins, surrounding an interior with a different structural fabric (Fig. 6). At Tellus Regio, specifically, lateral accretion of the margins possibly occurred after the formation of the structures in the facies of the plateau interior (Gilmore and Head

2018; Resor et al. 2021). Therefore, at least some tessera facies possibly formed prior to their incorporation via lateral accretion—and subsequent deformation during plateau formation.

Several lines of evidence show that tessera formation is linked to an extinct geodynamic regime. Buckle analysis of the wavelength of tesserae folds show that they require both elevated heat flows and strain rates relative to structures preserved in the plains, corona, and volcanoes (e.g., Brown and Grimm, 1997; 1999). This interpretation is valid for dry rocks of basaltic through felsic compositions if the rocks are not quartz-dominated (Resor et al. 2021). Multiple wavelengths of deformation might alternatively reflect physical layering in the crust (e.g., Romeo and Capote 2011), although this explanation may require layers that are thicker than observed (e.g., Byrne et al. 2021). The tesserae (average crustal thickness of ~20 km) are also currently isostatically compensated, again consistent with a lack of recent mantle contribution (e.g., Anderson and Smrekar, 2006; Maia and Wieczorek, 2022).

The composition of the tesserae has not yet been measured directly, but that of some tessera exposures can be inferred from both NIR and radar observations. Observations at ~1–1.2 μm from the Galileo flyby (Hashimoto et al. 2008) and VEx VIRTIS (Mueller et al. 2008; Gilmore et al. 2015) show that the Alpha Regio tessera has a lower emissivity than the global average, which is dominated by plains of presumably basaltic composition. Since emissivity near 1 μm is inversely correlated to Fe^{2+} content in minerals (e.g., Hunt and Salisbury 1970; Dyar et al. 2020), the signature of the tessera is consistent with rocks with lower Fe content, or more felsic compositions, assuming they are igneous rocks (e.g., Gilmore et al. 2023). The generation of substantial amounts of felsic melt (i.e., on the order of the volume of the tesserae) could require both water and a lithospheric recycling mechanism for formation (e.g., Campbell and Taylor 1983), and thus possibly must have formed during a more habitable era if they are ultimately shown to be chemically equivalent to Earth's continental crust (e.g., Campbell and Taylor 1983; Gilmore et al. 2023).

The interpretations above generally assume that the tesserae are igneous in origin. The complex structural fabric of tesserae makes it difficult to document the morphology of the original surfaces at the scale of the Magellan imagery, although Ivanov (2001) asserted from a survey that tessera precursor terrain is smooth and plains-like. However, layered beds have been identified in Tellus Regio, which resemble sedimentary beds on Earth and Mars exposed by erosion (Byrne et al., 2021). Additionally, Khawja et al. (2020) proposed that the topography of some tesserae is similar to fluvial drainage basins. It also should be recognized that the tesserae need not be structurally, morphologically, compositionally, or stratigraphically homogeneous: e.g., Brossier et al. (2020) showed that the radar emissivity properties of tesserae vary geographically, which may be evidence for differences in rock composition. The tesserae are also likely to contain sedimentary deposits from nearby, upwind craters (e.g., Campbell et al. 2015; Whitten and Campbell 2016) and internal mass wasting (e.g., Carter et al. 2023, this collection). The imaging, topography, and gravity data provided from VERITAS, DAVINCI and EnVision (Widemann et al. 2023, this collection; see also Sect. 6) will substantially advance our understanding of this important terrain type.

3.2 Rifts, Extension and Dykes

Long systems of extensional structures on Venus have variously been termed “fracture belts” or “groove belts” in the literature (e.g., Squyres et al. 1992; Ivanov and Head 2011) but, by analogy with Earth, are sites of crustal extension or rifting. These systems host normal faults that form graben and half graben with abundant evidence for fault linkage. Many of these systems are tens of kilometres across and hundreds of kilometres long. At larger scales, belts of extensional structures up to ten thousand kilometres long (Fig. 6) have been

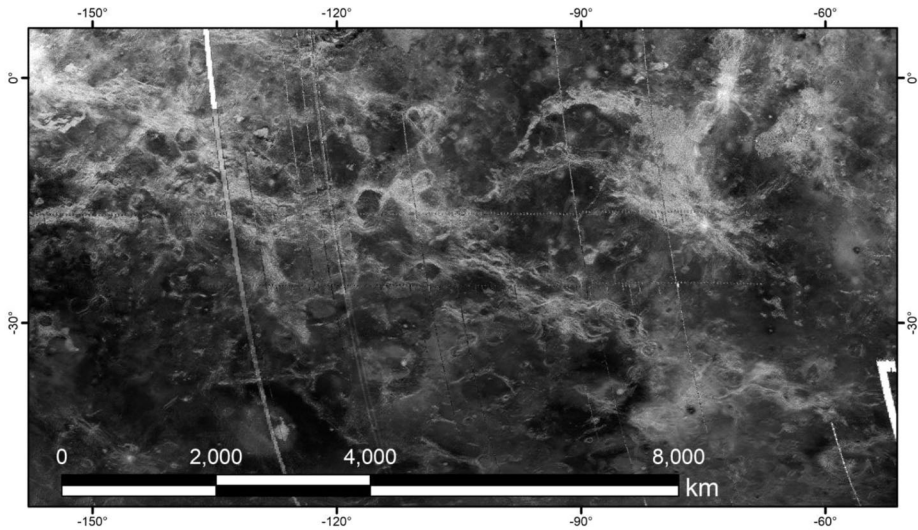


Fig. 7 - Parga Chasma, trending from NW to SE, or Atla Regio to Themis Regio, appears bright in Magellan SAR imagery. Note dozens of coronae in proximity to the rift

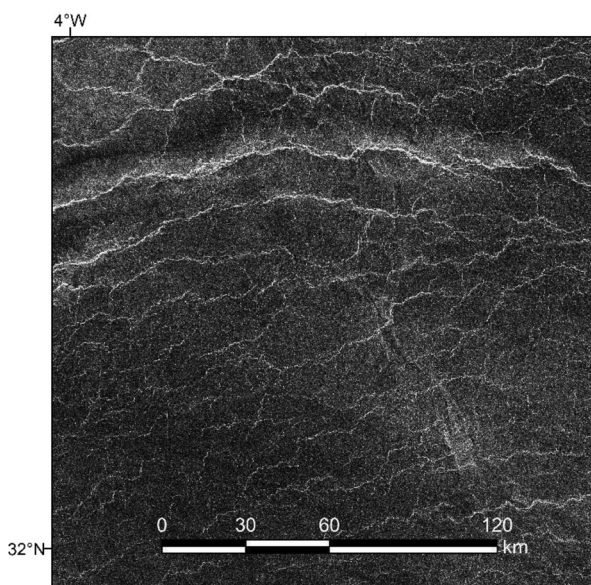
assigned the term chasmata or “rift zone” based on analogies to features on Earth and Mars (e.g., Solomon et al. 1991, 1992; Ivanov and Head 2011). These rifts form deep, elongated troughs, generally accompanied by broad expanses of effusive volcanic deposits, but are themselves typically located within regional topographic highs.

A large fraction of coronae are situated in proximity to the major rifts of Parga (Fig. 7), Hecate, and Dali/Diana (Hamilton and Stofan, 1996; Martin et al., 2007); many more occur in association with smaller rift zones (Glaze et al. 2002) (Sect. 2.1.3). Coronae at large rifts were found to have various age relationships with the rifts, such as coronae younger than the rift, synchronous formation with the rift, and post-tectonic (Hamilton and Stofan, 1996; Martin et al. 2007). At least one rift zone, Ganis Chasma, may be the site of active volcanism today (Shalygin et al. 2015). The collocation of rifts on Venus with elevated topography, together with considerable depths of compensation given by gravity–topography admittance functions, suggests that they are supported at least in part by mantle upwelling (e.g., Solomon et al. 1991; Smrekar et al. 2010). There are numerous examples of radiating extensional fracture systems on Venus (Grosfils and Head, 1994b) (Sect. 2.1.4), with at least 100 morphologically consistent with being associated with, and perhaps formed by, dyke emplacement (Ernst et al., 2001). Several of these (putative) radiating dyke swarms on Venus are associated with broad, domical swells comparable in size to mantle upwelling-induced uplifts on Earth (Grosfils and Head, 1994b).

3.3 Ridge Belts and Wrinkle Ridges

Where crustal shortening is spatially concentrated on Venus, such deformation is typically manifest as bands of structures interpreted as thrust faults and folds, and which have been termed “ridge belts” in the literature (e.g., Barsukov et al. 1986; Squyres et al., 1992, see Fig. 8). This term is not an established geologic one. Although it may be useful in certain circumstances, using more general terms such as “mountain ranges” may better align the study of Venus geology with the other terrestrial worlds (Klimczak et al., 2019). In any

Fig. 8 - Left-look Magellan SAR showing radar-bright wrinkle ridges trending \sim E-W with \sim 20 km spacing



case, these belts are by any measure orogenic, in that they represent the (local) convergence of crustal material. Generally appearing as broad, linear rises a few hundred metres in relief, tens of kilometres in width, and many hundreds of kilometres long (Squyres et al., 1992), these systems typically show multiple anastomosing secondary arches and ridges superposed on the larger rise that superficially resemble the “wrinkle ridge” anticlinal folds commonly observed elsewhere on Venus and on the Moon, Mars, and Mercury. Larger mountain ranges have long been recognized on Venus, and given their sizes are generally referred to as such (e.g., Barsukov et al. 1986). Those wrinkle ridges are typically tens to hundreds of kilometres long but only a few pixels across (corresponding to a width of a few hundred metres) when seen in Magellan data. Venus’s wrinkle ridges are likely thrust-fault-related folds, given their morphological similarity to such features on other planetary bodies, which individually denote low amounts of shortening strain. These structures are ubiquitous on the planet, deforming the two most dominant surface units (the so-called upper and lower “ridged plains”) mapped by Bilotti and Suppe (1999) and Ivanov and Head (2011).

3.4 Polygons and Distributed Deformation

In addition to wrinkle ridges, numerous other tectonic features occur in the plains, comprising polygonal fractures and small-scale fracture patterns (Fig. 9). Large fields of polygonal fractures with spacing ranging from a \sim 1–2 km (essentially the limit of resolution) up to 25 km have been identified in over 200 regions (Moreels and Smrekar, 2003). These features have been proposed to form as a result of cooling of lava flows, analogous to columnar fractures in basaltic lava flows, although extremely thick flows would be required for these Venus features (Johnson and Sandwell, 1992). In contrast, the largest columnar joint patterns on Earth are up to 30 m. For this reason, as well as their frequent association with volcanic features, Johnson and Sandwell (1994) favoured a model with thermal stresses from either cooling lava flows or heating at the base of the lithosphere. An alternative explanation is the propagation of climate-change driven cooling into the subsurface (e.g., Anderson

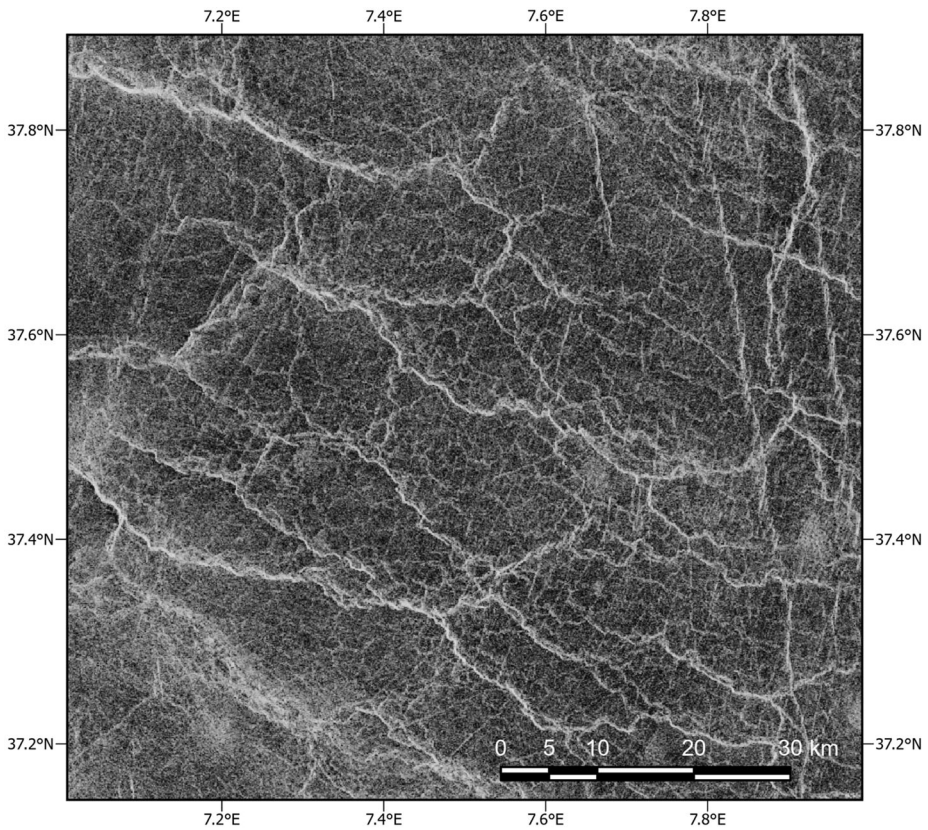


Fig. 9 - This section of FMAP 37N007 (Fig. 4 from Smrekar et al. 2002), shows two scales of polygons. The larger ones are controlled by intersections of NW-SE-trending wrinkle ridges

and Smrekar, 1999; Solomon et al., 1999; Smrekar et al. 2002). This hypothesis relies on huge volumes of volcanism, as predicted by the catastrophic resurfacing hypothesis, and associated outgassing as a driver for hundreds of degrees of climate change (Bullock and Grinspoon 1996; 2001). These two particular models differ in detail: Anderson and Smrekar (1999) used a continuous-plate model of deformation due to thermal stresses to assess the effect of large predicted positive and negative temperature changes, and found that thermal cooling stresses can predict the observed polygonal features, but that heating is insufficient to produce deformation. In contrast, Solomon et al. (1999) employed a broken-plate model, as had been used for mid-ocean ridge studies, and found that, in that configuration, heating can produce wrinkle ridges and cooling can produce polygonal fractures. The origin of these features may be tested by determining the minimum size of the polygons with higher-resolution imaging, and whether or not they occur as flows or other distinct topographic features using high resolution topography.

3.5 Subduction and Terrestrial-Style Plate Tectonics

Subduction is believed to be a necessary first step for plate tectonics (e.g., Whattam and Stern, 2015; Lithgow-Bertelloni and Richards, 1995). Since plate tectonics began long ago

on Earth (~4–1 Ga, still debated), neither the mechanism for initiation of subduction nor for plate tectonics is clearly identifiable. Thus, understanding the nature of subduction on Venus and the conditions that enable it to form would provide important insights into the initiation of terrestrial subduction. In addition to creating the slab-pull force that helps drive terrestrial plate tectonics, subduction plays a key role in recycling volatiles into the interior. These recycled volatiles can later be released back into the atmosphere, stabilizing Earth's climate. On Venus, subduction provides links to interior processes and contributes to heat loss (e.g., Gülcher et al. 2020, 2023), and a means to estimate local elastic and lithospheric thickness.

Numerous locations (e.g., Artemis Corona, Fig. 10) on Venus appear to exhibit 'rollback' subduction, a process in which a plate sinks into the mantle under some combination of surface loading and negative plate buoyancy, without requiring lateral plate motion. The plate 'rolls back' as the downward-flexed plate advances away from the original subduction location as the plate sinks further. By analogy with terrestrial subduction zones such as the arcuate trenches of the South Sandwich Islands, the Aleutian trench, and north Fiji Basin, McKenzie et al. (1992), Sandwell and Schubert (1992a, 1992b), and Schubert and Sandwell (1995) identified a dozen sites of possible subduction totalling 10,000 km in length. Their criteria included a deep, narrow trench with arcuate or linear planform (Fig. 10), a curvature $>10^{-7} \text{ m}^{-1}$ on the 'outer rise' side of the trench (the side attached to the subducting plate, e.g., on the southeast, outer side of Artemis), fractures parallel to the strike of the trench on both sides, and the absence of fractures cutting across the trenches. Hansen and Phillips (1993) presented an alternative interpretation of some of these features as resulting from mantle upwellings. This interpretation was based on the arcuate shape of many of these features, abundant volcanism in many locations, and fractures crossing the trench in one location.

Even with those examples of possible roll-back subduction associated with coronae, there is no evidence for a global network of tectonic plates diving into the planet's interior or being produced anew at spreading centres (e.g., Solomon et al. 1992). Harris and Bédard (2014, 2015) provided a general overview of strike-slip faulting on Venus. They argued for substantial lateral motions and indenter-like escape tectonics in Ishtar Terra, hypothesising that Lakshmi Planum collided with Ishtar Terra. These authors further suggested the presence of lateral displacements of hundreds to thousands of kilometres within shear zones in Ovda and Thetis Regiones. Harris and Bédard (2014, 2015) proposed that mantle flow tractions could have acted on the deep lithospheric keels of Lakshmi Planum and Ovda and Thetis Regiones, driving them across the planet in a manner akin to how large continental blocks move on Earth. Importantly, such motions produce the kinds of shortening and transpressional structures, and at the same approximate scales, as are recorded in the Archean rocks. If this hypothesis is correct, then the large-scale "drift" of major terranes on Venus may be a contemporary analogue of Archean Earth, when cratonic nuclei were mobile but modern plate tectonics, including subduction, had yet to take hold (Harris and Bédard 2014, 2015).

4 Crust, Lithosphere and Heat Flow

The surface geologic processes described above are a result of the interior heat loss mechanisms of convection and conduction. The crust, a compositional layer, and the lithosphere, a mechanical layer, strongly control the specific manifestation of these geologic processes. Models of both geologic processes and interior evolution require assumptions about crustal and lithospheric properties. In addition, viscous-deformation models require knowledge of

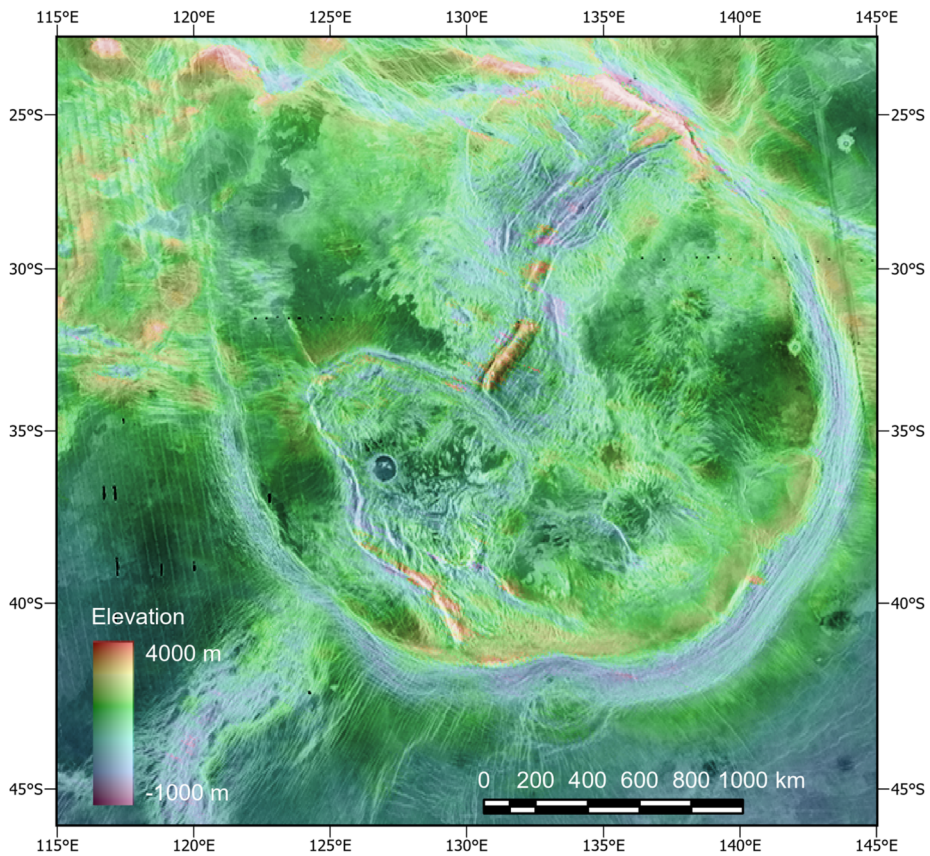


Fig. 10 - Magellan image data overlain on global topography of Artemis Corona. Artemis is the largest of all coronae, with a diameter of ~ 2600 km. Its southeast is a likely site of subduction. Relative topography is in m

strain rate since the material strength is a function of the rate at which stress is applied. Models of deformation require laboratory-derived relationships between stress and strain. Even for Earth studies, there are substantial open questions about how to apply these laboratory-derived rheological laws to geologic processes, with laboratory predictions, done at very high strain rates of necessity, apparently overpredicting the strength of rocks deforming at the lower but more geologically realistic strain rates. In this section, we describe the available data to constrain estimates of Venus' crustal and lithospheric rheology, and review what is inferred about the composition and thickness of the crust, the temperature and thickness of the lithosphere, and strain rates based on terrestrial analogy.

4.1 Crust and Upper Mantle

4.1.1 Crust and Surface Composition from Geochemical Constraints

The similar bulk densities of Venus and Earth imply that they have broadly similar elemental contents (e.g., Taylor and McLennan, 1995; Lee et al. 2009; Rubie et al., 2015; Weller and

Duncan 2015; Shellnutt 2016). However, the crusts of Venus and Earth could have quite different, and variable, compositions. In-situ data on crustal composition is limited to data from several Soviet landers in plains locations with instrumentation that measured elemental geochemistry (see Treiman 2007 for a review). Measured compositions in these locations were primarily mafic and likely basaltic (Surkov et al. 1984, 1986; Kargel et al. 1993). The rocks for which near-complete major elemental chemistry measurements were made are terrestrial equivalents of tholeiitic (Venera 14) and alkalic (Venera 13) basalt, whereas the Venera 8 rock could be similar (e.g., Kargel et al. 1993) or notably different, with anomalously high K, Th, and U concentrations similar to terrestrial granodiorite or dacite (e.g., Nikolayeva 1990). Trace elemental (K, Th, U) analyses at other landing sites (Vega 1, Venera 9, Venera 10) also indicated the presence of terrestrial basalt. On the basis of morphology, much of Venus is inferred to be covered in basaltic material, similar to the measured plains locations.

There is some evidence from flyby and orbital spectroscopy for felsic rock in the massive tessera plateaus (e.g., Hashimoto et al. 2008; Helbert et al., 2008; Mueller et al. 2008; Gilmore et al. 2015; Gilmore et al., 2023). A small suite of features such as ‘festoons’ also have morphologies arguably consistent with high viscosity silicious lavas (e.g., Pavri et al. 1992; Bridges 1997), but perhaps also with basaltic lavas (e.g., Stofan et al., 2000; Wroblewski et al. 2019). However, morphology is a poor indicator of composition and in no way a substitute for remote or in-situ chemical data. Thus, the degree and scale of crustal differentiation that has taken place on Venus is debated, with some arguing for less than Earth’s continents even in the tesserae and festoon flows (e.g., Kargel et al. 1993; Grimm and Hess, 1997; Treiman 2007; Treiman et al. 2016; Wroblewski et al., 2019).

Magma differentiation processes in terrestrial intraplate settings, thought to be the closest analogue for Venus tectonic settings (e.g., rifts, hotspots), are primarily related to crystallisation (i.e., equilibrium or fractional) and partial melting. In contrast, mixing or mingling is of secondary influence in comparison to convergent margin settings (Bachman and Bergantz, 2008; Christiansen and McCurry, 2008). Thus, forward petrological modelling using a range of magmatic conditions (i.e., water content, oxygen fugacity, and pressure), together with the rock compositions at the Venera 13 and Venera 14 landing sites and to a lesser extent the Vega 2 compositional measurements, can offer useful insight into the possible igneous rocks that could comprise a portion of the upper to middle crust. Fractional crystallisation modelling demonstrates that melt compositions similar to within-plate intermediate and silicic rocks (e.g., dacite, granodiorite, andesite, diorite, rhyolite, granite, trachyte, syenite), including the theoretical whole-rock composition of the Venera 8 landing site rocks and their K, Th, and U concentrations, can be produced at middle-to-upper crustal pressures (i.e., ~ 0.1 – 0.5 GPa) under reducing or oxidizing, and hydrous or anhydrous, conditions (Shellnutt 2013, 2018, 2019). The residual solid after fractionation is mostly composed of cumulus olivine, orthopyroxene, clinopyroxene, plagioclase, and Fe–Ti oxide minerals (i.e., titanomagnetite, ilmenite) and are analogous to the cumulate rocks of layered mafic–ultramafic intrusions of Earth, such as the Bushveld Complex, Stillwater Intrusion, and Skaergaard Intrusion. On Earth, rocks similar to the modelled residual silicic liquids and their mafic/ultramafic cumulate rocks are commonly found at intraplate settings associated with rifting and hotspot volcanism. Therefore, they are likely present within the crust of Venus as layered igneous complexes, and their silicic volcanic rocks may be associated with volcanic rises, coronae, pancake domes, and shield volcanoes. The lower viscosity of intraplate silicic volcanic rocks compared with convergent margin silicic volcanic rocks suggests that their volcanic edifices may not necessarily have meaningfully different morphologies from their mafic counterparts (Christiansen, 2005). As discussed above, volcanic morphology is *suggestive* of composition (e.g., Wroblewski et al. 2019), but not necessarily *definitively* so.

Partial melting of the mafic crust of Venus can also yield magmas with intermediate-to-silicic compositions under high pressure and temperature (~ 1 GPa, >1250 K) conditions expected for the lower crust of Venus (James et al. 2013; Shellnutt 2013). Of particular interest is the Venera 14 landing site, which could be very similar to basalts of terrestrial Archean greenstone belts. It is interesting because rocks of similar composition to those near Venera 14 can yield silicic liquids that are indistinguishable from the tonalite–trondhjemite–granodiorite (TTG) series of rocks found in Archean cratons (Shellnutt 2013, 2018; Johnson et al., 2017). The formation of some TTGs may be related to thickening of mafic crust and the subsequent partial melting of the lower parts of the thickened crust either by ambient geothermal conditions or by anomalously hot mantle plumes (Smithies, 2000; Moyen and Martin, 2012). Venus has regions of tectonically thickened crust and evidence for hotspot volcanism and high temperature, and low viscosity (perhaps ultramafic) lava flows (e.g., Lenardic et al., 1991; Komatsu and Baker 1994; Hansen et al., 1999) that may be experiencing similar processes. If TTG suites are generated on Venus, they might form within regions of thickened crust such as Ishtar Terra and Ovda Regio. Additionally, gravitational instabilities, in the form of rollback subduction, delamination, or lithospheric dripping (see Sect. 3.5. above), may occur on Venus. Such instabilities would lead to remelting of the crust, recycling of volatiles, and potentially to the production of more evolved lavas erupting at the surface, including even low-viscosity flows (Elkins-Tanton et al. 2007).

The basalt at the Venera 14 site is broadly similar to olivine tholeiite and possibly normal-mid-ocean ridge basalt (N-MORB) and thus may have originated from a mantle thermal regime similar to Earth (McKenzie et al., 1992; Kargel et al. 1993; Fegly Jr., 2003; Filiberto, 2014). The material measured at the Vega 2 landing site appears to be a mixture of soil or weathered material and rock, since the composition is broadly basaltic but the SO_3 content is extremely high ($\sim 4.7 \pm 1.5$ wt%). If those measurements were accurate, such rocks would not have a direct terrestrial equivalent, with the exception of a mixture of sulphate rock (e.g., gypsum, anhydrite) or sulphide ore with a mafic (basalt, gabbro) host rock that is typical of some basalt country rock relationships, layered intrusions, and/or volcanogenic mass-sulphide deposits (VMS). Sulphate rocks near Vega 2 might be related to the carbonate sulphate volcanism that was proposed to form the canali (e.g., Kargel et al. 1994).

4.1.2 Crustal Thickness and Upper Mantle Viscosity

Gravity and topography measurements are currently the only datasets available with which we can investigate the interior structure of Venus. Without more direct measurements, derivation of interior structure is inherently non-unique and subject to the assumptions made about such parameters as crust and mantle density, thermal gradient, and strain rate. A key challenge for Venus is the resolution of the measured gravity field, which ranges from ~ 400 to ~ 1000 km (Konopliv et al., 1999). The spherical harmonic field is expanded to degree and order 180 to prevent aliasing of the signal. The actual resolution of the field is represented by degree strength, which is a maximum of degree and order ~ 100 (Konopliv et al., 1999).

One approach to interpreting gravity and topography is to invert their spherical harmonics representation to provide an estimate of crustal thickness and upper-mantle viscosity and temperature (e.g., Banerdt, 1986; Herrick and Phillips, 1992; James et al. 2013). The correlations between thick/thin crust and hot/cold upper mantle with geologic surface features provides insight into the relationship between mantle convection and volcanism and tectonics. Different lithospheric properties and upper-mantle viscosity structures can be assumed in the inversions and the results then evaluated in terms of realism (e.g., are the temperature

anomalies consistent with expected mantle behaviour?). The relationship between gravity highs and lows and stress patterns has also been used to infer areas of present or recent activity (e.g. Smrekar, 1994). The long-wavelength geoid (the integral of the gravity field) can be interpreted as an anomalous density distribution that gives rise to lithospheric stresses (Sandwell et al., 1997).

Two-layer modelling with a low-order, pre-Magellan gravity field indicated that the mantle temperatures required to reproduce the observed gravity and topography become unrealistic if the viscosity structure includes an Earth-like asthenosphere (Herrick and Phillips, 1992). Other studies also suggested that Venus lacks a narrow, low-viscosity zone (e.g., Kiefer and Hager, 1991; Smrekar and Phillips 1991; Steinberger et al. 2010). However, different parameterizations (Pauer et al. 2006) and an approach of first removing large areas of thick crust (Maia et al. 2023) produced results that favor a ~ 200 km-thick zone below the lithosphere with a viscosity ~ 10 – 100 times lower than the mantle beneath, i.e., more akin to Earth's asthenosphere.

A low-viscosity asthenosphere on Venus may indicate that the interior of Venus is wet. Importantly, however, alternative explanations are possible. A low-viscosity zone can be produced by CO_2 rather than water (Sifré et al., 2014; Ghail 2015; Chantel et al., 2016) and by a specific dry olivine activation volume (Armann and Tackley 2012).

The associations between crustal thickness and inferred mantle convection with geologic features (e.g., James et al. 2013) clearly show that areas of thickened crust are associated with tessera plateaus, while significant mantle upwellings are associated with large volcanic rises (Fig. 11), some of which are connected by major rift systems.

The overall pattern of surface features relative to calculated mantle convection and crustal thickness can be used to make some inferences regarding the evolution of the interior over time. The correlation of the present gravity field with the global volcano–rift–corona pattern in many regions suggest that the large-scale mantle convection pattern has not changed dramatically during the time period over which these features were emplaced. The global wrinkle ridge pattern generally, but not everywhere, roughly parallels the geoid gradient, consistent with these features forming in response to current mantle patterns (Bilotti and Suppe, 1999; Sandwell et al., 1997). Laufey Regio, which hosts large volcanoes and concentric wrinkle ridges, appears to have formed in response to a mantle upwelling that has waned or become inactive (Brian et al. 2004). That there is no clear association of tessera plateaus with the inferred mantle convection pattern is consistent with most, but not necessarily all – Ishtar Terra is a notable exception, of these areas being inactive. While they may no longer be forming, high topography is likely to be gravitationally relaxing, depending on its crustal strength (e.g., Smrekar and Phillips, 1988; Nunes et al. 2004; Romeo and Turcotte 2008; Maia and Wieczorek, 2022; Nimmo and Mackwell 2023).

Most estimates of Venus' average crustal thickness are tens of km, with regional maxima up to ~ 70 – 90 km. Anderson and Smrekar (2006) and Jimenez-Daiz et al. (2015) both compiled global maps of crustal thickness using spectral admittance methods to solve for both local crustal and elastic thickness, without a contribution from mantle dynamics. Using somewhat different approaches, Anderson and Smrekar (2006) find an average crustal thickness on the order of ~ 10 – 20 km and Jimenez-Daiz et al. (2015) find ~ 20 – 25 km. James et al. (2013) employed a different method: analysing geoid to topography ratios and performing a two-layer layer inversion of crustal thicknesses and mantle forces to derive smoothed maps of global crustal thickness and dynamic mantle forces. They assumed a uniform elastic thickness of 20 km, which is reasonable (see the next subsection). They estimated a mean crustal thickness of ~ 8 – 25 km with the assumption that crustal thickness is non-zero everywhere and is limited by the transition of basalt to eclogite at ~ 60 – 70 km.

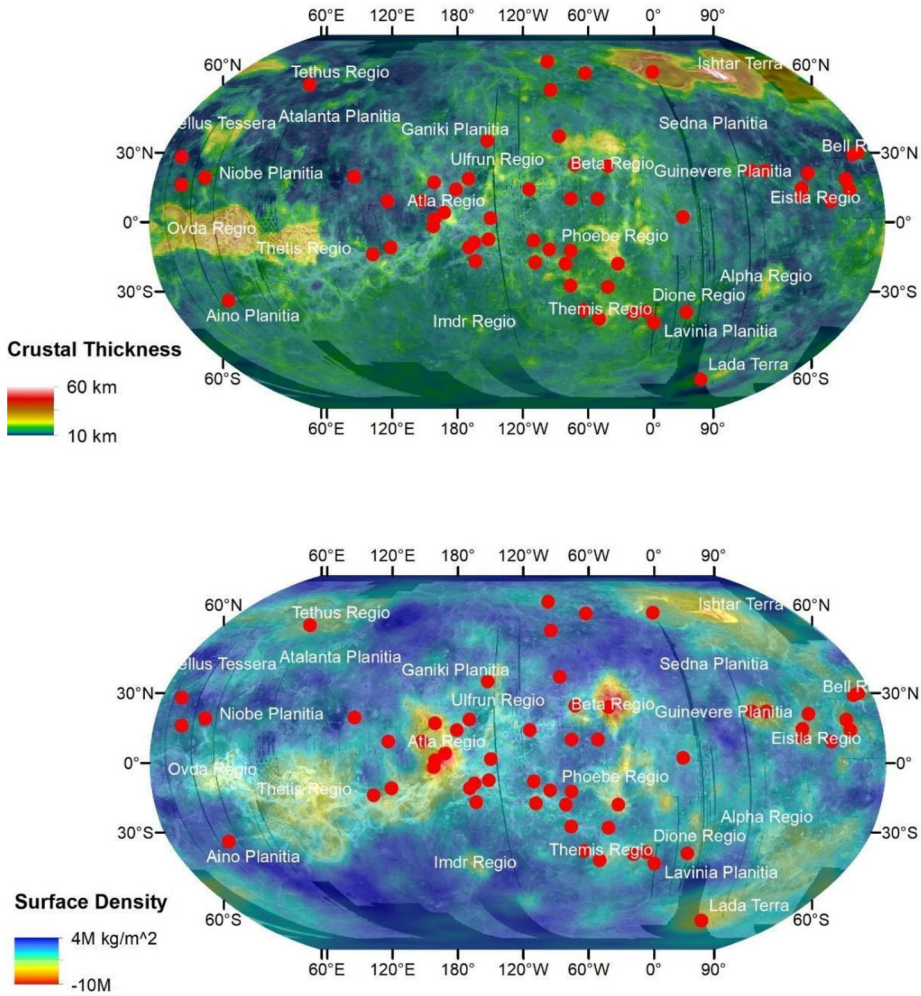


Fig. 11 Two-layer solution of James et al. (2013) superposed on Cycle 1 Magellan imaging of Venus. Top panel shows crustal thickness in km, and bottom panel density contrast in the uppermost mantle in kg m^{-2} . In the bottom panel, these Regios have been identified as hotspots: Imdr, Atla, Beta, Eistla (Western, Central, Eastern), Themis, Bell, Dione and Lada Terra (Stofan et al. 1995). Red dots show locations of large volcanoes in the database of Crumpler et al. (1997) with diameters >500 km. Among the many relationships between gravity, topography, and geology observable in these maps, large volcanoes are most often found in association with mantle upwellings or major rift zones and mostly avoid the areas of thickest crust, particularly tessera regions

Their calculated mean would increase to ~ 45 km if the Maxwell Montes formed tectonically in relatively recent times—meaning that they can be excluded from the assumption that crustal thickness cannot exceed ~ 70 km because of the basalt-eclogite phase transition has not reached completion, and/or the eclogite has not delaminated (e.g., Namiki and Solomon 1993; Jull and Arkani-Hamed, 1995).

Relatedly, convection models use gravity and topography to estimate a combination of crustal thickness and mantle properties (see Rolf et al. 2022, this collection, for more de-

tails). Such models typically focus on the longest-wavelength portion of the gravity spectrum, and tend to yield larger estimates of crustal thickness. Steinberger et al. (2010) found an average thickness of ~ 60 km using the range of the observed gravity spectrum that is likely dominated by crustal sources (i.e., above spherical harmonic degree 40). Wei et al. (2014) used models of Venus' mantle convection to include dynamical (mantle flow-sourced) contributions to derive a crustal thickness range of ~ 28 – 70 km, with the greatest values under highland regions such as Ishtar Terra and Aphrodite Terra.

4.2 Lithospheric Thickness and Heat Flow

A planet's lithosphere is the outermost part of the solid body. We can distinguish between three definitions of the lithosphere. First, the elastic lithosphere is the calculated thickness of a layer that is assumed to exhibit only elastic behavior. Second, the mechanical lithosphere represents a rheological layer that is too strong to convect even over long timescales. It encompasses the elastic lithosphere, and can additionally support loads via viscous deformation. Third, the thermal lithosphere contains the mechanical lithosphere and is defined as the layer in which heat is transported by thermal conduction, not convection. The thermal lithospheric thickness is usually defined by the depth to the mantle convection temperature, often taken as ~ 1575 K. In contrast, the crust and the uppermost mantle layers are defined by their composition. Composition implies a specific rheology, which has implications for the strength of the viscous portion of the mechanical lithosphere. The boundary between the crust and the uppermost mantle (or lithospheric mantle) may fall anywhere within these three layers, depending on parameters such as thermal gradient, strain rate, and rheology of the crust versus uppermost mantle.

The thermal lithosphere is essential to models of Venus's evolution. As the boundary layer, or 'lid,' of the convecting mantle, it couples the thermal state of the convecting interior to the surface. The heat transport across the thermal lithosphere limits the amount of heat leaving the mantle, determined by the thermal conductivity of mantle rocks, as well as the thickness and the temperature contrast across the lithosphere (i.e., Fourier's law). Both the temperature contrast and the thickness strongly depend on Venus' thermal history and its geodynamic regime (e.g., Rolf et al. 2022, this collection). The present thermal lithospheric thickness thus provides useful constraints on estimates of the thermal state of Venus' interior and how it may have evolved to this state.

Although convection models directly predict the thickness of the thermal lithosphere, it is the elastic lithospheric thickness that we can estimate more accurately. The wavelength at which the elastic lithosphere deforms in response to loads depends on its thickness. As discussed above, observations of gravity and topography thus yield quantitative estimates of the thickness of the elastic lithosphere. In idealized elastic models, lithospheric bending gives rise to internal stresses that increase linearly from zero at the mid-point of the elastic lithosphere and reach maximal values at its upper and lower boundaries. However, in reality, brittle failure and ductile flow limit the maximum possible stresses at the top and bottom of the mechanical lithosphere, respectively. Although the bottom of the mechanical lithosphere is viscous, it deforms only slowly and thus can also support surface topography or subsurface loads.

Specifically, the mechanical lithosphere encompasses both elastically and viscously strong parts, as defined by a yield-stress envelope. For a given rheological model of the lithosphere, the elastic thickness can be used to determine the mechanical thickness, which in turn is tied to the lithosphere's thermal state (e.g., McNutt 1984). The mechanical lithosphere is always thicker than the elastic lithosphere—but the total bending moments of both

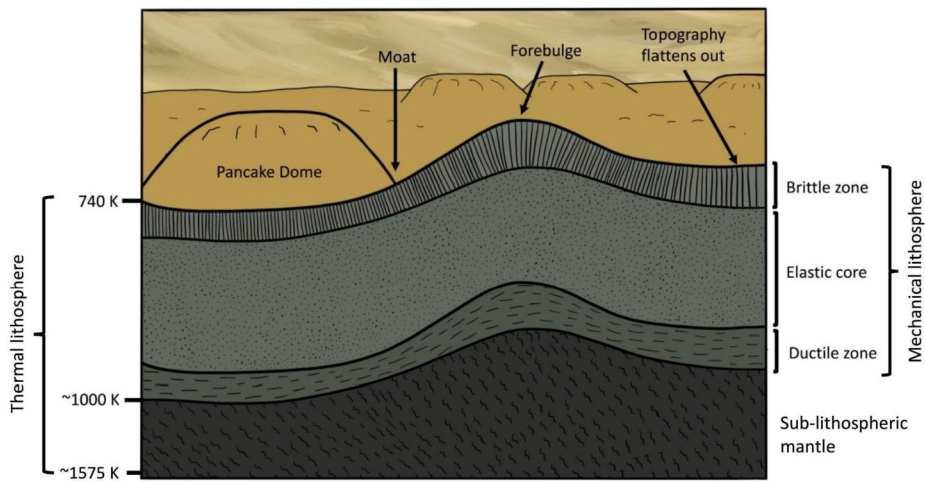


Fig. 12 - Volcanic features on Venus (here, a pancake dome) impose loads on the lithosphere. Even in the absence of gravity data, the topographic response of the lithosphere to these loads places constraints on models of lithospheric thickness. Rheological models enable conversions between inferred elastic and mechanical thicknesses—and then from mechanical thickness to the vertical thermal gradient and thus heat flow. Modified from Borrelli et al. (2021) with illustration by Joanna Wendel

(i.e., integrated over their yield strength envelopes) are equal. As shown in Fig. 12, the bottom of the mechanical lithosphere is associated with the temperature above which the ductile strength drops below a critical value (e.g., ~ 50 MPa). The corresponding critical temperature depends on the assumed rheology and strain rate but is typically ~ 1000 K for models with rheologies of dry olivine or diabase (e.g., Molnar, 2020). Stresses in the viscous layer can relax with time, such that the thickness of the mechanical layer can decrease with time. The thickness of the mechanical lithosphere can be used to estimate the thermal gradient due to the strong dependence of rock strength on temperature. Finally, the surface heat flow equals the product of the thermal gradient and the thermal conductivity of the lithosphere. Past papers have used a range of thermal conductivity values, from $\sim 2\text{--}4$ $\text{W m}^{-1} \text{K}^{-1}$ (e.g., Brown and Grimm 1996; Johnson and Sandwell 1994; Sandwell and Schubert 1992b; Solomon and Head 1982; Reese et al. 1998; O'Rourke and Smrekar 2018; Russell and Johnson 2021; Borrelli et al., 2021; Smrekar et al. 2023). Thus, comparing heat flow values from different studies requires normalizing them to a given thermal conductivity. In this paper, any reference to a heat flow value is normalized to a value of $3 \text{ W m}^{-1} \text{K}^{-1}$.

Strain rate is an essential parameter for calculating the thickness of the mechanical lithosphere and thus thermal gradient and heat flow. Similarly, strain rate directly influences calculated yield stress values used to approximate the complex deformation of the lithosphere in models of convective regime, as it determines whether an active or stagnant lid is predicted. At present there are no direct measurements of strain rates for Venus. Currently the only potential method of accurately constraining local strain rates under consideration for Venus is repeat-pass interferometry (RPI), which could measure active deformation on the timescale of years (Hensley et al., 2022). The strain rate for terrestrial intraplate deformation of $\sim 10^{-16} \text{ s}^{-1}$ is often applied to Venus as a best guess (e.g. Johnson and Sandwell 1994). However, numerous Earth studies have shown that, in actively deforming regions, and especially volcanically active regions, strain rates can be orders of magnitude higher (e.g., Fagereng and Biggs, 2019; Molnar, 2020) and these locally higher rates should also be

considered for the Venus lithosphere. The implication is that the strength of the lithosphere is likely higher during deformation than previously recognized. Ultimately, based on the effect of strain rate, lithospheric yield strength may be frequently underestimated.

Models of topographic profiles exhibiting flexural bending have been applied to deformation at a variety of features on Venus, including volcanic domes, coronae, and ridge belts. Interestingly, no flexural signatures have been found at larger volcanoes, possibly due to volcanic flooding of the moats (e.g., McGovern and Solomon, 1997). Most coronae have an elastic thickness of 20 km or less, with a handful of greater values mostly at larger coronae (Johnson and Sandwell 1994; Schubert and Sandwell 1995; O'Rourke and Smrekar 2018). Borrelli et al. (2021) examined topographic flexure at steep-sided volcanic domes (diameters of ~20–40 km). Topographic profiles at 20% of the ~60 domes on Venus show evidence of flexure, with most values of elastic thickness in the range from ~15–40 km. For some domes and small-scale features, topographic resolution may be a factor. McGovern et al. (2013) used magma-ascent models to predict that volcanoes may tend to form on thicker lithosphere than typical coronae. The lithospheric thicknesses estimated by Borrelli et al. (2021) generally support this hypothesis. Russell and Johnson (2021) estimated an elastic thickness of ~3–9 km for a small dome that sits on the fracture annulus of Aramaiti Corona. They advocated for the use of a lower Young's modulus and the resulting relatively low elastic thickness due to the presence of major fracturing in the annulus, as well as the best location of flexure per the location of fractures surrounding the dome. Borrelli et al. (2021) also noted that steep-sided domes in the vicinity of coronae tend to have lower elastic thickness than domes elsewhere.

Collectively, these studies found a wide range of heat flow values. The estimates of heat flow associated with coronae are typically $\sim >50\text{--}75\text{ mW m}^{-2}$, with a range of ~ 15 to $>200\text{ mW m}^{-2}$ (Johnson and Sandwell 1994; Schubert and Sandwell 1995; O'Rourke and Smrekar 2018; Smrekar et al. 2023). Steep-sided domes typically have a lower heat flow than common values for coronae (e.g., $\sim 50\text{ mW m}^{-2}$ for domes that are not near coronae; see Borrelli et al., 2021; Russell and Johnson, 2021), unless they are themselves near coronae. Additionally, most of the coronae identified as likely subduction zones (Schubert and Sandwell 1995) generally have greater elastic thicknesses and lower heat flows than average coronae values. Finally, the modelling of tectonic and impact features can also provide estimates of thermal gradient and heat flow. In a recent example, Bjonnes et al. (2021) simulated the multi-ring structure of Mead crater and found that the spacing of the ring faults can be explained by a thermal gradient of up to $\sim 14\text{ mK m}^{-1}$ (or a heat flow of $\sim 42\text{ mW m}^{-2}$, for a conductivity of $3\text{ W m}^{-1}\text{ K}^{-1}$), indicating a locally thick lithosphere at the time of formation. In contrast, models of tectonic deformation at other locations point to a very thin lithosphere and high heat flow (e.g., Smrekar and Solomon 1992; Raitala et al. 1995; Ruiz, 2007). As on Earth, the lithospheric thickness and heat flow are likely variable in time and space on Venus.

Elastic lithospheric thickness can also be estimated from the ratio of gravity and topography, or the admittance, due to the wavelength dependence of the deformation response. This method has been applied at numerous highland regions, typically returning estimates of elastic thickness of $\sim 20\text{--}30\text{ km}$ (e.g., Smrekar 1994; Simons et al., 1997)—hence the assumption of $\sim 20\text{ km}$ on average by James et al. (2013). Global admittance maps (Anderson and Smrekar 2006; Jiménez-Díaz et al. 2015) find a range of elastic thicknesses of $\sim 0\text{--}94\text{ km}$. Jiménez-Díaz et al. (2015) derive an average value of $\sim 30\text{--}40\text{ km}$, although this value is likely a bit high based on their approach of limiting the minimum value to 14 km.

Heat flow estimates are a strong constraint on the models of convective state and thermal evolution of a planetary body (see Rolf et al. 2022, this collection). Models of mantle con-

vection estimate thermal lithospheric thickness using geoid and topography data and magmatic activity as constraints (see Rolf et al. 2022, this collection). Using geoid–topography ratios, the average thermal lithospheric thickness may be 200 to 400 km, with reduced thickness below volcanic highlands (Moore & Schubert, 1997; Solomatov and Moresi, 1996). Larger average thicknesses of up to ~600 km may be feasible if geoid and topography can be explained by the thermal isostasy of a stagnant lid (Orth & Solomatov, 2011). The unknown temperature and viscosity of Venus' mantle allow for a very wide range of values from such models.

In contrast, a thinner thermal lithosphere of ~100–150 km is required to permit pressure-release melting at Venus hot spots (e.g., Smrekar & Parmentier 1996; Nimmo and McKenzie 1998), and to agree with estimates of heat flow (Smrekar et al. 2023). These estimates are compatible with mantle temperatures calculated from inferred compositions of basalts at the surface (e.g., Nimmo, 2002; Lee et al. 2009; Filiberto, 2014). Estimates of the mantle potential temperature (T_P) (i.e., the mantle adiabat projected up to the surface) have been derived based on data from Venera 13 ($T_P = 1732 \pm 73$ K) and Venera 14 ($T_P = 1603$ K, 1643 ± 70 K, 1732 ± 101 K)—within the range of ambient conditions of Earth (i.e., $T_P = 1623 \pm 50$ K). Of note, estimates based on measurements from Vega 2 ($T_P = 2051 \pm 167$ K) may be substantially higher but could be within the range of Earth's ambient mantle, too (e.g., McKenzie et al. 1992; Lee et al. 2009; Weller et al., 2015; Shellnutt 2016).

On Mars, where surface ages span several Gyr and flexural features can be dated back to the first ~1–3 Ga, it is possible to show a history of cooling with time based on increasing lithospheric thickness with the age of the terrain (e.g., McGovern et al., 2004). The inability to date individual areas on Venus means that different lithospheric thickness on Venus globally could reflect spatial or temporal variations. Given Venus' young surface age, the average lithospheric thickness may not have increased significantly over the last ~500–1000 Myr. The question remains as to whether the estimates of elastic thickness and heat flow reflect the present-day lithosphere or the time of lithospheric loading. In areas of thicker lithosphere, the loading signature from the time of loading may be 'frozen in' even if the lithosphere continues to cool and thicken with time. Smrekar et al. (2022b) argue that some regions with thin lithosphere and high heat flow, such as Parga Chasma, are likely to represent areas with high heat flow today. Even given some uncertainties, lithospheric thickness and heat flow can inform models of the present-day lithosphere and interior (e.g., Rolf et al. 2022, this collection).

5 Models for the Formation of Volcanic and Tectonic Features

Understanding the evolution of Venus and planets in general requires modelling of specific geologic processes to explore plausible conditions in the mantle (potential temperature, decompression melting including composition and volatile content, etc.) and the lithosphere (mechanical thickness, strength, thermal gradient, stress state, etc.). The key constraints described above form the recent or present conditions that evolutionary models should match. In this section, we discuss models of the origin of specific features and the conditions implied over the resurfacing age of Venus up to the present. We then use all these inputs to explore the hypothesis that conditions on Venus currently are much like those on early Earth. Rolf et al. 2022 (this collection) examines models of Venus' interior evolution, including the deep parts of the planet, across a billion-year timescale.

5.1 Formation of Volcanic Features

Despite their broad similarities, large volcanoes on Venus appear to have some differences in their formation relative to their Terrian and Martian counterparts (Fig. 1). Higher surface temperatures and pressures on Venus today yield smaller edifice heights than would otherwise be the case (e.g., Head and Wilson 1986; Bridges 1997; Head and Wilson 1992). Higher surface temperatures lead to smaller thermal gradients, shallower magma sources, hotter erupting lava, and therefore lava flows that spread farther laterally than on Earth (e.g., Flynn et al. 2023). The capacity of the thick, dense atmosphere to transport heat by radiation and convection also affects the spreading of lava flows (e.g., Snyder 2002; Flynn et al. 2023). The high surface pressure of Venus was also found to inhibit magma volatile exsolution, leading to fewer gas bubbles and thus potentially to less explosive volcanic eruptions than on Earth (e.g., Airey et al. 2015).

5.1.1 Plains Topography and Volcanism

Most of Venus' surface consists of volcanic plains. The plains are defined as regions of low elevation, low relief topography. As described above, there are a wide range of volcanic features in the plains. Studies to date have examined the formation of these plains via investigating the origin of the low lying topography as a possible result of thermal isostasy, and via numerical models that predict either global or regional volcanism. Globally, Venus' hypsometry is largely unimodal, lying within ± 1 km of the mean planetary radius (6051.8 km, although see Smrekar et al. 2018 for a discussion of elevations above 2 km). The hypsometry of the lowlands—and thus of the volcanic plains—is well-fit by a straight line (Rosenblatt et al., 1994), indicating that these regions are dominantly due to thermal isostasy. For an Earth-like mantle temperature, a thermal isostasy model applied to Venus gives a thermal lithospheric thickness of ~ 90 km. Means other than plate tectonic spreading centres can produce thermal isostasy (e.g., Morgan and Phillips 1983; Rosenblatt et al. 1994). For example, Morgan and Phillips (1983) showed that hot spot volcanism could produce the hypsometry of the plains. Ghail (2015) explained the plains topography as lithospheric rejuvenation—proposing that Venus may have a thin crust underlain by a localized asthenosphere activated by the presence of CO_2 in regions where the heat flow is relatively high, such as at mantle upwellings, plumes, or hot spots. Local topographic deviations from the global pattern of up to of several 100 m, such as those in Baltis Vallis, may be due to current convection-driven dynamic compensation of the topography (e.g. Conrad and Nimmo 2023).

Numerous geodynamic models predict widespread volcanism, or plains volcanism, and resurfacing, as discussed in detail in Rolf et al. 2022. These models predict volcanism and crustal thickness as a function of the lithospheric thickness, mantle temperature, and volatile content. We describe some example models here for completeness. In terms of explaining the occurrence of global plain volcanism on Venus, Parmentier and Hess (1992) and Head et al. (1994) presented a model linking the vertical accretion of a basaltic crust and the subsequent delamination linked to the emplacement of widespread volcanic plains. A 'catastrophic' tectonic resurfacing model initiated by delamination of negatively buoyant, depleted mantle was proposed to cause upwelling of warm, fertile mantle and pressure-release melting to produce extensive surface volcanism. Recent geodynamic modelling work by Adams et al. (2022) also focused on lithospheric delamination, in a 'peel-back' tectonic style, to be followed by the emplacement of hot, buoyant asthenosphere beneath the crust that may give rise to regional-scale volcanism. This style of resurfacing is proposed to occur on a more regional scale rather than a 'catastrophic' one.

Some geodynamic models focus on the role of mantle upwellings and decompression melting to understand the origins of plains volcanism. Reese et al. (2007) suggest that the lithosphere has thickened over the last 1 Ga, causing a decrease in melting consistent with the impact crater population and resurfacing history. Smrekar and Sotin (2012) focused on modeling the formation of mantle plumes capable of producing the hotspots. As discussed above, available thermal emissivity data from VIRTIS, as well as Magellan radar emissivity measurements, suggest that recent, large-scale volcanism is confined to hotspot/mantle plume settings. If this observation is borne out by future missions, it may turn out that tiny amounts of volatiles from the lower mantle are required to enable decompression melting in mantle plumes. Localized upwelling confined to the upper mantle may not be capable of crossing the solidus today due to desiccation of the upper mantle by prior, widespread melting (e.g., Smrekar and Sotin, 2012). This hypothesis is potentially consistent with the interpretation of Ar isotope data as indicating that Venus' interior volatiles are $\sim 25\%$ out-gassed (e.g., Kaula, 1999; O'Rourke and Korenga, 2015), if the upper mantle represents $\sim 25\%$ of the total mantle volume.

5.1.2 Lava Channels

Models of canali and sinuous rilles mainly focus on explaining their observed morphology, e.g., meander wavelengths, from Magellan radar images. Kargel et al. (1994) applied a scaling law, which describes the relationship between the meander wavelength and discharge at bank-full stage for streams on Earth, to estimate lava volumes required to form canali. These authors also calculated the duration of the lava flows from a simple estimate of how quickly canali meander could migrate, and found that a typical canale could form from $\sim 10^{13}$ to 10^{15} m³ of lava, which could cover up to $\sim 2.5 \times 10^6$ km² with ~ 500 -m thick flows. If the lava contained ~ 50 vol% carbonate minerals, the degassed CO₂ would have between 0.05% and 5% of the total mass of the present-day atmosphere. Perhaps older "generations" of canali once existed, contributing even more CO₂ to the atmosphere, but are not visible on the modern surface. Currently, Venus' atmosphere contains nearly as much carbon as exists in Earth's lithosphere and atmosphere (e.g., Lécuyer et al. 2000). However, studies have not yet fully elucidated how crustal or mantle differentiation on Venus could have produced huge volumes of carbonatite lava.

Few studies have attempted to estimate the depth profiles of lava channels on Venus because of the difficulty in making these estimates from the ~ 10 – 30 km horizontal footprint of Magellan altimetry data (Ford et al. 1993), which is substantially wider than the widths of most channels. However, post-Magellan studies have used radar clinometry at Baltis Vallis (Oshigami and Namiki, 2007) and six sinuous rilles and two valley networks (Oshigami et al. 2009) to obtain depth profiles that were resolved along the length of the channel.

One-dimensional models of channel formation by thermal erosion have been developed for application to Venus and other planets (e.g., Huppert and Sparks, 1985; Williams et al., 2001; Honda, 2005). Briefly, these models solve the heat balance for a lava flow to determine how far it can travel before solidifying given ground slope, the properties of the substrate, and lava composition, rheology, and thickness. For a certain type of lava, the thickness of the flow is adjusted to reproduce the observed length of the channel. The depth of the channel at the source is divided by the predicted vertical erosion rate to determine the effective duration of the lava flow. Oshigami et al. (2009) used this type of model to estimate that basaltic lava flows with initial thicknesses of ~ 2 – 6 m and durations of ~ 6 – 25 months could explain the lengths and depth profiles of six sinuous rilles, assuming present-day surface temperatures. The total lava volume associated with a typical sinuous rille on Venus is thus $\sim 10^{12}$ m³, ~ 1 – 3 orders of magnitude less than that suggested for a typical canale.

Existing modelling studies of lava channels on Venus have several limitations. First, they assume that Venus' surface temperature has remained constant, but it could have been higher or lower in the past. Second, models of sinuous rilles have not tested lava compositions other than Earth-like basalt. Third, no erosion models have been applied to canali. Since some proposed canali-forming lava compositions (e.g., carbonatite) have a lower melting temperature than the eroded substrate (i.e., basalt), mechanical erosion is likely more important than thermal erosion. Analogous models have been applied to the erosion of bedrock by water in attempts to calculate the discharge rates and volumes required to produce fluvial channels on Mars (e.g., Kleinhans 2005). Developing hybrid mechanical and thermal models of lava on Venus would be very useful for studies of channel formation. Measurements of the depth profiles of all channels, the grain sizes of the flow deposits and surrounding material, and any flow thicknesses via stratigraphy would provide key inputs to these models. Finally, any new information about the composition of surface material would help discriminate between models that feature different types of lavas and substrate materials.

5.1.3 Volcanic Rises

Volcanic rises are one of the few feature types for which there is an almost universally agreed formation mechanism: hotspots. The ten or so large volcanic rises on Venus are characterized by broad topographic swells, large positive gravity anomalies, and the presence of large volcanoes or coronae (e.g., McGill 1994), all of which are characteristic features of hotspots on Earth (see Sect. 2.1.2). Models of the interaction of plumes with the lithosphere seek to produce similar topographic uplift and gravity signatures (Kiefer and Hager, 1991) and decompression melting (Smrekar and Parmentier, 1996) consistent with the presence of large volcanoes. These studies indicate a thermal lithospheric thickness of 100 to 150 km and upwellings from the core–mantle boundary that are consistent with hotspot characteristics. Modelling the initiation of mantle plumes at the core–mantle boundary as well as the observed number of hotspots (e.g., Smrekar and Sotin, 2012) provides important information about mantle convective processes, as discussed in Rolf et al. 2022 (this collection).

As described in Sect. 3.2, more recent modelling work focuses on the lithosphere flexure associated with large volcano emplacement. McGovern and Solomon (1997) noted the lack of flexural induced moats and extensional faults around large (>100 km diameter) volcanoes on Venus. They then used flexural models to calculate the volumes of extrusive lava flows required to fill the expected (but not observed) flexural moat. McGovern and Solomon (1997) concluded that large volcanoes and the filled moat are one structurally coherent volcanic unit, unlike those on Earth and Mars that are partially filled by mass wasting or edifice collapse. The interaction of stresses—related to magma chamber growth and magma ascent, plus lithosphere flexure from the growing edifice—favour lateral subsurface flow as edifices grow, creating oblate magma chambers and promoting dyking (e.g., Galgana et al., 2011; McGovern and Solomon, 1998; McGovern et al. 2013, 2014).

5.1.4 Coronae and Novae

The wide range of corona characteristics (Sect. 2.1.3) have spawned numerous interpretations and models. Most of these modelling studies succeed in recreating at least some of the corona fracture annulus, topographic profiles, and/or gravity signatures, and point to a progression of topographic shapes over time.

Early work on corona formation focused on their generally circular shape, topography, and associated volcanism to conclude that some form of mantle upwelling must be involved

(Barsukov et al. 1986; Basilevsky 1986). A common proposition is that coronae form in response to stresses developed above an upwelling mantle plume or diapir, followed by gravitational relaxation or collapse due to magma withdrawal (e.g., Stofan et al. 1991, 1992; Janes et al. 1992; Squyres et al., 1992; Koch, 1994; Koch and Manga 1996; Grindrod and Hoogenboom, 2006; Gerya, 2014; Gülcher et al. 2020, 2023). Smrekar and Stofan (1997) introduced the first 2D numerical model incorporating plume-induced delamination, wherein lithospheric downwelling occurs at the edges of the laterally spreading plume head. These plume-induced delamination models were better at predicting the observed corona topographies than previous modelling, and placed the varying corona topographies into an evolutionary sequence (Smrekar and Stofan 1997; 1999). Some larger coronae may possess delamination or subduction, described below.

An additional class of models relies on volcanic construction to form coronae. Dombard et al. (2007) argued that partial melting above transient mantle plumes that impinge only on the base of the thermal lithosphere can cause magmatic loading of the crust above. Subsequent lateral crustal flow may cause surface deformation, producing the elevated rim surrounding an interior depression commonly observed at coronae, as first described in a simple model by Stofan et al. (1991). McGovern et al. (2013) suggested that the vertical loads exerted on the lithosphere by large volcanoes could influence magma ascent pathways from the mantle to the surface, which in the case of low elastic thickness may produce annular ridges of volcanic material at the surface, matching the topographic signatures of some coronae. Moreover, for higher values of elastic thickness ($\sim 10\text{--}40$ km), volcanoes are predicted to form instead of coronae. However, as discussed above, many larger coronae have elastic thickness of $\sim 20\text{--}40$ km.

The first study to use two-phase flow to model the pressure-release melting process at coronae shows that topographic rims can be produced by uplift above the buoyant melt concentrations (Schools and Smrekar 2024). This model also predicts high strain rate shearing that indicates the location of fracturing at rims. This model shows good agreement with a recent study of the shape of corona rim topography and the relationship to fracture locations (Sabbeth et al. 2024). This model creates rims at an early rather than late stage of evolution, suggesting an alternate evolutionary sequence to prior models.

The first 3D numerical study on corona formation involved thermal mantle plume impingement into warm and thin Venusian lithosphere (Gerya, 2014), assuming a thin elastic lithosphere (Anderson and Smrekar 2006). The results of this study suggest that plume-induced convection in a weak, ductile crust may be a plausible origin for some small-to-moderate sized (<200 km) coronae on Venus. This process may be analogous to those believed responsible for the formation of ancient terrestrial gneiss complexes (Campbell and Hill, 1988). Gerya (2014) noted that the first stage of uplift over a plume predicts radial fracturing, similar to ‘novae’ that are sometimes associated with coronae. Indeed, some prior studies did suggest that novae represent either an early stage or a “failed” corona (e.g., Janes and Squyres 1995; Stofan et al., 1997; Krassilnikov and Head 2003). Ernst et al. (2003) describe numerous radiating fracture patterns on Venus that they compare to dyke swarms on Earth. Gülcher et al. (2020) expanded on 3D numerical studies of plume-induced corona formation, defining different plume–lithosphere interaction scenarios possible at large coronae, such as lithospheric delamination, subduction (see Sect. 2.1.3), and an underplated plume, dependent on lithospheric and mantle plume properties. Gülcher et al. (2023) model lateral variations in crustal and/or lithospheric thicknesses to create asymmetric coronae with a prolonged tectonic and magmatic lifetime to develop, highlighting the importance of lateral variations in lithospheric properties for geodynamics on Venus.

Alternatively, models involving lithospheric downwelling with no associated mantle plume, such Rayleigh–Taylor instabilities, may also account for some of the topographic characteristics of coronae (e.g., Tackley and Stevenson, 1991; Grindrod and Hoogenboom, 2006; Hoogenboom and Houseman 2006). In these models, the nominal instability is caused by a dense mantle lithospheric layer over a less dense asthenosphere. A hybrid hypothesis involves the interaction between a mantle upwelling associated with large rifts and an adjacent downwelling instability, which may account for the spatial association of coronae with rift zones (Piskorz et al. 2014).

Since many different corona formation models can reproduce at least some of the key corona features, and both up- and downwelling of different sizes are common within the mantle convection regimes that may prevail within Venus (see Rolf et al. 2022, this collection), there may be multiple plausible formation scenarios for the diversity of observed coronae. Additionally, different corona morphologies may also represent different stages in their evolution. In particular, Gülcher et al. (2020) found that the topographic profile displayed by a corona may be completely isostatically inverted when an active plume interacting with the lithosphere cools down and fully crystallizes over time. These authors' analysis reveals that observed coronae on Venus may fall on a spectrum between early-stage (“active”) and late-stage (“inactive”) structures. However, different evolutionary sequences are possible (e.g., Schools and Smrekar 2024).

5.2 Formation of Tectonic Features

A key aspect of all modelling efforts to date is that subduction under Venusian conditions seems to be short-lived and, in contrast to modelling investigations under Earth-like conditions (e.g. Gerya et al. 2015; Baes et al., 2016), self-sustaining subduction zone does not develop on Venus. The exact conditions and behaviour of slab break-up is model- and condition dependent. For example, in the analogue models of Davaille et al. (2017), the slab separates into segments due to tearing caused by the brittle elasto–plastic behaviour of the lithosphere, while in the numerical models of Gülcher et al. (2020, 2023) the slab can coherently neck and detach, or tear into multiple segments that will caused directional slab retreat and detachment, based on the rheological parameters used. Moreover, the densification of slab material by eclogitization parameterized in the models seems to be a key factor in driving crustal recycling into the deeper mantle (Gülcher et al. 2023).

5.2.1 Rifts and Radiating Fracture Networks

Stoddard and Jurdy (2012) compared topographic profiles of selected rifts and hotspots on Earth and Venus. They calculated correlation coefficients between each topographic profile along a rift and the average of all profiles from that rift. These correlation coefficients were much higher for terrestrial rifts than Venusian rifts—the latter appeared most similar to terrestrial slow spreading rifts. Ghail (2015) found that the topographic profile across Venusian rifts are consistent with different rates of extension below a thermally-induced crustal detachment. Tectonic fractures characterize ‘slower’ rifts (e.g., Diana Chasma), while ‘faster’ rifts (e.g., Parga Chasma) host large numbers of coronae.

As discussed in Sect. 3.2, Venus possesses over 100 giant radial fracture systems, with an average radius of ~ 325 km and a maximum of >2000 km (e.g., Grosfils and Head 1994a, 1994b). Moreover, more such systems are likely to be found with future, higher-resolution radar imagery (Ernst et al. 2003). Early studies noted the similarity of the radial fractures to radial dyke swarms on Earth (McKenzie et al. 1992; Grosfils and Head 1994a, 1994b;

Ernst et al. 1995), although some modelled their formation as faults formed from dome uplift from a mantle upwelling (Stofan et al., 1991; Janes et al. 1992; Cyr and Melosh 1993), akin to novae formation. Conceptual and analytical models of the dyke formation mechanism (McKenzie et al. 1992; Grosfils and Head 1994a; Koenig and Pollard 1998) used terrestrial field and modelling work to estimate surface stresses and resultant strains on the Venus surface. Grindrod et al. (2005) found that the measured strain at four selected radial fracture centres is too large to be solely uplift related and must be primarily dyke driven, but concluded that the formation process is likely to be a combination of dyking and uplift. The numerical model of Galgana et al. (2013) accounted for both flexural stress from lithosphere uplift and the stress of magma chamber inflation. These authors found that edifice growth creates compressive stresses that eventually halt magma ascent and force existing, ascending dykes to grow laterally, thus becoming radial dykes. As previously discussed with corona models, it is probable that similar features such as radial corona fracture systems may have differing formation mechanisms dependent on emplacement conditions such as lithosphere thickness or strain from regional tectonics, and no single formati

5.2.2 Plume-Induced Subduction

The edges of some large coronae have been proposed to be sites of subduction (e.g., McKenzie et al. 1992; Sandwell and Schubert 1992b; 1995), with the concept of plume-induced subduction probably first described by Sandwell and Schubert (1992b) to explain coronae. Subsequent focus in the terrestrial community on understanding the initiation of subduction as the first step in developing plate tectonics led to a variety of models of plume-induced subduction (e.g., Ueda et al. 2008; Burov and Cloetingh 2010; Gerya et al. 2015). These models show how a long-lived, buoyant mantle plume can overcome the strength of and thus penetrate the lithosphere. The plume head then intrudes between the upper crust and dense mantle lithosphere, pushing the lithosphere downward into the asthenosphere, eventually initiating self-sustained subduction (Ueda et al. 2008; Stern and Gerya 2018).

Numerical explorations of this theory in 3D were undertaken to investigate subduction initiation by a thermal plume in the Archean on Earth (Gerya et al. 2015) and by a thermal-chemical plume on the modern Earth (Baes et al., 2016). Gerya et al. (2015) suggested that plume–lithosphere interactions on Archean Earth initiated subduction zones, which possibly led to the onset of plate tectonics. At a minimum, such complete breaks in the lithosphere are needed to allow individual plates to form. These workers proposed that a combination of three key physical factors is needed to trigger self-sustained, plume-induced subduction: a strong, negatively buoyant lithosphere, focused magmatic weakening leading to thinning of the lithosphere above the plume, and lubrication of the upper slab interface by hydrated crust (Gerya et al. 2015). The first and third factor may be (partially) absent on Venus (e.g. Huang et al. 2013). However, other means of weakening slab interfaces are possible in addition to hydrated crust, such as grain size reduction (Li and Gurnis 2023).

Gülcher et al. (2020) expanded on 3D numerical studies of plume-induced subduction, mapping out the dependency of different plume–lithosphere interaction scenarios on three key factors: plume buoyancy, lithospheric strength, and crustal thickness. Short-lived subduction episodes, leading to slab detachment, were identified in models that featured high plume buoyancy in combination with a low crust–mantle boundary temperature (by a relatively strong lithosphere through a colder lithosphere and/or a thin crust). For higher crust–mantle boundary temperatures (in that study found to be ~ 1100 K), lithospheric dripping developed instead of retreating slab segments. Follow-up work (Gülcher et al. 2023) on 3D plume-impingement upon laterally changing crustal thicknesses (i.e., lowland transitioning

into a plateau) confirmed the occurrence of a short-lived subduction arc on the lowland-side (thinned crust). Several key features of retreating subduction zones were reproduced in these 3D models, such as an outer rise surrounding a deep trench, a topographic feature observed at several Venusian coronae.

Theories of coronae formation involving plume-induced lithospheric subduction are supported by the successful reproduction of some of the tectonic features observed at several coronae margins in 3D analogue experiments (Davaille et al. 2017). They utilized analogue materials to represent the full range of structure and rheology for both the brittle lithosphere and convecting mantle, which is not achieved in numerical studies of corona formation. For example the lithosphere, which forms via drying of surface, has pervasive cracks that allow asymmetry to develop. In particular, this study is able to reproduce characteristic features observed at, for example, Artemis and Quetzalpetlal coronae, such as the arcuate outer rise surrounding a trench and rim. The outer rise of these coronae features extensional deformation, interpreted to result from bending of the subducting plate. Recent models of corona formation predict the locations of faulting where rims are flexed upward above buoyant partially molten regions at the base of the lithosphere (Schools and Smrekar 2024). In these models, topography surface faulting can be attributed to magmatic processes at depth due to plume evolution.

6 Is Venus the Archean Earth, Proterozoic Earth, or Something Completely Different?

Venus' apparent lack of modern Earth-like plate tectonics as well as its basaltic crust, mantle hotspots, and high surface temperature has led to tantalizing comparisons to Archean Earth (Morgan 1983; Hansen 2018; Harris and Bédard 2014). One challenge for assessing whether the Venus of today is a good representation of Earth of the past (i.e., Hadean and/or Archean) is that most of Earth's earliest history (i.e., 4.5–4.0 Ga) has been removed by plate tectonics, leaving primarily geochemical data from limited locations to piece together evidence of past processes. Similarly, very limited chemical data exist for Venus, and then only for a handful of locations. Venus and early Earth offer complementary, though very incomplete, views of the dominant processes on a pre-plate tectonic planet. Venus has been described as having vertical tectonics (Solomon and Head 1982; Phillips and Malin 1983; Morgan and Phillips 1983), dominated by mantle plumes. Similarly, Archean Earth was likely driven by vertical processes of mantle plume-initiated rifting and collision (Smithies et al., 2005a; Condie et al., 2016; Bédard 2018; Brown et al. 2020), and vertical return flow via lithospheric delamination (Johnson et al., 2014). As discussed below, this assumption is further supported by our understanding of Archean cratons and the known rock types and surface features of Venus (Hansen 2007, 2015, 2018; Harris and Bédard 2014, 2015).

6.1 Comparison with Archean Tectonic Systems

Little is known about the tectonic regime and development of the Archean (4.0–2.5 Ga) on Earth because the rock record is not widely exposed or preserved relative to younger terranes and cratons (Brown et al. 2020; Hawkesworth et al. 2020). There is debate on the timing of the initiation of plate tectonics and thus interpretations of a modern plate tectonic system cannot be robustly confirmed for the Archean (Condie and Kröner 2008; Stern 2008; Hamilton 2011, 1998). However, it is expected that the thermal regime under which the Archean crust developed had mantle potential temperatures (T_p) \sim 300–500 K higher than

ambient conditions today (1620 ± 50 K). There is almost no rock record for the Hadean (>4.0 Ga) as most of the information is inferred from detrital zircons, the Acasta gneiss, or isotopic model ages (Harrison 2009; O'Neil et al., 2012; Roth et al. 2014; O'Neil and Carlson, 2017; Reimink et al. 2020). Earth's Archean cratons are composed of two distinct belts or "terranes". One of these major terranes, the greenstone–granite belts, primarily record surficial rock sequences, whereas the other major terrane, the granulite–gneiss belts, record middle to lower crust metamorphic conditions (Condie 1981; Kröner 1985). Together, it is likely that greenstone–granite and granulite–gneiss belts represent a glimpse into the formation of primitive terrestrial crust or proto-continental crust (Smithies et al., 2005a; Thurston 2015; Bédard 2018).

Greenstone–granite belts are linear to curvilinear rock suites (i.e., ~ 10 – 25 km wide, ~ 100 – 300 km long, ~ 5 – 30 km thick). These dimensions are similar to those of the many tessera inliers distributed around Venus (e.g., Ivanov and Head, 2011). Terrestrial greenstone–granite belts have a characteristic stratigraphy of volcanic and volcanoclastic rocks, and sedimentary rocks accompanied by granitic rocks including tonalite–trondhjemite–granodiorite (TTG) suites (e.g., Condie 1981; Anhaeusser 2014; Thurston 2015). All greenstone belts are metamorphosed, but the degree (i.e., granulite, amphibolite, greenschist, prehnite–pumpellyite facies) and type (i.e. regional, contact, retrograde) of metamorphism are unique to each one. The volcanic suites are divided into an older subaqueous lower komatiite–tholeiitic basalt series and an upper, younger (by 3 to 30 Ma) bimodal sequence composed of tholeiitic basalt and calc-alkaline basalt, andesite, and rhyolite (Anhaeusser 2014; Thurston 2015). Greenstone belt formation and origin (i.e., a plate-tectonic origin or not) has yet to be resolved. However, they may be analogous to oceanic plateaus, volcanic arcs, ophiolites, or flood basalt suites that, at some level, may involve a mantle plume, particularly with respect to the eruption of the lower ultramafic–mafic volcanic series (de Wit and Ashwal, 1995; Smithies et al., 2005a; Bédard et al. 2003, 2013; Bédard 2006; Condie and Benn 2006; Anhaeusser 2014; Thurston 2015). The calc-alkaline nature of the upper silicic volcanic rocks is evidence that favours a volcanic arc-like origin, but similar rocks can be found in extensional tectonic settings since the calc-alkaline signature is a consequence of oxidizing magma conditions (Scott et al. 2002; Wyman et al. 2002; Arculus 2003; Smithies et al. 2005b; Bédard 2018). Modern (Cambrian to present) examples of greenstone-like belts exist and are associated with subduction and extensional tectonic settings but lack komatiitic rocks and banded-iron formations (Turner et al. 2014; Shellnutt and Dostal 2019).

At first glance, the topography of Venus resembles the continental and oceanic crustal dichotomy on Earth, in which tesserae are representative of 'continental' crust and the plains 'oceanic' crust (e.g. Smrekar et al. 2018). Near-infrared mapping spectrometer data suggest that, at least in one location, the plains and tesserae are compositionally different (Hashimoto et al. 2008; Mueller et al. 2008; Gilmore et al. 2015). Crustal thickness estimates indicate that plains are possibly ~ 10 – 20 km thick, whereas the tesserae may be ~ 65 km thick or more (see Sect. 3.1). These estimates are within the range of crustal thicknesses estimated for greenstone–granite belts and granulite–gneiss belts. The inferred compositional differences are consistent with the differences between terrestrial oceanic and continental crust. The major elemental composition of basalt measured at the Venera 14 landing site is very similar to olivine tholeiite of Archean greenstone belts, and the estimated primary melt compositions are ultramafic but not komatiitic (Shellnutt 2016, 2021). In comparison, the estimated composition of the rock at the Venera 8 landing site could be granodiorite/dacite and broadly resemble the calc-alkaline silicic rocks from the bimodal volcanic sequence of greenstone belts. However, uncertainty in its composition means that the Venera 8 rock could be lamprophyric (Nikolayeva 1990; Basilevsky et al. 1992; Kargel et al. 1993; Shellnutt 2019). Mantle

potential temperature estimates of Venusian basalts are variable: the rocks at the Venera 13 and Venera 14 sites are probably derived from a thermal regime similar to modern Earth, but estimates of the thermal regime for rocks at the Vega 2 landing site indicate an anomalously hot (2051 ± 167 K) regime (Lee et al. 2009; Weller and Duncan 2015; Shellnutt 2016).

There is debate on the precise composition of the tesserae, possible depositional processes, existence of a hydrosphere, formation of coronae, the mantle thermal regime, and the tectonic regime that was operating on ancient Venus. Recent studies indicate that the tesserae could be composed of mafic volcanic-sedimentary sequences rather than intermediate to silicic volcanic or plutonic rocks (Byrne et al. 2021). No *in situ* geochemical data exist for tesserae, and the high U (2.2 ± 0.7 ppm), Th (6.5 ± 2.2 ppm), and K₂O (4.0 ± 1.2 wt%) contents reported at the Venera 8 landing site could be indicative of a lamprophyre (alkali basalt) rather than a dacitic/syenitic rock (Basilevsky et al. 1992). It is possible that Venus had a hydrosphere during the Archean, but lithified sedimentary rocks (or their metamorphic equivalents) derived by mechanical weathering and chemical precipitation have not been verified (Florensky et al. 1977; Basilevsky et al. 1985). At present, the only evidence for the existence of sulphur-rich evaporites (e.g., gypsum, anhydrite) is the high SO₃ (4.7 ± 1.5 wt%) content measured at the Vega 2 landing site, but sulphates may form by weathering under current Venus conditions (Fegley and Prinn 1989; Fegley et al. 1997; Bullock and Grinspoon 2001; Dyar et al. 2021).

Earth's continental crust began to form during the Archean. One key reason why determining whether or not tesserae are true analogues of continents is that massive volumes of felsic crust require basaltic melt extraction from the mantle, ideally in the presence of water (e.g. Campbell 2002; Bonin 2012). Thus, tesserae may host the geochemical fingerprints of past water. This is a critical question not only for understanding the divergent evolution of Venus and Earth, but also for establishing Venus' potential habitability (Westall et al. 2023). Venus is the only other rocky body in the Solar System with a possible substantial volume of silicic crust (Shellnutt 2013; Wang et al. 2022). The formation and erosion of Earth's continental crust into the oceans is proposed to be the source of the elements needed for life to flourish (Duncan and Dasgupta 2017). In addition to the plume-induced subduction mechanism discussed above, some coronae types may form via delamination (Hoogenboom and Houseman 2006), possibly assisted by mantle flow due to extension (Piskorz et al. 2014). Moreover, Venus' large-scale ridge belts may be a result of compression above mantle downwelling (e.g. Zuber 1990). Thus, a variety of features on Venus may be indicative of crustal recycling and large-scale mantle melting.

Venus' high surface temperature creates a hot lithosphere and provides a thermal/mechanical analogue to conditions on early Earth. Davaille et al. (2017) argued that the apparent plume-induced subduction seen at features such as Artemis and Quetzelpetlatl Coronae are more likely to form under conditions of hot mantle and moderately thin lithosphere, as inferred for Venus today and Earth in the Archean. Hotter mantle temperatures allow for more buoyant plumes able to break a moderately strong lithosphere. The lithosphere cannot be too thin, or it will be too buoyant to subduct (e.g., Gülcher et al. 2020). Although many agree that subduction, which creates a complete break of the lithosphere, is the first step in plate tectonics, the evolution to mobile plates is not clear. Bercovici and Ricard (2014) suggested that the reason that Venus has developed subduction but has not yet developed Earth-like mobile plates is that breaks created by subduction are annealed over time due to the high temperatures, preventing the formation of large plates. This inference is consistent with the presence of many but moderately sized discrete blocks of lowland lithosphere, which appear to have jostled together since, at least in places, the emplacement of the locally youngest plains materials (Byrne et al. 2021).

When and how modern (oceanic) plate tectonics started on Earth is debated. There are advocates for plate tectonics having always operated and those that think it began at ~ 3.2 Ga, ~ 2.5 Ga, ~ 1.0 Ga, or ~ 0.8 Ga (e.g., Condie and Kröner 2008; Stern 2008; Hamilton 2011, 1998; Kusky et al. 2018; Windley et al., 2021). The precise origin of greenstone–granite and granulite–gneiss belts is still debated, and there are compelling arguments for and against the operation of plate tectonic-related processes in their development (de Wit and Ashwal, 1995; Anhaeusser 2014; Thurston 2015). Nevertheless, it appears that the generation of highly differentiated continental crust was either absent, very slow, or stunted on Venus. Currently, the continental crust represents $\sim 41\%$ of the surface area of the Earth and $\sim 0.7\%$ of its volume. It has taken ~ 4.5 Ga to create this volume of continental crust; however, although the rate of crustal growth throughout geologic time is uncertain (Honing and Spohn, 2016; Honing et al., 2019; Hawkesworth et al. 2019, 2020), we do know that this rate has not been constant. The three most common models for crustal growth are rapid development followed by steady-state; continuous growth; or episodic growth (Fig. 13). There are a number of uncertainties in these models, but perhaps the most important uncertainty is the timing of the initiation of modern plate tectonics (Honing and Spohn, 2016; Condie 2018; Windley et al. 2021). Assuming Venus is a close analogue of Earth and many fundamental planetary properties (e.g., thermal structure, abundances of heat-producing elements) are proportional to the size difference between the planets, then Venus' surface should have a similar area and volume of continental crust as Earth does today. Under the assumption that tesserae are similar to continental crust, then only $\sim 7.3\%$ of the surface area of Venus is continental crust (Ivanov and Head 2011; James et al. 2013)—that is, only 17% to 20% of the expected continental crust is present on Venus taking into consideration differences in crustal thickness estimates and that no crustal recycling occurred. According to different terrestrial crustal growth models (Fig. 13), Earth produced 17% to 20% of its current continental crust during one of three different time periods (Fig. 5): the Hadean to Eoarchean (~ 4.4 – 3.9 Ga); the Mesoarchean to Neoarchean (~ 3.1 – 2.7 Ga); or the Paleoproterozoic (~ 2.4 – 2.1 Ga). Thus, either the processes of crustal evolution on Venus have operated significantly more slowly than on Earth, or the development of continental crust was arrested relatively early. Alternatively, Ivanov and Head (1996) suggest that felsic crust could underlie as much as $\sim 55\%$ of Venus and that there may be only a surface veneer of basalt (~ 2 – 4 km thick). If this is the case, then Venus would have a larger surface area of continental crust than Earth.

Is Venus therefore analogous to Archean Earth? Possibly. However, our overall understanding of Venus' crustal evolution and overall geodynamics is in its infancy. A possible Venusian hydrosphere is currently only speculation. New geologic, geochemical, and isotopic surface measurements are required to thoroughly investigate the possibility that Venus can help us understand the nature and development of continental crust in the absence of modern plate tectonics, which may be, in turn, analogous to the Archean Earth.

6.2 Comparison with Proterozoic Tectonic Systems

By the end of the Archean, Earth was certainly developing its present-day dynamics. But there were also important tectonic, hydrospheric, atmospheric, and biological shifts that occurred during the Proterozoic that laid the foundation of Earth's present habitability. It is during the Archean–Proterozoic transition that the planetary evolution of Earth and Venus may have diverged. There are suggestions that by the Neoarchean (2.8 to 2.5 Ga), horizontal tectonic processes responsible for collision and accretion of island-arc-like terranes was becoming increasingly dominant (Zegers and van Keken, 2001; O'Neill et al. 2016; Windley et al., 2021). Once Earth transitioned into the Paleoproterozoic (2.5 to 1.6 Ga), some geologic

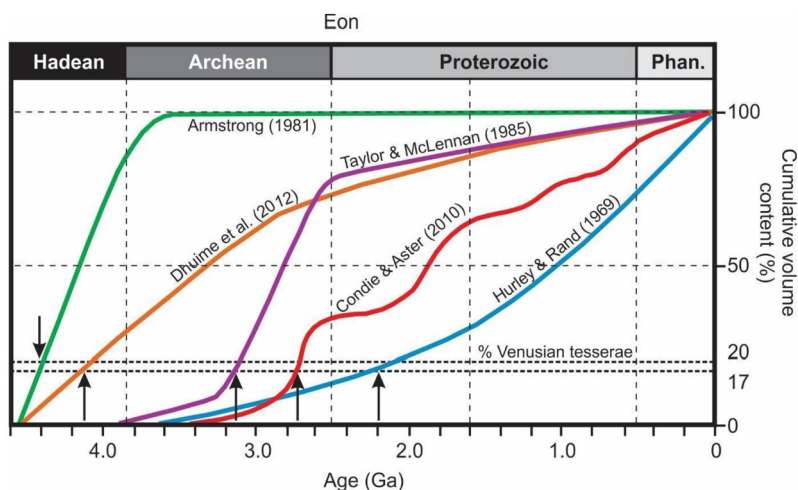


Fig. 13 - Terrestrial crustal growth curves showing the models that constrain the volume of crust in the Earth's past independent of present-day age distributions (modified from Cawood et al. 2013). The intersections (arrows) of the terrestrial crustal growth curves are shown at 17–20 vol.% crust to highlight the time periods when the amount of tesserae on Venus may have reached its present state if it evolved along the same path as Earth

features appeared (e.g., giant radiating mafic dyke swarms, anorthosite massifs, ophiolites) that were either rare or absent during the Archean.

A considerable proportion of the cratons that existed at the end of the Archean (~2.7–2.5 Ga) apparently amalgamated for the first time to form a supercontinent or multiple large continental blocks (Bleeker 2002; Pesonen et al., 2003). The emplacement of giant radiating mafic dyke swarms (e.g., Matachewan, Mistassini, Dharwar, Fort Frances, Kikkertavak, Black Range) and the possible existence of ophiolites at ~2.7–2.2 Ga indicates that a continent or continents broke up during the Early Paleoproterozoic (Cadman et al. 1993; Kusky et al. 2001; Ernst and Bleeker 2010; Sarma et al. 2020; Windley et al., 2021). Associated with these dykes are the correspondingly voluminous, and probably mantle plume-derived, flood basalt provinces that are collectively referred to as large igneous provinces (LIPs) (Ernst and Buchan 2001). The volcanic rocks of Paleoproterozoic LIPs are not commonly preserved due to erosion but their Neoproterozoic (~1.0–0.54 Ga old) and Phanerozoic (~0.54 Ga to present day) equivalents are better preserved. Archean giant radiating dyke swarms are rare. Their appearance during the latest Archean to earliest Paleoproterozoic marks a major shift in Earth's tectonic regime, becoming a common feature during the break-up of younger supercontinents (e.g., Rodinia, Pangea).

Complementary to the Paleoproterozoic dyke swarms and continental break-up events are well defined ophiolites that are within collisional and accretionary orogenic belts. The Purtuniqu, Jormua, and Kandra ophiolites demonstrate that oceanic crust was obducted at active continental margin settings at ~2.0–1.8 Ga (Scott et al. 1992; Peltonen and Kontinen 2004; Kumar et al. 2010). At ~1.9–1.8 Ga, a major global orogenic cycle occurred that is evidenced by the number of contemporaneous orogenic belts (e.g., Trans-Hudson, Thelon, Svecofennian), followed by post-collisional granites and anorthosite massifs were emplacement into the roots of the old orogens and another cycle of plate break-up, collisional/accretion orogens, and post-orogenic magmatism (Nance et al. 2014; Mitchell et al.

2021). The break-up and collision of cratons is indicative of the supercontinent cycle, which has become a defining characteristic of modern plate tectonics on Earth.

In comparison to Earth, the corresponding Proterozoic Eon of Venus was probably less geologically eventful. Per our current understanding, Venus appears not to have undergone the transition from a non-plate tectonic regime to a plate tectonic regime. Consequently, accretionary belts, island-arc terranes, ophiolites, and accretionary prisms are not expected to be found on Venus. Although collision-related mountains exist (e.g., Maxwell Montes) and underthrusting of crust probably occurred (Ansan and Vergely 1995; Davaille et al. 2017), the processes of proto-continental crust formation via the development of Earth-like subduction zones, their volcanic systems, and accretionary processes seemingly did not occur (Nimmo and McKenzie 1998). The converse of this is true as well: MORB-like oceanic crust did not develop either. From the Th/U ratios of Venusian basalt, it is likely that the overall internal heat budget generated by radioactive decay is the same as or similar to Earth (e.g., Steinberger et al. 2010; Armann and Tackley 2012; Taylor et al. 2018). Tonalite–trondhjemite–granodiorite suites, anorthosite, and post-collisional granite may be present within the crust of Venus as they do not require special geologic processes in order to form (Gilmore et al. 2015; Shellnutt and Manu Prasanth 2021; Wang et al. 2022). For example, anorthosite can be produced by crystallization and accumulation of plagioclase from a mafic parental magma, whereas post-collisional granite can develop after a period of compressive crustal stress. Since basalt and mountains generated by compressive stress are known to exist on Venus, it stands to reason that anorthosite and post-collisional granite could be present within the crust of Venus. Moreover, large, ore-bearing layered igneous complexes like the Bushveld intrusion or Great Dyke of Zimbabwe should be present as well, because they principally require large volumes of primitive mafic and ultramafic magma to differentiate. It is possible that some lobate or rounded smaller coronae of Venus are analogous to Bushveld-type complexes, but the Sudbury Igneous Complex-type intrusions may be unique to Earth since it was likely derived, in part, by bolide impact-induced melting (Therriault et al. 2002).

The major uncertainties in the Proterozoic evolution of Venus are the development of the atmosphere, hydrosphere, and biosphere. The current CO₂-rich atmosphere of Venus may or may not be primary, but it is likely that Venus lost a substantial amount of H₂ and without becoming O₂-rich like Earth (Donahue et al. 1997; Shaw 2008; Lammer et al. 2018). The evolution of Earth's atmosphere is directly related to the hydrosphere and biosphere, since the evolution of anaerobic cyanobacteria likely increased the amount of oxygen, whereas their subsequent demise due to the conversion of atmospheric CH₄ to CO₂ and H₂O may have assisted, along with lower solar luminosity, in the development of the Paleoproterozoic glaciations and reduced photosynthesis until after glacial retreat (Kopp et al. 2005). Could a similar process have occurred on Venus only for it to revert back to a CO₂-rich atmosphere? It depends on whether there was a hydrosphere and if life (i.e., cyanobacteria) evolved to the point where photosynthesis started to change the composition of the atmosphere. Venus may have lost a huge quantity of water during its early evolution, and surface water might have been stable until as recently as one billion years ago (Donahue et al. 1997; Way et al., 2016; Way and Del Genio, 2020). If Venus did indeed have a vibrant, Earth-like hydrosphere until ~1 Ga, then prokaryotic and possibly early eukaryotic life could have evolved. Furthermore, a hydrosphere would have permitted the chemical precipitation of limestone, banded-iron formations, primary and secondary sulphate rocks, and the formation of hydrothermal and hydro-magmatic mineral deposits (sulphate materials, along with Fe-oxides and Fe-sulfides, might also result from likely weathering of current surface rocks, see Gilmore et al, 2023, this collection). Nevertheless, if there was a global hydrosphere, Venus did not sustain a tropopause 'cold trap', allowing the hydrosphere to evaporate and generating a significant

volume of evaporites (i.e., carbonates, sulphates, halites). If all these events took place, how could the atmosphere become CO₂-rich again? The mostly likely explanation would be the devolatilization of carbonate and/or evaporite rocks due to contact metamorphism associated with magmatism (c.f., Aarnes et al. 2011; Pang et al. 2013). The possible implications of a Venusian hydrosphere are profound but purely speculative without evidence for chemically precipitated sedimentary rocks, glaciations, or hydro-magmatic mineral deposits. Although it is possible that Venus and Earth were similar during the Archean, they must have diverged by the Proterozoic. However, it is possible that life on both planets evolved in parallel until the loss of the Venusian hydrosphere.

7 Knowledge Gaps and Measurements Required to Fill Them

Venus is the least geologically understood of the terrestrial planetary bodies of the inner Solar System. Enormous knowledge gaps remain (Treiman 2007; Glaze et al., 2018). The thick, cloudy atmosphere of Venus is a formidable challenge to remote sensing of the surface, motivating the need for surface or near-surface measurements. New missions will greatly advance our understanding and lead to new questions about the evolution of Venus through time (Widemann et al. 2023, this collection, and references therein). Additionally, fundamental geophysical techniques of seismology, electromagnetic sounding, heat flow, and magnetometry have yet to be exploited for interrogating the interior.

7.1 Geochemistry

Venera landers provided in situ data at four sites, providing images, atmospheric composition, wind speed, temperature, and the composition of surface materials. Major elemental compositions were reported at three sites, and Th, U, K contents at two others, with the Vega 2 site providing the only measurements of both major and trace elemental compositions (Surkov et al. 1984, 1986; Kargel et al. 1993).

First-order geochemical measurements of the surface rocks and regolith are needed. Advances in X-ray fluorescence spectrometry, particle X-ray spectrometry, Mössbauer spectrometry, and sample preparation, as well as the development of laser-induced breakdown spectrometry (LIBS) and remote micro-imager (RMI) technology, permit smaller equipment to be included in surface landers (e.g., Gorevan et al. 2003; Treiman 2007; Clegg et al. 2009; Wiens et al. 2012). The measurement accuracy and precision of the various techniques would be a substantial improvement over the data reported from the Venera and Vega probes (c.f., Treiman 2007). The elements that can be measured range from major elements (Si, Ti, Al, Fe, Mg, Ca, Na, K, P) to many trace elements (Li, Sr, Rb, Mn). Depending on the rock type (ultramafic, mafic, felsic) additional elements (e.g., Ni, Cr, V) may be of a suitable concentration for measurements. The key problem with Venus is the harsh surface conditions (93 bars, 740 K), and any spectrometer would have to be properly prepared to overcome these extreme environmental conditions.

Of critical importance are the landing sites. The Venera and Vega probes landed at equatorial to tropical latitudes within 2 km of the mean planetary radius in eastern Aphrodite Terra and eastern to southeastern Beta Regio (Kargel et al. 1993). If possible, suitable landing sites should be considered across the various landscapes of Venus (in tesserae, coranae, and hotspots). The highland regions of Ishtar Terra, Aphrodite Terra, Beta Regio, and Lada Terra should be prioritized as likely preserving the oldest rocks and the greatest diversity of lithologies and compositions (e.g., Hashimoto et al. 2008; Gilmore et al. 2015,

2017; Treiman et al. 2016; Gilmore and Head 2018; Byrne et al. 2021; Resor et al. 2021). From the surface rocks and regolith, a number of important processes and geologic conditions can potentially be investigated, including crustal differentiation, magma crystallization and mineral chemistry, lava viscosity, eruptive temperature, formation of magmatic mineral deposits, mantle source composition, mantle redox conditions, mantle potential temperature, depositional environment, metamorphic facies (pressure, temperature, fO_2), stress and strain rates, as well as investigations of whether any evidence exists in support of ancient hydrological cycles, phreatomagmatic eruptions, hydro-magmatic and hydrothermal mineral deposits, water composition, paleoenvironment, and biosphere development. Clarity on any or all of these facets of Venus geology and geophysics would offer a huge advancement in our understanding of the interior properties and development of the planet.

Of equal importance to basic surface geochemistry, but technologically problematic to measure, is the isotopic systematics of Venusian rocks. Light and heavy stable isotopes (e.g., H, O, C, S, Fe, Zn, Mo) and radiogenic isotopes (e.g., Sr, Nd, Pb, Hf, Os) are invaluable for addressing the interior and surficial development of a planetary body. The stable isotopes offer insight into mass-dependent fractionation, primarily of atmosphere–lithosphere interactions that involve the hydrosphere, biosphere, mantle volatile budget, and climate, and can also be useful for assessing mantle evolution and mineral deposits (e.g., Hoefs 2009). The radiogenic isotopes of Venusian rocks offer insight to planetary accretion, interior differentiation of the core, mantle, and crust, and secular mantle and crust evolution (e.g., Faure 2001). Most of the isotopic systems require the application of relatively intense laboratory preparation prior to measurement and would not be practical for a surface lander. The return of surface samples or the identification of Venusian rocks in the meteorite collection are currently the only viable means to measure some or all of the stable and radiogenic isotopic systems. However, there are breakthroughs in the measurement of some radiogenic isotopes by in situ laser (~20–50 mm beam size) ablation methods (Bolea-Fernandez et al. 2016; Spencer et al. 2020). Sr and Hf isotopes can be measured with a suitable degree of accuracy by in situ methods with minimal sample preparation but rely on the presence of Rb–Sr- and Lu–Hf-rich silicate minerals such as feldspar ($KAlSi_3O_8$ – $NaAlSi_3O_8$ – $CaAl_2Si_2O_8$) and zircon ($ZrSiO_4$). If the in-situ measurement of Sr ($^{87}Sr/^{86}Sr$) and Hf ($^{176}Hf/^{177}Hf$, $^{176}Lu/^{177}Hf$) isotopic ratios can be achieved by a lander, such measurements would provide a major advance in the understanding of planetary accretion and internal differentiation of Venus.

Perhaps the most ambitious and desirable measurement that can be achieved is radioisotopic geochronology of rocks and minerals from the surface (e.g., Coleman et al. 2012; Cohen et al., 2019). Crater retention and distribution, and relative geologic relationships, are the only methods for estimating the average surface age (<1 Ga) and general stratigraphy (e.g., Strom et al. 1994; Ivanov and Head 2015), in which, for example, tesserae are usually regarded as older than the plains (e.g., Basilevsky and Head, 2002; Gilmore and Head 2018). However, radiometric dating is the only method that can return a measure of the absolute age of a rock. Over the past twenty years, in situ geochronology has exploded in the geologic literature and, on Earth, is a common, reliable, affordable, and low-intensity sample preparation method of choice (Spencer et al., 2016). Under ideal circumstances, a rock sample from Venus would be necessary for mineral separation and measurement but, it may be feasible to measure the isotopic ratios directly with minimal sample preparation by in situ methods. Specifically, U–Pb dating of zircon, a common accessory mineral of granitic rocks, can provide a robust measurement of the $^{207}Pb/^{206}Pb$, $^{207}Pb/^{235}U$, and $^{206}Pb/^{238}U$ ratios with an uncertainty in the range ~2–4% (Spencer et al., 2016). Another possibility is the application of the Rb/Sr isochron method on minerals (e.g., feldspar, biotite, amphibole, pyroxene) using the measured $^{87}Sr/^{86}Sr$ ratio and Rb and Sr concentrations to estimate the $^{87}Rb/^{86}Sr$

ratio (Coleman et al. 2012; Bolea-Fernandez et al. 2016). Although the uncertainty of the Rb/Sr isochron method makes it less reliable, it would be useful (i.e., better than ± 100 Ma) and in situ Rb/Sr geochronology may be more practical because the potential target minerals are common in mafic to silicic rocks. Regardless, the first step in the application of in situ geochronology methods would be the positive identification of differentiated igneous rocks (i.e., intermediate to silicic) by surface geochemical remote sensing.

7.2 Seismology

A better knowledge of Venus' seismicity would majorly improve our understanding of rock rheology, deformation mechanisms, and Venus geotherms, as well as help us constrain estimates of crustal thickness, mantle viscosity, and core properties. As described above, Venus' young surface has a wide range of volcanic and tectonic features capable of producing substantial seismicity. The spatial distribution of seismic events related to tectonic features, like faults and volcanoes, is much more homogeneous on Venus than on other planets, due in part to the extremely limited erosion. Seismicity estimates have assumed an intraplate level of seismic activity because Venus lacks Earth-like plate tectonics. As expected, this approach leads to a lower predicted rate of activity than on Earth (e.g., Stofan et al., 1993; Stevenson et al. 2015). Sources of uncertainty come from the limited constraints on heat flow and rock rheology discussed above. Lognonné and Johnson (2007) predicted >100 quakes >Mw5 per year, with a maximum seismic moment magnitude of ~ 6.5 based on analogy to terrestrial intraplate activity. This low maximum quake magnitude calculation assumed a thickness of the seismogenic layer to be 30 km. Knapmeyer et al. (2006) estimated seismicity on Mars based on extensive (albeit hillshade-based) mapping of surface faults and their conversion into quake magnitudes. This approach, which has large error bars, predicts a range of seismicity consistent with seismic data from the InSight mission (Giardini et al. 2020). Sabbeth et al. (2023) applied a similar approach to a specific fault type on Venus, predicting an order of magnitude higher level of seismicity at Venus than InSight measured in Cerberus Fossae on Mars. This estimate was based on fault lengths. Future high-resolution topography would allow fault throw to be measured as well, providing greater fidelity to this approach. Seismic sources due to meteoroid impacts are likely to be rare because the thick atmosphere destroys impactors that produce craters less than a few kilometres in diameter (e.g., Zahnle 1992; Korycansky and Zahnle 2005). Airbursts due to impactor disruption and breakup in the thick Venus atmosphere could help provoke a seismic signal, although an impactor large enough to airburst in the lower atmosphere is statistically unlikely to hit Venus in the next several decades (e.g., McKinnon et al. 1997).

Although long duration, in-situ seismic measurements would be ideal, Venus' surface temperature motivates a range of possible methods, including orbital searches for atmospheric airglow or balloon-born infrasound measurements (Stevenson et al. 2015). If present, aerial platforms could detect infrasound from explosive volcanism (e.g., Brissaud et al. 2021; Garcia et al. 2022; Rossi et al. 2023). Pyroclastic flows, likely from explosive volcanism (e.g., Ganesh et al. 2021), appear to be rare but indicate that such eruptions have occurred on Venus (e.g., Campbell et al. 2017; Ganesh et al. 2022). See also a review of future seismic investigations and concepts in Widemann et al. 2023, Sect. 10 (This collection).

7.3 Electromagnetic Sounding

Future missions could use electromagnetic (EM) sounding to probe properties of the lithosphere that influence volcanic and tectonic processes. Grimm et al. (2012) proposed exploiting Schumann resonances at ~ 10 – 40 Hz to determine the depth profiles of conductivity and

temperature within the lithosphere. If the lithosphere is dry as expected, then EM sounding could probe depths of hundreds of kilometres on Venus. If the lithosphere is wet (i.e., with hundreds of ppm H₂O), then sounding would be limited to depths of <20 km—but the discovery of a wet lithosphere would be a major result by itself. Speculatively, EM sounding could also search for molten salt aquifers as proposed by Kargel et al. (1994). An aerial platform could perform EM sounding with instruments such as magnetometers and electrometers at ~55-km altitudes in the clouds (e.g., Wilson et al. 2012; Cutts et al. 2022). However, no previous mission has confirmed the presence of Schumann resonances.

On Earth, frequent lightning discharges (tens each second) dump so much EM energy below the ionosphere that Schumann resonances exist always around the globe (e.g., Grimm et al. 2012). Observations of whistler waves from Venus Express and Pioneer Venus Orbiter have been claimed to reveal that lightning happens on Venus several times more often than on Earth (e.g., Hart et al. 2022). However, these whistlers might have a non-lightning origin (George et al. 2023). Recently, the Parker Solar Probe mission observed whistlers at Venus during a gravity assist and measured their direction of propagation for the first time. Whereas lightning-generated whistlers would propagate outwards from the atmosphere, the observed whistlers travelled towards Venus from its nightside magnetotail (George et al. 2023). Multiple processes can produce whistlers at Venus, but no existing measurement provides proof of lightning. Long-duration observations from an orbiter would provide much better statistical constraints on the rate of lightning-derived whistlers.

Lightning could be absent or extremely rare on Venus (see also Lorenz 2018 for a comprehensive review). The Akatsuki mission (Lorenz et al. 2019; Takahashi et al. 2020) and earlier ground-based observations (Hansell et al., 1995) have identified <10 optical flashes total that are potentially attributable to lightning, yielding a rate of only a few flashes per hour on all of Venus—less than 10⁻⁵ times the rate of cloud-based lightning on Earth. Other processes may have produced some or all of these flashes, including meteors (e.g., Blaske et al. 2023) and instrument artifacts (Lorenz et al. 2018), meaning that the rate of cloud-level lightning on Venus could be (nearly) zero. In principle, explosive volcanism and/or aeolian processes on the surface could generate lightning, albeit likely not at high rates (e.g., Lorenz et al. 2018). Unlike lightning in the clouds, near-surface lightning probably would create EM signals but not optical flashes detectable via remote observation. Ultimately, our ignorance about the EM environment below the ionosphere is profound and coupled to our struggles to understand and explore volcanism on Venus generally.

7.4 Magnetometry

Crustal remanent magnetism has revealed the history of volcanism and tectonics on other terrestrial planets. Most notably, scientists found “smoking gun” evidence for plate tectonics in the 1950s in the form of “stripes” of magnetized crust painted with alternating polarities outwards from spreading centres in the seafloor. As described in the introductory article of this collection (O’Rourke et al. 2023, this collection), no mission has so far discovered any crustal remanent magnetism on Venus. However, the detection limits are so weak that huge amounts of magnetized crust could await detection (O’Rourke et al. 2019)—for example, equivalent to the magnetic anomalies detected in the crusts of Mercury, Mars, Earth, and the Moon. As with EM sounding, we cannot promise to use crustal magnetometry to study volcanism and tectonics at Venus. Perhaps Venus never had a strong, global magnetic field that would enable lava or magma to acquire remnant magnetization. Maybe surface temperatures were higher in the recent past (e.g., Bullock and Grinspoon 2001; Warren and Kite 2023), which would have demagnetized any magnetized rocks in the crust. Again, as for

EM sounding, an aerial platform could characterize the magnetic environment below the ionosphere of Venus for the first time—and determine if measurements that are so powerful on Earth and other planets are applicable to Venus.

7.5 In Situ Heat Flow

Heat-flow data would provide valuable new information on local thermal gradients and, coupled with crustal thickness and thermal evolution models, the abundance and distribution of radiogenic elements. Heat flow is also a key discriminator between different modes of mantle convection (see Rolf et al. 2022, this collection). One approach is to measure the heat coming out of the interior with a flux plate (e.g., Kremic et al. 2020). However, scientists have inferred small (~ 1 K) diurnal surface temperature variations from remote observations of thermal emission (e.g., Mueller et al. 2008) and global climate models (e.g., Lebonnois et al. 2018). Such small changes in surface temperature could be problematic for the flux plate approach, but these estimates could change after future measurements of surface brightness temperature, acquired from orbit. Analyses could compensate for the effects of these variations if a long enough baseline of surface temperature could be made (i.e., over multiple Venus days). Alternatively, subsurface drilling could deploy a more traditional heat flow probe (Widemann et al. 2023, this collection, and references therein). As for surface seismology, the engineering challenge of drilling is considerable. Given the high scientific value of heat flow measurements to understanding the planet's interior evolution, new technologies to enable this kind of science investigation are important to develop.

8 Conclusion

In this article, we have explored how Venus' tectonic and volcanic processes provide essential insights on Venus' evolution, as any rocky body's crustal layer provides a complex archive for the planet's long term evolution. A primary constraint on the interpretation of geologic processes on another planet is the size and spatial distribution of impact craters, the study of tectonic processes that removed older terrains, which remains controversial. Our understanding of current processes and surface structures effectively provides boundary conditions for extrapolating back into Venus' geologic and convective history: the size, type and distribution of volcanic features provide a window into interior processes such as upwelling/downwelling, melting and mantle temperature. We have introduced the fact that a completely stagnant lid does not provide sufficient heat loss, leading to the idea that Venus has either cycled between a stagnant lid and past plate tectonic regimes, or has undergone regional equilibrium resurfacing: these different interpretations address the fundamental role that both the mean surface age and local variability play in framing the long-term geologic evolution of Venus, and in interpreting interior properties.

Tectonic features provide separate constraints on the rheology, thickness of the lithosphere, and the origin and magnitude of driving stress fields. Gravity data provide further information on the thickness of the crust, the lithosphere, and subsurface density variations due to processes such as mantle upwellings. The goal of this review work has been not to provide a single view, but rather to represent a range of possible interpretations, the constraints available from current data, and to outline specific needs for future datasets. Global mapping of the tessera terrain shows that most tessera margins are embayed by plains, thus establishing the tessera as the oldest materials in a proposed global stratigraphic column. Their composition has not yet been measured directly, but that of some tessera exposures

can be inferred from both NIR and radar observations. The generation of such large amounts of felsic melt could require both water and a lithospheric recycling mechanism for formation, and thus possibly must have formed during a more habitable era, assuming the tesserae are igneous in origin.

Volcanic and tectonic constraints on the evolution of Venus are therefore particularly important to our understanding of terrestrial planets' habitability, providing a natural laboratory to understand its evolution in time. A renaissance in Venus exploration is underway with ESA's EnVision orbiter mission, NASA's VERITAS orbiter and the DAVINCI in-situ probe missions all going to Venus by the early 2030s. VERITAS's payload is composed of two instruments crafted to study Venus' surface coupled with a radio science investigation to measure the gravity field. The two instruments are an X-band interferometric synthetic aperture radar, VISAR, and a fourteen-band infrared spectrometer, VEM (Smrekar et al., 2022a). DAVINCI's Venus Descent Imager (VenDI), a near-IR descent-imaging system will deliver clear, high contrast, high SNR images, providing the first geologic constraints on the tesserae surface environment at 2–200 m length scales (Garvin et al., 2022). EnVision's suite of investigations will perform targeted surface imaging as well as polarimetric and stereo imaging, radiometry, and altimetry, a subsurface radar that will sound the upper crust in search of material boundaries, and a suite three spectrometers operating in the UV and Near- and Short Wave-IR (Widemann et al. 2023, this collection). Together, the three missions will fundamentally improve our understanding of the planet's long term history, current activity and evolutionary path.

Declarations

Competing Interests The authors have no competing interests to declare that are relevant to the content of this article and no funding was received to assist with the preparation of this manuscript.

Open Access This article is licensed under a Creative Commons Attribution 4.0 International License, which permits use, sharing, adaptation, distribution and reproduction in any medium or format, as long as you give appropriate credit to the original author(s) and the source, provide a link to the Creative Commons licence, and indicate if changes were made. The images or other third party material in this article are included in the article's Creative Commons licence, unless indicated otherwise in a credit line to the material. If material is not included in the article's Creative Commons licence and your intended use is not permitted by statutory regulation or exceeds the permitted use, you will need to obtain permission directly from the copyright holder. To view a copy of this licence, visit <http://creativecommons.org/licenses/by/4.0/>.

References

- Aarnes I, Fristad F, Planke S, Svensen H (2011) The impact of host-rock composition on devolatilization of sedimentary rocks during contact metamorphism around mafic sheet intrusions. *Geochem Geophys Geosyst* 12:Q10019. <https://doi.org/10.1029/2011GC003636>
- Adams AC, Stegman DR, Smrekar SE, Tackley PJ (2022) Regional-scale lithospheric recycling on Venus via peel-back delamination. *J Geophys Res, Planets* 127:e2022JE007460. <https://doi.org/10.1029/2022JE007460>
- Addington EA (2001) A stratigraphic study of small volcano clusters on Venus. *Icarus* 149(1):16–36. <https://doi.org/10.1006/icar.2000.6529>
- Airey MW, Mather TA, Pyle DM, Glaze LS, Ghail RC, Wilson CF (2015) Explosive volcanic activity on Venus: the roles of volatile contribution, degassing, and external environment. *Planet Space Sci* 113–114:33–48. <https://doi.org/10.1016/j.pss.2015.01.009>
- Aittola M, Kostama VP (2002) Chronology of the formation process of Venusian novae and the associated coronae. *J Geophys Res, Planets* 107(E11):22-1–22-26. <https://doi.org/10.1029/2001JE001528>
- Anderson FS, Smrekar SE (1999) Tectonic effects of climate change on Venus. *J Geophys Res* 104(E12):30743–30756. <https://doi.org/10.1029/1999JE001082>

- Anderson FS, Smrekar SE (2006) Global mapping of crustal and lithospheric thickness on Venus. *J Geophys Res, Planets* 111:E08006. <https://doi.org/10.1029/2004JE002395>
- Anhaeusser CR (2014) Archaean greenstone belts and associated granitic rocks – a review. *J Afr Earth Sci* 100:684–732. <https://doi.org/10.1016/j.jafrearsci.2014.07.019>
- Ansan V, Vergely P (1995) Evidence of vertical and horizontal motions on Venus: Maxwell Montes. *Earth Moon Planets* 69:285–310. <https://doi.org/10.1007/BF00643789>
- Arculus RJ (2003) Use and abuse of the terms calcalkaline and calcalkalic. *J Petrol* 44:929–935. <https://doi.org/10.1093/petrology/44.5.929>
- Armann M, Tackley PJ (2012) Simulating the thermochemical magmatic and tectonic evolution of Venus's mantle and lithosphere: Two-dimensional models. *J Geophys Res, Planets* 117(E12). <https://doi.org/10.1029/2012JE004231>
- Bachmann O, Bergantz GW (2008) Deciphering magma chamber dynamics from styles of compositional zoning in large silicic ash flow sheets. *Rev Mineral Geochem* 69(1):651–674. <https://doi.org/10.2138/rmg.2008.69.17>
- Baes M, Gerya T, Sobolev SV (2016) 3-D thermo-mechanical modeling of plume-induced subduction initiation. *Earth Planet Sci Lett* 453:193–203. <https://doi.org/10.1016/j.epsl.2016.08.023>
- Baker VR, Komatsu G, Parker TJ, Gulick VC, Kargel JS, Lewis JS (1992) Channels and valleys on Venus: preliminary analysis of Magellan data. *J Geophys Res, Planets* 97(E8):13421–13444. <https://doi.org/10.1029/92JE00927>
- Banerdt WB (1986) Support of long-wavelength loads on Venus and implications for internal structure. *J Geophys Res, Solid Earth* 91(B1):403–419. <https://doi.org/10.1029/JB091iB01p00403>
- Barsukov VL, Basilevsky AT, Burba GA, Bobinna NN, Kryuchkov VP, Kuzmin RO, Nikolaeva OV, Pronin AA, Ronca LB, Chernaya IM, Shashkina VP, Garanin AV, Kushky ER, Markov MS, Sukhanov AL, Kotelnikov VA, Rzhiga ON, Petrov GM, Alexandrov YN, Sidorenko AI, Bogomolov AF, Skrypnik GI, Bergman MY, Kudrin LV, Bokshstein IM, Kronrod MA, Chochia PA, Tyuffin YS, Kadnichansky SA, Akim EL (1986) The geology and geomorphology of the Venus surface as revealed by the radar images obtained by Veneras 15 and 16. *J Geophys Res, Solid Earth* 91(B4):378–398. <https://doi.org/10.1029/JB091iB04p0D378>
- Basilevsky AT, Head JW (1996) Evidence for rapid and widespread emplacement of volcanic plains on Venus: stratigraphic studies in the Baltis Vallis region. *Geophys Res Lett* 23(12):1497–1500. <https://doi.org/10.1029/96GL00975>
- Basilevsky AT, Head JW (2002) Venus: timing and rates of geologic activity. *Geology* 30(11):1015–1018. [https://doi.org/10.1130/0091-7613\(2002\)030<1015:VTAROG>2.0.CO;2](https://doi.org/10.1130/0091-7613(2002)030<1015:VTAROG>2.0.CO;2)
- Basilevsky AT, Kuzmin RO, Nikolaeva OV, Pronin AA, Ronca LB, Avduvsky VS, Uspensky GR, Chermukhina ZP, Semenchenko VV, Ladygin VM (1985) The surface of Venus as revealed by the Venera landings: part II. *Geol Soc Am Bull* 96(1):137–144. [https://doi.org/10.1130/0016-7606\(1985\)96<137:TSOVAR>2.0.CO;2](https://doi.org/10.1130/0016-7606(1985)96<137:TSOVAR>2.0.CO;2)
- Basilevsky AT, Nikolaeva OV, Weitz CM (1992) Geology of the Venera 8 landing site region from Magellan data: morphological and geochemical considerations. *J Geophys Res, Planets* 97:16315–16335. <https://doi.org/10.1029/92JE01557>
- Bédard JH (2006) A catalytic delamination-driven model for coupled genesis of Archaean crust and sub-continental lithospheric mantle. *Geochim Cosmochim Acta* 70(5):1188–1214. <https://doi.org/10.1016/j.gca.2005.11.008>
- Bédard JH (2018) Stagnant lids and mantle overturns: implications for Archaean tectonics, magmagenesis, crustal growth, mantle evolution, and the start of plate tectonics. *Geosci Front* 9(1):19–49. <https://doi.org/10.1016/j.gsf.2017.01.005>
- Bédard JH, Brouillette P, Madore L, Berclaz A (2003) Archaean cratonization and deformation in the northern Superior Province, Canada: an evaluation of plate tectonic versus vertical tectonic models. *Precambrian Res* 127:61–87. [https://doi.org/10.1016/S0301-9268\(03\)00181-5](https://doi.org/10.1016/S0301-9268(03)00181-5)
- Bédard JH, Harris LB, Thurston PC (2013) The hunting of the snArc. *Precambrian Res* 229:20–48. <https://doi.org/10.1016/j.precamres.2012.04.001>
- Bercovici D, Ricard Y (2014) Generation of plate tectonics with two-phase grain-damage and pinning: source-sink model and toroidal flow. *Earth Planet Sci Lett* 365:275–288. <https://doi.org/10.1016/j.epsl.2013.02.002>
- Bilotti F, Suppe J (1999) The global distribution of wrinkle ridges on Venus. *Icarus* 139(1):137–157. <https://doi.org/10.1006/icar.1999.6092>
- Bindschadler DL, Parmentier EM (1990) Mantle flow tectonics: the influence of a ductile lower crust and implications for the formation of topographic uplands on Venus. *J Geophys Res, Solid Earth* 95(B13):21329–21344. <https://doi.org/10.1029/JB095iB13p21329>
- Bindschadler DL, Schubert G, Kaula WM (1992) Coldspots and hotspots: global tectonics and mantle dynamics of Venus. *J Geophys Res, Planets* 97(E8):13495–13532. <https://doi.org/10.1029/92JE01165>

- Bjornes E, Johnson BC, Evans AJ (2021) Estimating Venusian thermal conditions using multiring basin morphology. *Nat Astron* 5:498–502. <https://doi.org/10.1038/s41550-020-01289-6>
- Blaske CH, O'Rourke JG, Desch SJ, Borrelli ME (2023) Meteors may masquerade as lightning in the atmosphere of Venus. *J Geophys Res, Planets* 128(9):e2023JE007914. <https://doi.org/10.1029/2023JE007914>
- Bleeker W (2002) The late Archean record: a puzzle in ca. 35 pieces. *Lithos* 71:99–134. <https://doi.org/10.1016/j.lithos.2003.07.003>
- Bolea-Fernandez E, Van Malderen SJM, Balcaen L, Resano M, Vanhaecke F (2016) Laser ablation-tandem ICP-mass spectrometry (LA-ICP-MS/MS) for direct Sr isotopic analysis of solid samples with high Rb/Sr ratios. *J Anal At Spectrom* 31:464–472. <https://doi.org/10.1039/C5JA00404G>
- Bondarenko NV, Head JW, Ivanov MA (2010) Present-day volcanism on Venus: evidence from microwave radiometry. *Geophys Res Lett* 37(23). <https://doi.org/10.1029/2010GL045233>
- Bonin B (2012) Extra-terrestrial igneous granites and related rocks: a review of their occurrence and petrogenesis. *Lithos* 153:3–24. <https://doi.org/10.1016/j.lithos.2012.04.007>
- Borrelli ME, O'Rourke JG, Smrekar SE, Ostberg CM (2021) A global survey of lithospheric flexure at steep-sided domical volcanoes on Venus reveals intermediate elastic thicknesses. *J Geophys Res, Planets* 126(7):e2020JE006756. <https://doi.org/10.1029/2020JE006756>
- Brian AW, Stofan ER, Guest JE, Smrekar SE (2004) Lafeys Regio: a newly discovered topographic rise on Venus. *J Geophys Res, Planets* 109(E7). <https://doi.org/10.1029/2002JE002010>
- Bridges NT (1997) Ambient effects on basalt and rhyolite lavas under Venusian, subaerial, and subaqueous conditions. *J Geophys Res, Planets* 102(E4):9243–9255. <https://doi.org/10.1029/97JE00390>
- Brissaud Q, Krishnamoorthy S, Jackson JM, Bowman DC, Komjathy A, Cutts JA, Zhan Z, Pauken MT, Izraelvitz JS, Walsh GJ (2021) The first detection of an earthquake from a balloon using its acoustic signature. *Geophys Res Lett* 48(12):e2021GL093013. <https://doi.org/10.1029/2021GL093013>
- Brossier JF, Gilmore MS, Toner K (2020) Low radar emissivity signatures on Venus volcanoes and coronae: new insights on relative composition and age. *Icarus* 343:113693. <https://doi.org/10.1016/j.icarus.2020.113693>
- Brown CD, Grimm RE (1995) Tectonics of Artemis Chasma: a Venusian “Plate” boundary. *Icarus* 117(2):219–249. <https://doi.org/10.1006/icar.1995.1155>
- Brown CD, Grimm RE (1996) Lithospheric rheology and flexure at Artemis Chasma, Venus. *J Geophys Res* 101(E5):12697–12708. <https://doi.org/10.1029/96JE00834>
- Brown CD, Grimm RE (1997) Tessera deformation and the contemporaneous thermal state of the plateau highlands. *Venus, Earth and Planetary Science Letters* 147(1):1–10. [https://doi.org/10.1016/S0012-821X\(97\)00007-1](https://doi.org/10.1016/S0012-821X(97)00007-1)
- Brown CD, Grimm RE (1999) Recent tectonic and lithospheric thermal evolution of Venus. *Icarus* 139(1):40–48. <https://doi.org/10.1006/icar.1999.6083>
- Brown M, Johnson T, Gardiner NJ (2020) Plate tectonics and the Archean Earth. *Annu Rev Earth Planet Sci* 48:291–320. <https://doi.org/10.1146/annurev-earth-081619-052705>
- Bullock MA, Grinspoon DH (2001) The recent evolution of climate on Venus. *Icarus* 150:19–37. <https://doi.org/10.1006/icar.2000.6570>
- Burov E, Cloetingh S (2010) Plume-like upper mantle instabilities drive subduction initiation. *Geophys Res Lett* 37(3). <https://doi.org/10.1029/2009GL041535>
- Byrne PK, Krishnamoorthy S (2022) Estimates on the frequency of volcanic eruptions on Venus. *J Geophys Res, Planets* 127:e2021JE007040. <https://doi.org/10.1029/2021JE007040>
- Byrne PK, Ghail RC, Gilmore MS, Şengör AMC, Klimczak C, Senske DA, Whitten JL, Khawja S, Ernst RE, Solomon SC (2021) Venus tesserae feature layered, folded, and eroded rocks. *Geology* 49:81–85. <https://doi.org/10.1130/G47940.1>
- Cadman AC, Heaman L, Tarney J, Wardle R, Krogh TE (1993) U-Pb geochronology and geochemical variation within two Proterozoic mafic dyke swarms. *Labrador Canad J Earth Sci* 30:1490–1504. <https://doi.org/10.1139/e93-128>
- Campbell IH (2002) Implications of the Nb/U, Th/U and Sm/Nd in plume magmas for the relationship between continental and oceanic crust formation and the development of depleted mantle. *Geochim Cosmochim Acta* 66(9):1651–1661. [https://doi.org/10.1016/S0016-7037\(01\)00856-0](https://doi.org/10.1016/S0016-7037(01)00856-0)
- Campbell IH, Hill RI (1988) A two-stage model for the formation of the granite-greenstone terrains of the Kalgoorlie-Norseman area, Western Australia. *Earth Planet Sci Lett* 90(1):11–25. [https://doi.org/10.1016/0012-821X\(88\)90107-0](https://doi.org/10.1016/0012-821X(88)90107-0)
- Campbell IH, Taylor SR (1983) No water, no granites - no oceans, no continents. *Geophys Res Lett* 10(11):1061–1064. <https://doi.org/10.1029/GL010i011p01061>
- Campbell BA, Campbell DB, Morgan GA, Carter LM, Nolan MC, Chandler JF (2015) Evidence for crater ejecta on Venus tessera terrain from Earth-based radar images. *Icarus* 250:123–130. <https://doi.org/10.1016/j.icarus.2014.11.025>

- Campbell BA, Morgan GA, Whitten JL, Carter LM, Glaze LS, Campbell DB (2017) Pyroclastic flow deposits on Venus as indicators of renewed magmatic activity. *J Geophys Res, Planets* 122(7):1580–1596. <https://doi.org/10.1002/2017JE005299>
- Carter LM, Gilmore MS, Ghail RC, Byrne PK, Smrekar SE, Ganey TM, Izenberg N (2023) Sedimentary processes on Venus. *Space Sci Rev* 219:85. <https://doi.org/10.1007/s11214-023-01033-2>
- Cawood PA, Hawkesworth CJ, Dhuime B (2013) The continental record and the generation of continental crust. *Geol Soc Am Bull* 125(1–2):14–32. <https://doi.org/10.1130/B30722.1>
- Chantel J, Manthilake G, Andrault D, Novella D, Yu T, Wang YB (2016) Experimental evidence supports mantle partial melting in the asthenosphere, Experimental evidence supports mantle partial melting in the asthenosphere. *Sci Adv* 2, e1600246. <https://doi.org/10.1126/sciadv.1600246>. 2016
- Christiansen RL (2005) Post-Laramide Tectonomagmatics of the U.S. Cordillera. *Geochimica et Cosmochimica Acta Supplement* 69(10), Supplement, 2005, A136
- Christiansen EH, McCurry M (2008) Contrasting origins of Cenozoic silicic volcanic rocks from the western Cordillera of the United States. *Bull Volcanol* 70:251–267. <https://doi.org/10.1007/s00445-007-0138-1>
- Clegg SM, Sklute E, Dyar MD, Barefield JE, Wiens RC (2009) Multivariate analysis of remote laser-induced breakdown spectroscopy spectra using partial least squares, principal component analysis, and related techniques. *Spectrochim Acta, Part B, At Spectrosc* 64(1):79–88. <https://doi.org/10.1016/j.sab.2008.10.045>
- Cohen BA, Malespin CA, Farley KA, Martin PE, Cho Y, Mahaffy PR (2019) In situ geochronology on Mars and the development of future instrumentation. *Astrobiology* 19(11):1303–1314. <https://doi.org/10.1089/ast.2018.1871>
- Coleman M, Hecht M, Hurowitz J, Neidholdt E, Polk J, Sinha MP, Sturhahn W, Zimmerman W (2012) In situ geochronology as a mission-enabling technology. In: 2012 IEEE aerospace conference, pp 1–8. <https://doi.org/10.1109/AERO.2012.6187053>
- Condie KC (1981) Archean greenstone belts. *Dev Precambrian Geol* 3:1–434
- Condie KC (2018) A planet in transition: the onset of plate tectonics on Earth between 3 and 2 Ga? *Geosci Front* 9(1):51–60. <https://doi.org/10.1016/j.gsf.2016.09.001>
- Condie KC, Benn K (2006) Archean geodynamics: similar to or different from modern geodynamics? In: Benn K, Mareschal J-C, Condie KC (eds) *Archean geodynamics and environments*. Geophysical monograph series, vol 164, pp 47–59
- Condie KC, Kröner A (2008) When did plate tectonics begin? Evidence from the geologic record. In: Condie KC, Pease V (eds) *When did plate tectonics begin on planet Earth?* *Spec Pap Geol Soc Am*, vol 440, pp 281–294
- Condie KC, Aster RC van Hunen J (2016) A great thermal divergence in the mantle beginning 2.5 Ga: geochemical constraints from greenstone basalts and komatiites. *Geosci Front* 7(4):543–553. <https://doi.org/10.1016/j.gsf.2016.01.006>
- Conrad JW, Nimmo F (2023) Constraining characteristic morphological wavelengths for Venus using Baltis Vallis. *Geophys Res Lett* 50(10):e2022GL101268. <https://doi.org/10.1029/2022GL101268>
- Cordier D, Bonhommeau DA, Port S, Chevrier V, Lebonnois S, García-Sánchez F (2019) The physical origin of the Venus low atmosphere chemical gradient. *Astrophys J* 880:2. <https://doi.org/10.3847/1538-4357/ab27bd>
- Crumpler LS, Head JW, Aubele JC (1993) Relation of major volcanic center concentration on Venus to global tectonic patterns. *Science* 261(5121):591–595. <https://doi.org/10.1126/science.261.5121.591>
- Crumpler LS, Aubele JC, Senske DA, Keddie ST, Magee KP, Head JW (1997) Volcanoes and centers of volcanism on Venus. In: Bougher SW, Hunten DM, Phillips RJ (eds) *Venus II*. University of Arizona Press, Tucson, pp 697–756
- Crumpler LS, Aubele JC (2000) Volcanism on Venus. In: Sigurdsson H et al (eds) *Encyclopedia of volcanoes*. Academic Press, New York, pp 727–770
- Cutts J, Baines K, Dorsky L, Frazier W, Izraelvitz J, Krishnamoorthy S et al (2022) Exploring the clouds of Venus: science driven Aerobot missions to our sister planet. In: 2022 IEEE aerospace conference (AERO), pp 1–20. <https://doi.org/10.1109/AERO53065.2022.9843740>
- Cyr KE, Melosh HJ (1993) Tectonic patterns and regional stresses near Venesian coronae. *Icarus* 102(2):175–184. <https://doi.org/10.1006/icar.1993.1042>
- Davaille A, Smrekar SE, Tomlinson S (2017) Experimental and observational evidence for plume-induced subduction on Venus. *Nat Geosci* 10(5):349–355. <https://doi.org/10.1038/ngeo2928>
- Dawson JB (1962) Sodium Carbonate Lavas from Oldoinyo Lengai. *Tanganyika Nat* 195(4846):1075–1076. <https://doi.org/10.1038/1951075a0>
- Dawson JB, Pinkerton H, Norton GE, Pyle DM (1990) Physicochemical properties of alkali carbonatite lavas: data from the 1988 eruption of Oldoinyo Lengai. *Tanzania Geol* 18(3):260–263. [https://doi.org/10.1130/0091-7613\(1990\)018<0260:PPOACL>2.3.CO;2](https://doi.org/10.1130/0091-7613(1990)018<0260:PPOACL>2.3.CO;2)
- de Wit MJ, Ashwal LD (1995) Greenstone belts: what are they? *S Afr J Geol* 98:505–520

- D’Incecco P, Müller N, Helbert J, D’Amore M (2017) Idunn Mons on Venus: location and extent of recently active lava flows. *Planet Space Sci* 136:25–33. <https://doi.org/10.1016/j.pss.2016.12.002>
- Dombard AJ, Johnson CL, Richards MA, Solomon SC (2007) A magmatic loading model for coronae on Venus. *J Geophys Res, Planets* 112(E4). <https://doi.org/10.1029/2006JE002731>
- Donahue TM, Grinspoon DH, Hartle RE, Hodges RR (1997) Ion/neutral escape of hydrogen and deuterium: evolution of water. In: Bougher SW, Hunten DM, Phillips RJ (eds) *Venus II*. Univ. Arizona Press, Tucson, pp 385–414
- Duncan M, Dasgupta R (2017) Rise of Earth’s atmospheric oxygen controlled by efficient subduction of organic carbon. *Nat Geosci* 10:387–392. <https://doi.org/10.1038/ngeo2939>
- Dyar MD, Helbert J, Marturilli A, Müller NT, Kappel D (2020) Probing Venus surface iron contents with six-band visible near-infrared spectroscopy from orbit. *Geophys Res Lett* 47(23):e2020GL090497. <https://doi.org/10.1029/2020GL090497>
- Dyar MD, Helbert J, Cooper RC, Sklute EC, Marurilli A, Mueller NT, Kappel D, Smrekar SE (2021) Surface weathering on Venus: constraints from kinetic, spectroscopic, and geochemical data. *Icarus* 358:114139. <https://doi.org/10.1016/j.icarus.2020.114139>
- Elkins-Tanton LT, Smrekar SE, Hess PC, Parmentier EM (2007) Volcanism and volatile recycling on a one-plate planet: Applications to Venus. *J Geophys Res, Planets* 112(E4). <https://doi.org/10.1029/2006JE002793>
- Ernst R, Bleeker W (2010) Large igneous provinces (LIPs), giant dyke swarms, and mantle plumes: significance for break-up events within Canada and adjacent regions from 2.5 Ga to the present. *Can J Earth Sci* 47:695–739. <https://doi.org/10.1139/E10-025>
- Ernst RE, Buchan KL (2001) Large mafic magmatic events through time and links to mantle plume heads. In: Buchan RE, Buchan KL (eds) *Mantle plumes: their identification through time*. *Spec Pap Geol Soc Am*, vol 352, pp 483–575. <https://doi.org/10.1130/0-8137-2352-3.483>
- Ernst RE, Head JW, Parfitt E, Grosfils E, Wilson L (1995) Giant radiating dyke swarms on Earth and Venus. *Earth-Sci Rev* 39(1):1–58. [https://doi.org/10.1016/0012-8252\(95\)00017-5](https://doi.org/10.1016/0012-8252(95)00017-5)
- Ernst RE, Grosfils EB, Mège D (2001) Giant Dike Swarms: Earth, Venus, and Mars. *Annu Rev Earth Planet Sci* 29:489–534. <https://doi.org/10.1146/annurev.earth.29.1.489>
- Ernst RE, Dosnoyers DW, Head JW, Grosfils EB (2003) Graben–fissure systems in Guinevere Planitia and Beta Regio (264°–312°E, 24°–60°N), Venus, and implications for regional stratigraphy and mantle plumes. *Icarus* 164:282–316. [https://doi.org/10.1016/S0019-1035\(03\)00126-X](https://doi.org/10.1016/S0019-1035(03)00126-X)
- Fagereng Å, Biggs J (2019) New perspectives on ‘geological strain rates’ calculated from both naturally deformed and actively deforming rocks. *J Struct Geol* 125:100–110. <https://doi.org/10.1016/j.jsg.2018.10.004>
- Faure G (2001) *Origin of igneous rocks: the isotopic evidence*. Springer, Heidelberg
- Fegley B Jr, Prinn RG (1989) Estimation of the rate of volcanism on Venus from reaction rate measurements. *Nature* 337:55–58. <https://doi.org/10.1038/337055a0>
- Fegley B (2003) Venus. In: Holland HD, Turekian KK (eds) *Treatise on geochemistry*, vol 1. Elsevier, Amsterdam, pp 487–507. <https://doi.org/10.1016/b0-08-043751-6/01150-6>
- Fegley B, Klingelhofer G, Lodders K, Widemann T (1997) Geochemistry of surface-atmosphere interactions on Venus. In: Bougher SW, Hunten DM, Phillips RJ (eds) *Venus II*. University of Arizona Press, Tucson, pp 591–636
- Filiberto J (2014) Magmatic diversity on Venus: constraints from terrestrial analog crystallization experiments. *Icarus* 231:131–136. <https://doi.org/10.1016/j.icarus.2013.12.003>
- Filiberto J, Trang D, Treiman AH, Gilmore MS (2020) Present-day volcanism on Venus as evidenced from weathering rates of olivine. *Sci Adv* 6(1):eaax7445. <https://doi.org/10.1126/sciadv.aax7445>
- Florensky CP, Ronca LB, Basilevsky AT, Burba GA, Nikolaeva OV, Pronin AA, Trakhtman AM, Volkov VP, Zazetsky VV (1977) The surface of Venus as revealed by Soviet Venera 9 and 10. *Geol Soc Am Bull* 88(11):1537–1545. [https://doi.org/10.1130/0016-7606\(1977\)88<1537:TsovAr>2.0.CO;2](https://doi.org/10.1130/0016-7606(1977)88<1537:TsovAr>2.0.CO;2)
- Flynn ITW, Chevrel MO, Ramsey MS (2023) Adaptation of a thermorheological lava flow model for Venus conditions. *J Geophys Res, Planets* 128(7):e2022JE007710. <https://doi.org/10.1029/2022JE007710>
- Ford JP, Plaut JJ, Weitz CM, Farr TG, Senske DA, Stofan ER, Michaels G, Parker TJ (1993) Guide to Magellan image interpretation. *JPL Publ* 93(24)
- Galgana GA, McGovern PJ, Grosfils EB (2011) Evolution of large Venusian volcanoes: Insights from coupled models of lithospheric flexure and magma reservoir pressurization. *Journal of Geophysical Research Planets* 116(E3). <https://doi.org/10.1029/2010JE003654>
- Galgana GA, Grosfils EB, McGovern PJ (2013) Radial dike formation on Venus: insights from models of uplift, flexure and magmatism. *Icarus* 225(1):538–547. <https://doi.org/10.1016/j.icarus.2013.04.020>
- Ganesh I, McGuire LA, Carter LM (2021) Modeling the dynamics of dense pyroclastic flows on Venus: insights into pyroclastic eruptions. *J Geophys Res, Planets* 126(9):e2021JE006943. <https://doi.org/10.1029/2021JE006943>

- Ganesh I, Carter LM, Henz TN (2022) Radar backscatter and emissivity models of proposed pyroclastic density current deposits on Venus. *J Geophys Res, Planets* 127(10):e2022JE007318. <https://doi.org/10.1029/2022JE007318>
- Garcia RF, Klotz A, Hertzog A, Martin R, G erier S, Kassarian E, Bordereau J, Venel S, Mimoun D (2022) Infrasonic from large earthquakes recorded on a network of balloons in the stratosphere. *Geophys Res Lett* 49(15):e2022GL098844. <https://doi.org/10.1029/2022GL098844>
- Garvin JB, Getty SA, Arney GN, Johnson NM, Kohler E, Schwer KO, Sekerak M, Bartels A, Saylor RS, Elliott VE, Goodloe CS, Garrison MB, Cottini V, Izenberg N, Lorenz R, Malespin CA, Ravine M, Webster CR, Atkinson DH, Aslam S, Atreya S, Bos BJ, Brinckerhoff WB, Campbell B, Crisp D, Filiberto JR, Forget F, Gilmore M, Gorius N, Grinspoon D, Hofmann AE, Kane SR, Kiefer W, Lebonnois S, Mahaffy PR, Pavlov A, Trainer M, Zahnle KJ, Zolotov M (2022) Revealing the mysteries of Venus: the DAVINCI mission. *Planet Sci J* 3:117. <https://doi.org/10.3847/psj/ac63c2>
- George H, Malaspina DM, Goodrich K, Ma Y, Ramstad R, Connor D, Bale SD, Curry S (2023) Non-lightning-generated whistler waves in near-Venus space. *Geophys Res Lett* 50(19):e2023GL105426. <https://doi.org/10.1029/2023GL105426>
- Gerya T (2014) Precambrian geodynamics: concepts and models. *Gondwana Res* 25:442–463. <https://doi.org/10.1016/j.gr.2012.11.008>
- Gerya TV, Stern RJ, Baes M, Sobolev S, Whattam SA (2015) Plate tectonics on the Earth triggered by plume-induced subduction initiation. *Nature* 527:221–225. <https://doi.org/10.1038/nature15752>
- Ghail RC (2002) Structure and evolution of southeast Thetis Regio. *J Geophys Res, Planets* 107(E8):4–1–4–7. <https://doi.org/10.1029/2001JE001514>
- Ghail RC (2015) Rheological and petrological implications for a stagnant lid regime on Venus. *Planet Space Sci* 113–114:2–9. <https://doi.org/10.1016/j.pss.2015.02.005>
- Ghent RR, Hansen VL (1999) Structural and kinematic analysis of eastern Ovda Regio, Venus: implications for crustal Plateau formation. *Icarus* 139(1):116–136. <https://doi.org/10.1006/icar.1999.6085>
- Ghent RR, Tibuleac IM (2002) Ribbon spacing in Venusian tessera: implications for layer thickness and thermal state. *Geophys Res Lett* 29(20):61. <https://doi.org/10.1029/2002GL015994>
- Giardini D, Lognonn  P, Banerdt WB et al (2020) The seismicity of Mars. *Nat Geosci* 13:205–212. <https://doi.org/10.1038/s41561-020-0539-8>
- Gilmore MS, Head JW (2000) Sequential deformation of plains at the margins of Alpha Regio, Venus: implications for tessera formation. *Meteorit Planet Sci* 35(4):667–687. <https://doi.org/10.1111/j.1945-5100.2000.tb01451.x>
- Gilmore MS, Head JW (2018) Morphology and deformational history of Tellus Regio, Venus: evidence for assembly and collision. *Planet Space Sci* 154:5–20. <https://doi.org/10.1016/j.pss.2018.02.001>
- Gilmore MS, Ivanov MA, Head JW, Basilevsky AT (1997) Duration of tessera deformation on Venus. *J Geophys Res, Planets* 102(E6):13357–13368. <https://doi.org/10.1029/97JE00965>
- Gilmore MS, Collins GC, Ivanov MA, Marinangeli L, Head JW (1998) Style and sequence of extensional structures in tessera terrain, Venus. *J Geophys Res Planets* 103(E7):16813–16840. <https://doi.org/10.1029/98JE01322>
- Gilmore MS, Mueller N, Helbert J (2015) VIRTIS emissivity of Alpha Regio, Venus, with implications for tessera composition. *Icarus* 254:350–361. <https://doi.org/10.1016/j.icarus.2015.04.008>
- Gilmore M, Treiman A, Helbert J, Smrekar S (2017) Venus surface composition constrained by observation and experiment. *Space Sci Rev* 212(3–4):1511–1540
- Gilmore MS, Dyar MD, Mueller N et al (2023) Mineralogy of the Venus Surface. *Space Sci Rev* 219:52. <https://doi.org/10.1007/s11214-023-00988-6>
- Glaze LS, Stefan ER, Smrekar SE, Baloga SM (2002) Insights into corona formation through statistical analyses. *J Geophys Res, Planets* 107(E12):18–1–18–12. <https://doi.org/10.1029/2002JE001904>
- Glaze LS, Wilson CF, Zasova LV, Nakamura M, Limaye S (2018) Future of Venus research and exploration. *Space Sci Rev* 214:89. <https://doi.org/10.1007/s11214-018-0528-z>
- Global Volcanism Program (2023). [Database] Volcanoes of the World (v. 5.1.5; 15 Dec 2023). Distributed by Smithsonian Institution, compiled by Venzke, E. <https://doi.org/10.5479/si.GVP.VOTW5-2023.5.1>
- Gorevan SP, Myrick T, Davis K, Chau JJ, Bartlett P, Mukherjee S, Anderson R, Squyres SW, Arvidson RE, Madsen MB, Bertelsen P, Goetz W, Binau CS, Richter L (2003) Rock Abrasion Tool: Mars Exploration Rover mission. *J Geophys Res, Planets* 108(E12). <https://doi.org/10.1029/2003JE002061>
- Griffiths RW, Campbell IH (1990) Stirring and structure in mantle starting plumes. *Earth Planet Sci Lett* 99(1–2):66–78. [https://doi.org/10.1016/0012-821X\(90\)90071-5](https://doi.org/10.1016/0012-821X(90)90071-5)
- Grimm RE, Hess PC (1997) The crust of Venus. In: *Venus II*. University of Arizona Press, Tucson, pp 1205–1244
- Grimm RE, Barr AC, Harrison KP, Stillman DE, Neal KL, Vincent MA, Delory GT (2012) Aerial electromagnetic sounding of the lithosphere of Venus. *Icarus* 217(2):462–473. <https://doi.org/10.1016/j.icarus.2011.07.021>

- Grindrod PM, Hoogenboom T (2006) Venus: the corona conundrum. *Astron Geophys* 47(3):3.16–3.21. <https://doi.org/10.1111/j.1468-4004.2006.47316.x>
- Grindrod PM, Nimmo F, Stofan ER, Guest JE (2005) Strain at radially fractured centers on Venus. *J Geophys Res, Planets* 110(E12):E12002. <https://doi.org/10.1029/2005JE002416>
- Grindrod PM, Stofan ER, Guest JE (2010) Volcanism and resurfacing on Venus at the full resolution of Magellan SAR data. *Geophys Res Lett* 37(15). <https://doi.org/10.1029/2010GL043424>
- Grosfils E, Head JW (1994a) Emplacement of a radiating dike swarm in western Vinmara Planitia, Venus: interpretation of the regional stress field orientation and subsurface magmatic configuration. *Earth Moon Planets* 66:153–171. <https://doi.org/10.1007/BF00644129>
- Grosfils E, Head JW (1994b) The global distribution of giant radiating dike swarms on Venus: implications for the global stress state. *Geophys Res Lett* 21(8):701–704. <https://doi.org/10.1029/94GL00592>
- Grosfils E, Aubele J, Crumpler L, Gregg T, Sakimoto S (2000) Volcanism on Earth's Seafloor and Venus. In: Zimbelman JR, Gregg TKP (eds) *Environmental effects on volcanic eruptions: from deep oceans to deep space*
- Guest JE, Stofan ER (1999) A new view of the stratigraphic history of Venus. *Icarus* 139(1):55–66. <https://doi.org/10.1006/icar.1999.6091>
- Gülcher AJP, Gerya TV, Montési LGJ, Munch J (2020) Corona structures driven by plume–lithosphere interactions and evidence for ongoing plume activity on Venus. *Nat Geosci* 13(8):547–554. <https://doi.org/10.1038/s41561-020-0606-1>
- Gülcher AJP, Yu T-Y, Gerya TV (2023) Tectono-magmatic evolution of asymmetric coronae on Venus: topographic classification and 3D thermo-mechanical modeling. *J Geophys Res, Planets* 123(1):e2023JE007978. <https://doi.org/10.1029/2023JE007978>
- Hahn RM, Byrne PK (2022) Kernel density analysis of volcanoes on Venus at varying spatial scales. *Lun Planet Sci Conf* 53:2437
- Hamilton WB (1998) Archean magmatism and deformation were not products of plate tectonics. *Precambrian Res* 91(1–2):143–179. [https://doi.org/10.1016/S0301-9268\(98\)00042-4](https://doi.org/10.1016/S0301-9268(98)00042-4)
- Hamilton WB (2011) Plate tectonics began in Neoproterozoic time, and plumes from deep mantle have never operated. *Lithos* 123:1–20. <https://doi.org/10.1016/j.lithos.2010.12.007>
- Hamilton VE, Stofan ER (1996) The geomorphology and evolution of Hecate Chasma, Venus. *Icarus* 121(1):171–194. <https://doi.org/10.1006/icar.1996.0077>
- Hansell SA, Wells WK, Hunte DH (1995) Optical detection of lightning on Venus. *Icarus* 117(2):345–351. <https://doi.org/10.1006/icar.1995.1160>
- Hansen VL (2007) Venus: a thin-lithosphere analog for early Earth? In: Van Kranendonk MJ, Smithies RH, Bennett VC (eds) *Earth's oldest rocks, developments in Precambrian geology* 15, pp 987–1012
- Hansen VL (2015) Impact origin of Archean cratons. *Lithosphere* 7(5):563–578. <https://doi.org/10.1130/L371.1>
- Hansen VL (2018) Global tectonic evolution of Venus, from exogenic to endogenic over time, and implications for early Earth processes. *Philos Trans R Soc A376*:20170412. <https://doi.org/10.1098/rsta.2017.0412>
- Hansen VL, Phillips RJ (1993) Tectonics and volcanism of eastern Aphrodite Terra, Venus: no subduction, no spreading. *Science* 260(5107):526–530. <https://doi.org/10.1126/science.260.5107.526>
- Hansen VL, Willis JA (1996) Structural analysis of a sampling of tesserae: implications for Venus geodynamics. *Icarus* 123(2):296–312. <https://doi.org/10.1006/icar.1996.0159>
- Hansen VL, Banks BK, Ghent RR (1999) Tessera terrain and crustal plateaus, Venus. *Geology* 27(12):1071–1074. [https://doi.org/10.1130/0091-7613\(1999\)027<1071:TTACPV>2.3.CO;2](https://doi.org/10.1130/0091-7613(1999)027<1071:TTACPV>2.3.CO;2)
- Hansen VL, Phillips RJ, Willis JJ, Ghent RR (2000) Structures in tessera terrain, Venus: issues and answers. *J Geophys Res, Planets* 105(E2):4087–4368. <https://doi.org/10.1029/1999JE001137>
- Harris LB, Bédard JH (2014) Crustal evolution and deformation in a non-plate-tectonic Archean Earth: comparisons with Venus. In: Dilek Y, Furnes H (eds) *Evolution of Archean crust and early life, modern approaches in solid Earth sciences*, pp 215–291
- Harris LB, Bédard JH (2015) Interactions between continent-like 'drift' rifting and mantle flow on Venus: gravity interpretations and Earth analogues. In: Plattz T, Massironi M, Byrne PK, Hiesinger H (eds) *Volcanism and tectonism across the inner solar system*. *Geologic society of London special publication*, vol 401, pp 327–356
- Harrison TM (2009) The hadean crust: evidence from >4 Ga zircons. *Annu Rev Earth Planet Sci* 37:479–505. <https://doi.org/10.1146/annurev.earth.031208.100151>
- Hart RA, Russell CT, Zhang T (2022) Statistical study of lightning-generated whistler-mode waves observed by Venus Express. *Icarus* 380:114993. <https://doi.org/10.1016/j.icarus.2022.114993>
- Hashimoto GL, Roos-Serote M, Sugita S, Gilmore MS, Kamp LW, Carlson RW, Baines K-H (2008) Felsic highland crust on Venus suggested by Galileo near-infrared mapping spectrometer data. *J Geophys Res, Planets* 113:E00B24. <https://doi.org/10.1029/2008JE003134>

- Hawkesworth CJ, Cawood PA, Bhuime B (2019) Rates of generation and growth of the continental crust. *Geosci Front* 10:165–173. <https://doi.org/10.1016/j.gsf.2018.02.004>
- Hawkesworth CJ, Cawood PA, Bhuime B (2020) The evolution of the continental crust and the onset of plate tectonics. *Front Earth Sci* 8:326. <https://doi.org/10.3389/feart.2020.00326>
- Head JW (1990) Processes of crustal formation and evolution on Venus: an analysis of topography, hypsometry, and crustal thickness variations. *Earth Moon Planets* 50(1):25–55. <https://doi.org/10.1007/BF00142388>
- Head JW, Wilson L (1986) Volcanic processes and landforms on Venus: theory, predictions, and observations. *J Geophys Res, Solid Earth* 91(B9):9407–9446. <https://doi.org/10.1029/JB091iB09p09407>
- Head JW, Wilson L (1992) Magma reservoirs and neutral buoyancy zones on Venus: implications for the formation and evolution of volcanic landforms. *J Geophys Res, Planets* 97(E3):3877–3903. <https://doi.org/10.1029/92JE00053>
- Head JW, Crumpler LS, Aubele JC, Guest JE, Saunders RS (1992) Venus volcanism: classification of volcanic features and structures, associations, and global distribution from Magellan data. *J Geophys Res, Planets* 97(E8):13153–13197. <https://doi.org/10.1029/92JE01273>
- Head JW, Parmentier EM, Hess PC (1994) Venus: vertical accretion of crust and depleted mantle and implications for geologic history and processes. *Planet Space Sci* 42(10):803–811. [https://doi.org/10.1016/0032-0633\(94\)90061-2](https://doi.org/10.1016/0032-0633(94)90061-2)
- Heaman LM, Kjarsgaard BA (2000) Timing of eastern North American kimberlite magmatism: continental extension of the Great Meteor hotspot track? *Earth Planet Sci Lett* 178(3):253–268. [https://doi.org/10.1016/S0012-821X\(00\)00079-0](https://doi.org/10.1016/S0012-821X(00)00079-0)
- Helbert J, Müller N, Kostama P, Marinangeli L, Piccioni G, Drossart P (2008) Surface brightness variations seen by VIRTIS on Venus Express and implications for the evolution of the Lada Terra region. *Venus Geophys Res Lett* 35(11):L11201. <https://doi.org/10.1029/2008GL033609>
- Hensley S, Wallace MS, Martin J, Perkovic-Martin D, Smrekar S, Younis M, Lachaise M, Prats P, Rodriguez M, Zebker H, Campbell B, Mastrogioseppe M (2022) Planned differential interferometric SAR observations at Venus by the Veritas mission. In: Proceedings of IGARSS 2022, International Geoscience and Remote Sensing Symposium, Kuala Lumpur, Indonesia, 17–22 July, 2022
- Herrick RR, Hensley S (2023) Surface changes observed on a Venusian volcano during the Magellan mission. *Science* 379(6638):1205–1208. <https://doi.org/10.1126/science.abm7735>
- Herrick RR, Phillips RJ (1992) Geological correlations with the interior density structure of Venus. *J Geophys Res, Planets* 97(E10):16017–16034. <https://doi.org/10.1029/92JE01498>
- Herrick RR, Rumpf ME (2011) Postimpact modification by volcanic or tectonic processes as the rule, not the exception, for Venusian craters. *J Geophys Res, Planets* 116(E2). <https://doi.org/10.1029/2010JE003722>
- Herrick RR, Stahlke DL, Sharpton VL (2012) Fine-scale Venusian topography from Magellan stereo data. *Eos, Trans Am Geophys Union* 93(12):125–132. <https://doi.org/10.1029/2012EO120002>
- Herrick RR, Bjonnes ET, Carter LM, Gerya T, Ghail RC, Gillmann C, Gilmore MS, Hensley S, Ivanov MA, Izenberg NR, Mueller NT, O'Rourke JG, Rolf T, Smrekar SE, Weller MB (2023) Resurfacing history and volcanic activity of Venus. *Space Sci Rev* 219:29. <https://doi.org/10.1007/s11214-023-00966-y>
- Hess PC, Head JW (1990) Derivation of primary magmas and melting of crustal materials on Venus: some preliminary petrogenetic considerations. *Earth Moon Planets* 50–51(1):57–80. <https://doi.org/10.1007/BF00142389>
- Hoefs J (2009) Stable isotope geochemistry. Springer, Berlin. <https://doi.org/10.1007/978-3-540-70708-0>
- Hoggard MJ, Parnell-Turner R, White N (2020) Hotspots and mantle plumes revisited: towards reconciling the mantle heat transfer discrepancy. *Earth Planet Sci Lett* 542:116317. <https://doi.org/10.1016/j.epsl.2020.116317>
- Honda C, Fujimura A (2005) Formation process of lunar sinuous rilles by thermal erosion of basaltic lava flow. In: Lunar and Planetary Science Conference XXXVI, Abstract 1562. <https://www.lpi.usra.edu/meetings/lpsc2005/pdf/1562.pdf>
- Höning D, Spohn T (2016) Continental growth and mantle hydration as intertwined feedback cycles in the thermal evolution of Earth. *Phys Earth Planet Inter* 255:27–49. <https://doi.org/10.1016/j.pepi.2016.03.010>
- Höning D, Tosi N, Spohn T (2019) Carbon cycling and interior evolution of water-covered plate tectonics and stagnant-lid planets. *Astron Astrophys* 627:A48. <https://doi.org/10.1051/0004-6361/201935091>
- Hoogenboom T, Houseman GA (2006) Rayleigh–Taylor instability as a mechanism for corona formation on Venus. *Icarus* 180(2):292–307. <https://doi.org/10.1016/j.icarus.2005.11.001>
- Huang J, Yang A, Zhong S (2013) Constraints of the topography, gravity and volcanism on Venusian mantle dynamics and generation of plate tectonics. *Earth Planet Sci Lett* 362:207–214. <https://doi.org/10.1016/j.epsl.2012.11.051>

- Hunt GR, Salisbury JW (1970) Visible and near-infrared spectra of minerals and rocks: I silicate minerals. *Mod Geol* 1:283–300
- Huppert HE, Sparks RSJ (1985) Komatiites I: eruption and flow. *J Petrol* 26:694–725. <https://doi.org/10.1093/ptrology/26.3.694>
- Ivanov MA (2001) Morphology of the Tessera Terrain on Venus: implications for the composition of Tessera material. *Sol Syst Res* 35:1–17. <https://doi.org/10.1023/A:1005289305927>
- Ivanov MA, Basilevsky AT (1993) Density and morphology of impact craters on Tessera Terrain. *Venus Geophys Res Lett* 20(23):2579–2582. <https://doi.org/10.1029/93GL02692>
- Ivanov MA, Head JW (1996) Tessera terrain on Venus: a survey of the global distribution, characteristics, and relation to surrounding units from Magellan data. *J Geophys Res, Planets* 101(E6):14861–14908. <https://doi.org/10.1029/96JE01245>
- Ivanov MA, Head JW (2004) Stratigraphy of small shield volcanoes on Venus: Criteria for determining stratigraphic relationships and assessment of relative age and temporal abundance. *J Geophys Res, Planets* 109(E10). <https://doi.org/10.1029/2004JE002252>
- Ivanov MA, Head JW (2011) Global geologic map of Venus. *Planet Space Sci* 59(13):1559–1600. <https://doi.org/10.1016/j.pss.2011.07.008>
- Ivanov MA, Head JW (2013) The history of volcanism on Venus. *Planet Space Sci* 84:66–92. <https://doi.org/10.1016/j.pss.2013.04.018>
- Ivanov MA, Head JW (2015) Volcanically embayed craters on Venus: testing the catastrophic and equilibrium resurfacing models. *Planet Space Sci* 106:116–121. <https://doi.org/10.1016/j.pss.2014.12.004>
- James PB, Zuber MT, Phillips RJ (2013) Crustal thickness estimates and support of topography on Venus. *J Geophys Res, Planets* 118(4):859–875. <https://doi.org/10.1029/2012JE004237>
- Janes DM, Squyres SW (1995) Viscoelastic relaxation of topographic highs on Venus to produce coronae. *J Geophys Res, Planets* 100(E10):21173–21187. <https://doi.org/10.1029/95JE01748>
- Janes DM, Squyres SW, Bindshadler DL, Baer G, Schubert G, Sharpton VL, Stofan ER (1992) Geophysical models for the formation and evolution of coronae on Venus. *J Geophys Res, Planets* 97(E10):16055–16067. <https://doi.org/10.1029/92JE01689>
- Janle P, Jannsen D, Basilevsky AT (1988) Tepev Mons on Venus: morphology and elastic bending models. *Earth Moon Planets* 41(2):127–139. <https://doi.org/10.1007/BF00056398>
- Jeffery AJ, Gertisser R (2018) Peralkaline Felsic Magmatism of the Atlantic Islands. *Front Earth Sci* 6. <https://doi.org/10.3389/feart.2018.00145>
- Jellinek AM, Manga M (2004) Links between Long-Lived Hot Spots, Mantle Plumes, D'', and Plate Tectonics. *Rev Geophys* 42(3). <https://doi.org/10.1029/2003RG000144>
- Jiménez-Díaz A, Ruiz J, Kirby JF, Romeo I, Tejero R, Caupto R (2015) Lithospheric structure of Venus from gravity and topography. *Icarus* 260:215–231. <https://doi.org/10.1016/j.icarus.2015.07.020>
- Johnson CL, Sandwell DT (1992) Joints in Venusian lava flows. *J Geophys Res, Planets* 97(E8):13601–13610. <https://doi.org/10.1029/92JE01212>
- Johnson CL, Sandwell DT (1994) Lithospheric flexure on Venus. *Geophys J Int* 119(2):627–647. <https://doi.org/10.1111/j.1365-246X.1994.tb00146.x>
- Johnson TE, Brown M, Kaus BJP, VanTongeren JA (2014) Delamination and recycling of Archaean crust caused by gravitational instabilities. *Nat Geosci* 7:47–52. <https://doi.org/10.1038/ngeo2019>
- Johnson TE, Brown M, Gardiner NJ, Kirkland CL, Smithies RH (2017) Earth's first stable continents did not form by subduction. *Nature* 543(7644):239–242. <https://doi.org/10.1038/nature21383>
- Jull MG, Arkani-Hamed J (1995) The implications of basalt in the formation and evolution of mountains on Venus. *Phys Earth Planet Inter* 89(3–4):163–175. [https://doi.org/10.1016/0031-9201\(95\)03015-O](https://doi.org/10.1016/0031-9201(95)03015-O)
- Kargel JS, Komatsu G, Baker VR, Strom RG (1993) The volcanology of Venera and VEGA landing sites and the geochemistry of Venus. *Icarus* 103:253–275. <https://doi.org/10.1006/icar.1993.1069>
- Kargel JS, Kirk RL, Fegley Jr B, Treiman AH (1994) Carbonate-sulfate volcanism on Venus? *Icarus* 112(1):219–252. <https://doi.org/10.1006/icar.1994.1179>
- Kasbohm J, Schoene B (2018) Rapid eruption of the Columbia River flood basalt and correlation with the mid-Miocene climate optimum. *Sci Adv* 4(9):eaat8223. <https://doi.org/10.1126/sciadv.aat8223>
- Kaula WM (1999) Constraints on Venus evolution from radiogenic argon. *Icarus* 139(1):32–39. <https://doi.org/10.1006/icar.1999.6082>
- Keller J, Krafft M (1990) Effusive natrocarbonatite activity of Oldoinyo Lengai, June 1988. *Bull Volcanol* 52(8):629–645. <https://doi.org/10.1007/BF00301213>
- Khawja S, Ernst RE, Samson C, Byrne PK, Ghail RC, MacLellan LM (2020) Tesserae on Venus may preserve evidence of fluvial erosion. *Nat Commun* 11:5789. <https://doi.org/10.1038/s41467-020-19336-1>
- Kiefer WS, Hager BH (1991) A mantle plume model for the equatorial highlands of Venus. *J Geophys Res* 96:20947–20966. <https://doi.org/10.1029/91JE02221>
- Kleinshans MG (2005) Flow discharge and sediment transport models for estimating a minimum timescale of hydrological activity and channel and delta formation on Mars. *J Geophys Res* 110:E1. <https://doi.org/10.1029/2005JE002521>

- Klimczak C, Byrne PK, Şengör AM, Solomon SC (2019) Principles of structural geology on rocky planets. *Can J Earth Sci* 56(12):1437–1457. <https://doi.org/10.1139/cjes-2019-0065>
- Klose KB, Wood JA, Hashimoto A (1992) Mineral equilibria and the high radar reflectivity of Venus mountaintops. *J Geophys Res, Planets* 97(E10):16353–16369. <https://doi.org/10.1029/92JE01865>
- Knapmeyer M, Oberst J, Hauber E, Wählisch M, Deuchler C, Wagner R (2006) Working models for spatial distribution and level of Mars' seismicity. *J Geophys Res, Planets* 111(E11). <https://doi.org/10.1029/2006JE002708>
- Koch DM (1994) A spreading drop model for plumes on Venus. *J Geophys Res, Planets* 99(E1):2035–2052. <https://doi.org/10.1029/93JE03097>
- Koch DM, Manga M (1996) Neutrally buoyant diapirs: a model for Venus coronae. *Geophys Res Lett* 23(3):225–228. <https://doi.org/10.1029/95GL03776>
- Koenig E, Pollard DD (1998) Mapping and modeling of radial fracture patterns on Venus. *J Geophys Res, Solid Earth* 103(B7):15183–15202. <https://doi.org/10.1029/98JB00577>
- Komatsu G, Baker VR (1994) Meander properties of Venusian channels. *Geology* 22(1):67–70. [https://doi.org/10.1130/0091-7613\(1994\)022<0067:MPOVC>2.3.CO;2](https://doi.org/10.1130/0091-7613(1994)022<0067:MPOVC>2.3.CO;2)
- Komatsu G, Baker VR, Gulick VC, Parker TJ (1993) Venusian channels and valleys: distribution and volcanological implications. *Icarus* 102(1):1–25. <https://doi.org/10.1006/icar.1993.1029>
- Komatsu G, Gulick VC, Baker VR (2001) Valley networks on Venus. *Geomorphology* 37(3):225–240. [https://doi.org/10.1016/S0169-555X\(00\)00084-2](https://doi.org/10.1016/S0169-555X(00)00084-2)
- Konopliv AS, Banerdt WB, Sjogren WL (1999) Venus gravity: 180th degree and order model. *Icarus* 139(1):3–18. <https://doi.org/10.1006/icar.1999.6086>
- Kopp RE, Kirschvink JL, Hilburn IA, Nash CZ (2005) The Paleoproterozoic snowball Earth: a climate disaster triggered by the evolution of oxygenic photosynthesis. *Proc Natl Acad Sci* 102(32):11131–11136. <https://doi.org/10.1073/pnas.0504878102>
- Korycansky DG, Zahnle KJ (2005) Modeling crater populations on Venus and Titan. *Planet Space Sci* 53(7):695–710. <https://doi.org/10.1016/j.pss.2005.03.002>
- Krassilnikov AS, Head JW (2003) Novae on Venus: Geology, classification, and evolution. *J Geophys Res, Planets* 108(E9). <https://doi.org/10.1029/2002JE001983>
- Kremic T, Ghail R, Gilmore M, Hunter G, Kiefer W, Limaye S, Pauken M, Tolbert C, Wilson C (2020) Long-duration Venus lander for seismic and atmospheric science. *Planet Space Sci* 190:104961. <https://doi.org/10.1016/j.pss.2020.104961>
- Kröner A (1985) Evolution of the Archean continental crust. *Annu Rev Earth Planet Sci* 13:49–74. <https://doi.org/10.1146/annurev.ea.13.050185.000405>
- Kumar KV, Ernst WG, Leelandadam C, Wooden JL, Grove MJ (2010) First Paleoproterozoic ophiolite from Gondwana: geochronologic-geochemical documentation of ancient oceanic crust from Kandra, SE India. *Tectonophysics* 487:22–32. <https://doi.org/10.1016/j.tecto.2010.03.005>
- Kusky TM, Li J-H, Tucker RD (2001) The Archean Dongwanzi ophiolite complex, North China craton: 2.505-billion-year-old oceanic crust and mantle. *Science* 292(5519):1142–1145. <https://doi.org/10.1126/science.1059426>
- Kusky TM, Windley BF, Polat A (2018) Geologic evidence for the operation of plate tectonics throughout the Archean: records from Archean paleo-plate boundaries. *J Earth Sci* 29:1291–1303. <https://doi.org/10.1007/s12583-018-0999-6>
- Lammer H, Zerkle AL, Gebauer S, Tost N, Noack L, Scherf M, Pilat-Lohinger E, Güdel M, Grenfell JL, Godolt M, Nikalau A (2018) Origin and evolution of the atmospheres of early Venus, Earth and Mars. *Astron Astrophys Rev* 26:2. <https://doi.org/10.1007/s00159-018-0108-y>
- Lancaster MG, Guest JE, Magee KP (1995) Great lava flow fields on Venus. *Icarus* 118(1):69–86. <https://doi.org/10.1006/icar.1995.1178>
- Lang NP, López I (2015) The magmatic evolution of three Venusian coronae. *Geol Soc (Lond) Spec Publ* 401(1):77–95. <https://doi.org/10.1144/SP401.3>
- Lebonnois S, Schubert G (2017) The deep atmosphere of Venus and the possible role of density-driven separation of CO₂ and N₂. *Nat Geosci* 10(7):473–477. <https://doi.org/10.1038/ngeo2971>
- Lebonnois S, Schubert G, Forget F, Spiga A (2018) Planetary boundary layer and slope winds on Venus. *Icarus* 314:149–158. <https://doi.org/10.1016/j.icarus.2018.06.006>
- Lécuyer C, Simon L, Guyot F (2000) Comparison of carbon, nitrogen and water budgets on Venus and the Earth. *Earth Planet Sci Lett* 181(1):33–40. [https://doi.org/10.1016/S0012-821X\(00\)00195-3](https://doi.org/10.1016/S0012-821X(00)00195-3)
- Lee CT-A, Luffi P, Plank T, Dalton H, Leeman WP (2009) Constraints on the depths and temperatures of basaltic magma generation on Earth and other terrestrial planets using new thermobarometers for mafic magmas. *Earth Planet Sci Lett* 279:20–33. <https://doi.org/10.1016/j.epsl.2008.12.020>
- Lenardic A, Kaula WM, Bindschadler DL (1991) The tectonic evolution of Western Ishtar Terra, Venus. *Geophys Res Lett* 18(12):2209–2212. <https://doi.org/10.1029/91GL02734>

- Li Y, Gurnis M (2023) Strike slip motion and the triggering of subduction initiation. *Front Earth Sci* 11:1156034. <https://doi.org/10.3389/feart.2023.1156034>
- Lithgow-Bertelloni C, Richards MA (1995) Cenozoic plate driving forces. *Geophys Res Lett* 22:1317–1320. <https://doi.org/10.1029/95GL01325>
- Lognonné P, Johnson C (2007) 10.03—Planetary seismology. In: Schubert G (ed) *Treatise on geophysics*. Elsevier, Amsterdam, pp 69–122. <https://doi.org/10.1016/B978-0-44452748-6.00154-1>
- Lorenz RD (2018) Lightning detection on Venus: a critical review. *Prog Earth Planet Sci* 5:34. <https://doi.org/10.1186/s40645-018-0181-x>
- Lorenz RD, Imai M, Takahashi Y, Sato M, Yamazaki A, Imamura T, Satoh T, Nakamura M (2019) Constraints on Venus lightning from Akatsuki's first 3 years in orbit. *Geophys Res Lett* 46(14):7955–7961. <https://doi.org/10.1029/2019GL083311>
- Lourenço DL, Rozel AB, Ballmer MD, Tackley PJ (2020) Plutonic-squishy lid: a new global tectonic regime generated by intrusive magmatism on Earth-like planets. *Geochem Geophys Geosyst* 21(4):e2019GC008756. <https://doi.org/10.1029/2019GC008756>
- Magee KP, Head JW (2001) Large flow fields on Venus: implications for plumes, rift associations, and resurfacing. In: Ernst RE, Buchan KL (eds) *Mantle plumes: their identification through time*. *Spec Pap Geol Soc Am*, vol 352, pp 81–101. <https://doi.org/10.1130/0-8137-2352-3.81>
- Maia JS, Wieczorek MA (2022) Lithospheric structure of Venusian crustal plateaus. *J Geophys Res, Planets* 127:e2021JE007004. <https://doi.org/10.1029/2021JE007004>
- Marcq E, Bertaux J-L, Montmessin F, Belyaev D (2013) Variations of sulphur dioxide at the cloud top of Venus's dynamic atmosphere. *Nat Geosci* 6:25–28. <https://doi.org/10.1038/ngeo1650>
- Martin P, Stofan ER, Glaze LS, Smrekar SE (2007) Corona of Parga Chasma, Venus. *J Geophys Res, Planets* 112:E04S03. <https://doi.org/10.1029/2006JE002758>
- McGill GE (1994) Hotspot evolution and Venusian tectonic style. *J Geophys Res, Planets* 99(E11):23149–23161. <https://doi.org/10.1029/94JE02319>
- McGovern PJ, Solomon SC (1997) Filling of flexural moats around large volcanoes on Venus: implications for volcano structure and global magmatic flux. *J Geophys Res* 102:16303–16318
- McGovern PJ, Solomon SE (1998) Growth of large volcanoes on Venus: mechanical models and implications for structural evolution. *J Geophys Res, Planets* 103(E5):11071–11101. <https://doi.org/10.1029/98JE01046>
- McGovern PJ, Sean C, Solomon SC, Smith DE, Zuber MT, Simons M, Wieczorek MA, Phillips RJ, Neumann GA, Aharonson O, Head JW (2004) Correction to “Localized gravity/topography admittance and correlation spectra on Mars: implications for regional and global evolution” by Patrick J. McGovern, Sean C. Solomon, David E. Smith, Maria T. Zuber, Mark Simons, Mark A. Wieczorek, Roger J. Phillips, Gregory A. Neumann, Oded Aharonson, and James W. Head. *J Geophys Res* 107(E12):5136. <https://doi.org/10.1029/2002JE001854>
- McGovern PJ, Rumpf ME, Zimbelman JR (2013) The influence of lithospheric flexure on magma ascent at large volcanoes on Venus. *J Geophys Res, Planets* 118(11):2423–2437. <https://doi.org/10.1002/2013JE004455>
- McGovern PJ, Galgana GA, Verner KR, Herrick RR (2014) New constraints on volcanotectonic evolution of large edifices on Venus from stereo topography-derived strain estimates. *Geology* 42:59–62. <https://doi.org/10.1130/G34919.1>
- McKenzie DP, Ford PG, Johnson CL, Parsons B, Sandwell DT, Saunders RS, Solomon SC (1992) Features on Venus generated by plate boundary processes. *J Geophys Res, Planets* 97(E8):13533–13544. <https://doi.org/10.1029/92JE01350>
- McKinnon WB, Zahnle KJ, Ivanov BA, Melosh HJ (1997) Cratering on Venus: models and observations. In: Bougher SW, Hunten DM, Phillips RJ (eds) *Venus II*. University of Arizona Press, Tucson, pp 969–1014
- McNutt MK (1984) Lithospheric flexure and thermal anomalies. *J Geophys Res, Solid Earth* 89(B13):11180–11194. <https://doi.org/10.1029/JB089iB13p11180>
- Mitchell RN, Zhang N, Salminen J, Liu Y, Spencer CJ, Steinberger B, Murphy JB, Li Z-X (2021) The super-continent cycle. *Nature Rev Earth Environ* 2:358–374. <https://doi.org/10.1038/s43017-021-00160-0>
- Molnar N, Cruden A, Betts P (2020) The role of inherited crustal and lithospheric architecture during the evolution of the Red Sea: insights from three dimensional analogue experiments. *Earth Planet Sci Lett* 544:116377. <https://doi.org/10.1016/j.epsl.2020.116377>
- Moore WB, Schubert G (1997) Venusian crustal and lithospheric properties from nonlinear regressions of highland geoid and topography. *Icarus* 128:415–428. <https://doi.org/10.1006/icar.1997.5750>
- Moreels P, Smrekar SE (2003) Identification of polygonal patterns on Venus using mathematical morphology. *IEEE, Trans Image Proc* 1. <https://doi.org/10.1109/TIP.2003.814254>
- Morgan WJ (1972) Deep mantle convection plumes and plate Motions1. *AAPG Bull* 56(2):203–213. <https://doi.org/10.1306/819A3E50-16C5-11D7-8645000102C1865D>

- Morgan P (1983) Hot spot heat loss and tectonic style on Venus and in the Earth's Archean. *Lunar and Planetary Science XIV*, 515–516
- Morgan P, Phillips RJ (1983) Hot spot heat transfer: its application to Venus and implications to Venus and Earth. *J Geophys Res, Solid Earth* 88(B10):8305–8317. <https://doi.org/10.1029/JB088iB10p08305>
- Moyen JF, Martin H (2012) Forty years of TTG research. *Lithos* 148:312–336. <https://doi.org/10.1016/j.lithos.2012.06.010>
- Mueller N, Helbert J, Hashimoto GL, Tsang CCC, Erard S, Piccioni G, Drossart P (2008) Venus surface thermal emission at 1 μm in VIRTIS imaging observations: evidence for variation of crust and mantle differentiation conditions. *J Geophys Res, Planets* 113(E5):E00B17. <https://doi.org/10.1029/2008JE003118>
- Namiki N, Solomon SC (1993) The gabbro-eclogite phase transition and the elevation of mountain belts on Venus. *J Geophys Res, Planets* 98:15025–15031. <https://doi.org/10.1029/93JE01626>
- Nance RD, Murphy JB, Santosh M (2014) The supercontinent cycle: a retrospective essay. *Gondwana Res* 25(1):4–29. <https://doi.org/10.1016/j.gr.2012.12.026>
- Nikolayeva OV (1990) Geochemistry of the Venera 8 material demonstrates the presence of continental crust on Venus. *Earth Moon Planets* 50:329–341. <https://doi.org/10.1007/BF00142398>
- Nimmo F (2002) Why does Venus lack a magnetic field? *Geology* 30(987). [https://doi.org/10.1130/0091-7613\(2002\)030<0987:WDVLAM>2.0.CO;2](https://doi.org/10.1130/0091-7613(2002)030<0987:WDVLAM>2.0.CO;2)
- Nimmo F, Mackwell S (2023) Viscous relaxation as a probe of heat flux and crustal Plateau composition on Venus. *Proc Natl Acad Sci* 120(3):e2216311120. <https://doi.org/10.1073/pnas.2216311120>
- Nimmo F, McKenzie D (1998) Volcanism and tectonics on Venus. *Annu Rev Earth Planet Sci* 26:23–51. <https://doi.org/10.1146/annurev.earth.26.1.23>
- Nunes DC, Phillips RJ, Brown CD, Dombard AJ (2004) Relaxation of compensated topography and the evolution of crustal plateaus on Venus. *J Geophys Res, Planets* 109(E1):E01006. <https://doi.org/10.1029/2003JE002119>
- O'Neil J, Carlson RW (2017) Building Archean cratons from Hadean mafic crust. *Science* 355:1199–1202. <https://doi.org/10.1126/science.aah3823>
- O'Neil J, Carlson RW, Paquette JL, Francis D (2012) Formation age and metamorphic history of the Nuvvuagittuq Greenstone Belt. *Precambrian Res* 220:23–44. <https://doi.org/10.1016/j.precamres.2012.07.009>
- O'Neill C, Lenardic A, Weller M, Moresi L, Quenette S, Zhang S (2016) A window for plate tectonics in terrestrial planet evolution? *Phys Earth Planet Inter* 255:80–92. <https://doi.org/10.1016/j.pepi.2016.04.002>
- O'Rourke JG, Korenaga J (2015) Thermal evolution of Venus with argon degassing. *Icarus* 260:128–140. <https://doi.org/10.1016/j.icarus.2015.07.009>
- O'Rourke JG, Smrekar SE (2018) Signatures of lithospheric flexure and elevated heat flow in stereo topography at coronae on Venus. *J Geophys Res, Planets* 123(2):369–389. <https://doi.org/10.1002/2017JE005358>
- O'Rourke JG, Buz J, Fu RR, Lillis RJ (2019) Detectability of remanent magnetism in the Crust of Venus. *Geophys Res Lett* 46(11):5768–5777. <https://doi.org/10.1029/2019GL082725>
- O'Rourke JG, Wilson CF, Borrelli ME, Byrne PK, Dumoulin C, Ghail R, Gülcher AJP, Jacobson SA, Korabely O, Spohn T, Way MJ, Weller M, Westall F (2023) Venus, the planet: introduction to the evolution of Earth's sister planet. *Space Sci Rev* 219:10. <https://doi.org/10.1007/s11214-023-00956-0>
- Orth CP, Solomatov VS (2011) The isostatic stagnant lid approximation and global variations in the Venusian lithospheric thickness. *Geochem Geophys Geosyst* 12:Q07018. <https://doi.org/10.1029/2011GC003582>
- Oshigami S, Namiki N (2007) Cross-sectional profiles of Baltis Vallis channel on Venus: reconstructions from Magellan SAR brightness data. *Icarus* 190(1,Pages):1–14. <https://doi.org/10.1016/j.icarus.2007.03.011>
- Oshigami S, Namiki N, Komatsu G (2009) Depth profiles of venusian sinuous rilles and valley networks. *Icarus* 199(2):250–263. <https://doi.org/10.1016/j.icarus.2008.10.012>
- Pang K-N, Arnd N, Svensen H, Polozov A, Polteau S, Iizuka Y, Chung S-L (2013) A petrologic, geochemical and Sr-Nd isotopic study on contact metamorphism and degassing of Devonian evaporates in the Norilsk aureoles. *Siberia Contrib Mineral Petrol* 165(4):683–704
- Parfitt EA, Head JW (1993) Buffered and unbuffered dike emplacement on Earth and Venus: implications for magma reservoir size, depth, and rate of magma replenishment. *Earth Moon Planets* 61(3):249–281. <https://doi.org/10.1007/BF00572247>
- Parmentier EM, Hess PC (1992) Chemical differentiation of a convecting planetary interior: consequences for a one plate planet such as Venus. *Geophys Res Lett* 19(20):2015–2018. <https://doi.org/10.1029/92GL01862>
- Pauer M, Fleming K, Čadek O (2006) Modeling the dynamic component of the geoid and topography of Venus. *J Geophys Res, Planets* 111(E11). <https://doi.org/10.1029/2005JE002511>
- Pavri B, Head III JW, Klose KB, Wilson L (1992) Steep-sided domes on Venus: characteristics, geologic setting, and eruption conditions from Magellan data. *J Geophys Res, Planets* 97(E8):13445–13478. <https://doi.org/10.1029/92JE01162>

- Peltonen P, Kontinen A (2004) The Jormua Ophiolite: a mafic-ultramafic complex from an ancient ocean-continent transition zone. *Dev Precambrian Geol* 13:35–71. [https://doi.org/10.1016/S0166-2635\(04\)13001-6](https://doi.org/10.1016/S0166-2635(04)13001-6)
- Pesonen LJS-A, Elming SÅ, Meranen S, Pisarevsky S, D'Agrella-Filho MS, Meert JG, Schmidt PW, Abrahamson N, Bylund G (2003) Palaeomagnetic configuration of supercontinents during the Proterozoic. *Tectonophysics* 375:289–324. [https://doi.org/10.1016/S0040-1951\(03\)00343-3](https://doi.org/10.1016/S0040-1951(03)00343-3)
- Phillips RJ, Hansen VL (1998) Geological evolution of Venus: rises, plains, plumes, and plateaus. *Science* 279(5356):1492–1497. <https://doi.org/10.1126/science.279.5356.1492>
- Phillips RJ, Malin MC (1983) The interior of Venus and tectonic implications. In: Hunten DM, Colin L, Donahue TM, Moroz VI (eds) *Venus*. Univ. Arizona Press, Tucson, pp 159–214.
- Phillips RJ, Raubertas RF, Arvidson RE, Sarkar IC, Herrick RR, Izenberg N, Grimm RE (1992) Impact craters and Venus resurfacing history. *J Geophys Res, Planets* 97(E10):15293–15948. <https://doi.org/10.1029/92JE01696>
- Piskorz D, Elkins-Tanton LT, Smrekar SE (2014) Coronae formation on Venus via extension and lithospheric instability. *J Geophys Res, Planets* 119(12):2568–2582
- Raitala J, Kauhanen K, Black M, Tokkonen T (1995) Crustal bending at Salme Dorsa on Venus. *Planet Space Sci* 43(8):1001–1012. [https://doi.org/10.1016/0032-0633\(95\)00004-0](https://doi.org/10.1016/0032-0633(95)00004-0)
- Reese CC, Solomatov VS, Moresi LN (1998) Heat transport efficiency for stagnant lid convection with dislocation viscosity: application to Mars and Venus. *J Geophys Res* 103(E6):13643–13657. <https://doi.org/10.1029/98je01047>
- Reese CC, Solomatov VS, Orth CP (2007) Mechanisms for cessation of magmatic resurfacing on Venus. *J Geophys Res* 112:E04S04. <https://doi.org/10.1029/2006JE002782>
- Reimink JR, Davies JHFL, Bauer AM, Chacko T (2020) A comparison between zircons from the Acasta gneiss complex and the Jack Hills region. *Earth Planet Sci Lett* 561:115975. <https://doi.org/10.1016/j.epsl.2019.115975>
- Resor PG, Gilmore MS, Straley B, Senske DA, Herrick RR (2021) Felsic tesserae on Venus permitted by lithospheric deformation models. *J Geophys Res, Planets* 126(4):e2020JE006642. <https://doi.org/10.1029/2020JE006642>
- Robinson CA, Wood JA (1993) Recent volcanic activity on Venus: evidence from radiothermal emissivity measurements. *Icarus* 102(1):26–39. <https://doi.org/10.1006/icar.1993.1030>
- Rolf T, Steinberger B, Sruthi U, Werner SC (2018) Inferences on the mantle viscosity structure and the post-overture evolutionary state of Venus. *Icarus* 313:107–123. <https://doi.org/10.1016/j.icarus.2018.05.014>
- Rolf T, Weller M, Gülcher A et al (2022) Dynamics and evolution of Venus' mantle through time. *Space Sci Rev* 218:70. <https://doi.org/10.1007/s11214-022-00937-9>
- Romeo I, Capote R (2011) Tectonic evolution of Ovda Regio: an example of highly deformed continental crust on Venus? *Planet Space Sci* 59(13):1428–1445. <https://doi.org/10.1016/j.pss.2011.05.013>
- Romeo I, Turcotte DL (2008) Pulsating continents on Venus: an explanation for crustal plateaus and tessera terrains. *Earth Planet Sci Lett* 276(1–2):85–97. <https://doi.org/10.1016/j.epsl.2008.09.00>
- Rosenblatt P, Pinet PC, Thouvenot E (1994) Comparative hypsometric analysis of Earth and Venus. *Geophys Res Lett* 21(6):465–468. <https://doi.org/10.1029/94GL00419>
- Rossi F, Saboia M, Krishnamoorthy S, Vander Hook J (2023) Proximal exploration of Venus volcanism with teams of autonomous buoyancy-controlled balloons. *Acta Astronaut* 208:389–406. <https://doi.org/10.1016/j.actaastro.2023.03.003>
- Roth ASG, Bourdon B, Mojzsis SJ, Rudge JF, Guitreau M, Blichert-Toft J (2014) Combined ^{147}Sm – ^{143}Nd constraints on the longevity and residence time of early terrestrial crust. *Geochem Geophys Geosyst* 15(6):2329–2345. <https://doi.org/10.1002/2014GC005313>
- Rubie DC, Jacobson SA, Morbidelli A, O'Brien DP, Young ED, de Vries J, Nimmo F, Palme H, Frost DJ (2015) Accretion and differentiation of the terrestrial planets with implications for the compositions of early-formed Solar System bodies and accretion of water. *Icarus* 248:89–108. <https://doi.org/10.1016/j.icarus.2014.10.015>
- Ruiz J (2007) The heat flow during the formation of ribbon terrains on Venus. *Planet Space Sci* 55(14):2063–2070. <https://doi.org/10.1016/j.pss.2007.05.003>
- Russell MB, Johnson CL (2021) Evidence for a locally thinned lithosphere associated with recent Volcanism at Aramaiti Corona, Venus. *J Geophys Res, Planets* 126(8):e2020JE006783. <https://doi.org/10.1029/2020JE006783>
- Sabbeth L, Smrekar SE, Stock JM (2023) Estimated seismicity of Venusian wrinkle ridges based on fault scaling relationships. *Earth Planet Sci Lett* 619:118308. <https://doi.org/10.1016/j.epsl.2023.118308>
- Sabbeth L, Carrington MA, Smrekar SE (2024) Constraints on corona formation from an analysis of topographic rims and fracture annuli. *Earth Planet Sci Lett* 633:118568. <https://doi.org/10.1016/j.epsl.2024.118568>

- Sandwell DT, Schubert G (1992b) Flexural ridges, trenches, and outer rises around coronae on Venus. *J Geophys Res, Planets* 97(E10):16069–16083. <https://doi.org/10.1029/92JE01274>
- Sandwell DT, Schubert G (1992a) Evidence for retrograde lithospheric subduction on Venus. *Science* 257(5071):766–770. <https://doi.org/10.1126/science.257.5071.766>
- Sandwell DT, Johnson CL, Bilotti F, Suppe J (1997) Driving Forces for Limited Tectonics on Venus. *Icarus* 129(1):232–244. <https://doi.org/10.1006/icar.1997.5721>
- Sarma DS, Parachuramulu V, Santosh M, Nagaraju E, Babu NR (2020) Pb-Pb baddeleyite ages of mafic dyke swarms from the Dharwar craton: implications for Paleoproterozoic LIPs and diamond potential of mantle keel. *Geosci Front* 11:2127–2139
- Schaber GG, Strom RG, Moore HJ, Soderblom LA, Kirk RL, Chadwick DJ, Dawson DD, Gaddis LR, Boyce JM, Russell J (1992) Geology and distribution of impact craters on Venus: what are they telling us?. *J Geophys Res, Planets* 97(E8):13257–13301. <https://doi.org/10.1029/92JE01246>
- Schools J, Smrekar SE (2024) Formation of coronae topography and fractures via plume buoyancy and melting. *Earth Planet Sci Lett* 633:118643. <https://doi.org/10.1016/j.epsl.2024.118643>.
- Schubert G, Sandwell DT (1995) A global survey of possible subduction sites on Venus. *Icarus* 117(1):173–196. <https://doi.org/10.1006/icar.1995.1150>
- Scott DJ, Helmstaedt H, Bickle MJ (1992) Purtuniqu ophiolite, Cape Smith belt, northern Quebec, Canada: a reconstructed section of Early Proterozoic oceanic crust. *Geology* 20(2):173–176. [https://doi.org/10.1130/0091-7613\(1992\)020<0173:POCSBN>2.3.CO;2](https://doi.org/10.1130/0091-7613(1992)020<0173:POCSBN>2.3.CO;2)
- Scott CR, Mueller WU, Pilote P (2002) Physical volcanology, stratigraphy, and lithochemistry of an Archean volcanic arc: evolution from plume-related volcanism to arc rifting of SE Abitibi greenstone belt, Val d'Or, Canada. *Precamb Res* 115:223–260. [https://doi.org/10.1016/S0301-9268\(02\)00011-6](https://doi.org/10.1016/S0301-9268(02)00011-6)
- Senske DA, Schaber GG, Stofan ER (1992) Regional topographic rises on Venus: geology of Western Eistla Regio and comparison to Beta Regio and Atla Regio. *J Geophys Res, Planets* 97(E8):13395–13420. <https://doi.org/10.1029/92JE01167>
- Shalygin EV, Markiewicz WJ, Basilevsky AT, Titov DV, Ignatiev NI, Head JW (2015) Active volcanism on Venus in the Ganiki Chasma rift zone. *Geophys Res Lett* 42(12):4762–4769. <https://doi.org/10.1002/2015GL064088>
- Shaw GH (2008) Earth's atmosphere – Hadean to early Proterozoic. *Chem Erde* 68(3):235–264. <https://doi.org/10.1016/j.chemer.2008.05.001>
- Shellnutt JG (2013) Petrological modeling of basaltic rocks from Venus: a case for the presence of silicic rocks. *J Geophys Res, Planets* 118(6):1350–1364. <https://doi.org/10.1002/jgre.20094>
- Shellnutt JG (2016) Mantle potential temperature estimates of basalt from the surface of Venus. *Icarus* 277:98–102. <https://doi.org/10.1016/j.icarus.2016.05.014>
- Shellnutt JG (2018) Derivation of intermediate to silicic magma from the basalt analyzed at the Vega 2 landing site. *Venus Public Library of Science PLOS ONE* 13(3):e0194155. <https://doi.org/10.1371/journal.pone.0194155>
- Shellnutt JG (2019) The curious case of the rock at Venera 8. *Icarus* 321:50–61. <https://doi.org/10.1016/j.icarus.2018.11.001>
- Shellnutt JG (2021) Construction of a Venusian greenstone belt: a petrological perspective. *Geosci Can* 48(3):97–116. <https://doi.org/10.12789/geocanj.2021.48.176>
- Shellnutt JG, Dostal J (2019) Haida Gwaii (British Columbia, Canada): a Phanerozoic analogue of a subduction-unrelated Archean greenstone belt. *Sci Rep* 9:3251. <https://doi.org/10.1038/s41598-019-39818-7>
- Shellnutt JG, Manu Prasanth MP (2021) Modeling results for the composition and typology of non-primary Venusian anorthositic. *Icarus* 366:114531. <https://doi.org/10.1016/j.icarus.2021.114531>
- Sifré D, Gardés E, Massuyeau M, Hashim L, Hier-Majumder S, Gaillard F (2014) Electrical conductivity during incipient melting in the oceanic low-velocity zone. *Nature* 509:81–85. <https://doi.org/10.1038/nature13245>
- Simons M, Solomon SC, Hager BH (1997) Localization of gravity and topography: constraints on the tectonics and mantle dynamics of Venus. *Geophys J Int* 131(1):24–44. <https://doi.org/10.1111/j.1365-246X.1997.tb00593.x>
- Smithies RH (2000) The Archean tonalite-trondhjemite-granodiorite (TTG) series is not an analogue of Cenozoic adakite. *Earth Planet Sci Lett* 182(1):115–125. [https://doi.org/10.1016/S0012-821X\(00\)00236-3](https://doi.org/10.1016/S0012-821X(00)00236-3)
- Smithies RH, Champion DC, Van Kranendonk MJ, Howard HM, Hickman AH (2005b) Modern-style subduction processes in the Mesoarchaean: geochemical evidence from the 3.12 Ga Whundo intra-oceanic arc. *Earth Planet Sci Lett* 231:221–237. <https://doi.org/10.1016/j.epsl.2004.12.026>
- Smithies RH, Van Kranendonk MJ, Champion DC (2005a) It started with a plume – early Archean basaltic proto-continental crust. *Earth Planet Sci Lett* 238:284–297. <https://doi.org/10.1016/j.epsl.2005.07.023>

- Smrekar SE (1994) Evidence for active hotspots on Venus from analysis of Magellan Gravity Data. *Icarus* 112:2–26. <https://doi.org/10.1006/icar.1994.1166>
- Smrekar SE, Parmentier EM (1996) The interaction of mantle plumes with surface thermal and chemical boundary layers: applications to hotspots on Venus. *J Geophys Res, Solid Earth* 101:5397–5410. <https://doi.org/10.1029/95jb02877>
- Smrekar SE, Phillips RJ (1988) Gravity-driven deformation of the crust on Venus. *Geophys Res Lett* 15(7):693–696. <https://doi.org/10.1029/GL0151007p00693>
- Smrekar SE, Phillips RJ (1991) Venusian highlands: geoid to topography ratios and their implications. *Earth Planet Sci Lett* 107(3–4):582–597. [https://doi.org/10.1016/0012-821X\(91\)90103-O](https://doi.org/10.1016/0012-821X(91)90103-O)
- Smrekar SE, Solomon SC (1992) Gravitational spreading of high terrain in Ishtar Terra, Venus. *J Geophys Res, Planets* 97(E10):16121–16148. <https://doi.org/10.1029/92JE01315>
- Smrekar SE, Sotin C (2012) Constraints on mantle plumes on Venus: implications for volatile history. *Icarus* 217(2):510–523. <https://doi.org/10.1016/j.icarus.2011.09.011>
- Smrekar SE, Stofan ER (1997) Corona formation and heat loss on Venus by coupled upwelling and delamination. *Science* 277(5330):1289–1294. <https://doi.org/10.1126/science.277.5330.1289>
- Smrekar SE, Kiefer WS, Stofan ER (1997) Large Volcanic Rises on Venus. In: Bougher SW, Hunten DM, Phillips RJ, Matthews MS, Ruskin AS, Guerrieri ML (eds) *Venus II. Geology, geophysics, atmosphere, and solar wind environment*. University of Arizona Press, Tucson, pp 845–878
- Smrekar SE, Moreels P, Franklin BJ (2002) Characterization and formation of polygonal fractures on Venus. *J Geophys Res, Planets* 107(E11):1–17. <https://doi.org/10.1029/2001JE001808>
- Smrekar SE, Stofan ER, Mueller NT, Treiman AH, Elkins-Tanton LT, Helbert J, Piccioni G, Drossart P (2010) Recent hotspot volcanism on Venus from VIRTIS emissivity data. *Science* 328(5978):605–608. <https://doi.org/10.1126/science.1186785>
- Smrekar SE, Davaille A, Sotin C (2018) Venus interior structure and dynamics. *Space Sci Rev* 214:88. <https://doi.org/10.1007/s11214-018-0518-1>
- Smrekar SE, Hensley S, Nybakken R, Wallace MS, Perkovic-Martin D, You T-H, Nunes D, Brophy J, Ely T, Burst E, Dyar MD, Helbert J, Miller B, Hartley J, Kallemeyn P, Whitte J, Iess L, Mastrogiuseppe M, Younis M, Prts P, Rodriguez M, Mazarico R (2022a) VERITAS (Venus emissivity, radio science, InSAR, topography, and spectroscopy): a discovery mission. In: 2022 institute for electrical and electronics engineers/IEEE Aerospace Conference (AERO), pp 1–20. <https://doi.org/10.1109/AERO53065.2022.9843269>
- Smrekar SE, Ostberg C, O'Rourke JG (2022b) Evidence for active rifting and Earth-like lithospheric thickness and heat flow on Venus. *Nat Geosci*. <https://doi.org/10.1038/s41561-022-01068-0>
- Smrekar SE, Ostberg C, O'Rourke JG (2023) Earth-like lithospheric thickness and heat flow on Venus consistent with active rifting. *Nat Geosci* 16:13–18. <https://doi.org/10.1038/s41561-022-01068-0>
- Snyder D (2002) Cooling of lava flows on Venus: the coupling of radiative and convective heat transfer. *J Geophys Res, Planets* 107(E10):5080. <https://doi.org/10.1029/2001JE001501>
- Solomatov VS, Moresi L-N (1996) Stagnant lid convection on Venus. *J Geophys Res, Planets* 101:4737–4753. <https://doi.org/10.1029/95je03361>
- Solomon SC, Head JW (1982) Mechanisms for lithospheric heat transport on Venus: implications for tectonic style and volcanism. *J Geophys Res, Solid Earth* 87(B11):9236–9246. <https://doi.org/10.1029/JB087iB11p09236>
- Solomon SC, Head JW, Kaula WM, McKenzie D, Parsons B, Phillips RJ, Schubert G, Talwani M (1991) Venus tectonics: initial analysis from Magellan. *Science* 252(5003):297–312. <https://doi.org/10.1126/science.252.5003.297>
- Solomon SC, Smrekar SE, Bindschadler DL, Grimm RE, Kaula WM, McGill GE, Phillips RJ, Saunders RS, Schubert G, Squyres SW, Stofan ER (1992) Venus tectonics: an overview of Magellan observations. *J Geophys Res, Planets* 97(E8):13199–13255. <https://doi.org/10.1029/92JE01418>
- Solomon SC, Bullock MA, Grinspoon DH (1999) Climate change as a regulator of tectonics on Venus. *Science* 286(5437):87–90. <https://doi.org/10.1126/science.286.5437.87>
- Spencer CJ, Kirkland CL, Taylor RJM (2016) Strategies towards statistically robust interpretations of in situ U–Pb zircon geochronology. *Geosci Front* 7(4):581–589. <https://doi.org/10.1016/j.gsf.2015.11.006>
- Spencer CJ, Kirkland CL, Roberts NMW, Evans NJ, Liebmann J (2020) Strategies towards robust interpretations of in situ zircon Lu–Hf isotope analyses. *Geosci Front* 11(3):843–853. <https://doi.org/10.1016/j.gsf.2019.09.004>
- Squyres SW, Jankowski DG, Simons M, Solomon SC, Hager BH, McGill GE (1992) Plains tectonism on Venus: the deformation belts of Lavinia Planitia. *J Geophys Res* 97(E8):13579–13599. <https://doi.org/10.1029/92JE00481>
- Steinberger B, Werner SC, Torsvik TH (2010) Deep versus shallow origin of gravity anomalies, topography and volcanism on Earth, Venus and Mars. *Icarus* 207:564–577. <https://doi.org/10.1016/j.icarus.2009.12.025>

- Stern RJ (2008) Modern-style plate tectonics began in Neoproterozoic time: an alternative interpretation of Earth's tectonic history. In: Condie KC, Pease V (eds) When did plate tectonics begin on planet Earth? Spec Pap Geol Soc Am, vol 440, pp 265–280
- Stern RJ, Gerya T (2018) Subduction initiation in nature and models: a review. *Tectonophysics* 746:173–198. <https://doi.org/10.1016/j.tecto.2017.10.014>
- Stevenson DJ, Cutts J, Mimoun D, Arrowsmith S, Banerdt B, Blom P, Brageot E, Brissaud Q, Chin G, Gao P, Garcia R, Hall J, Hunter G, Jackson J Kerzhanovic V, Kiefer W, Komjathy A, Lee C, Lognonné P, Lorenz R, Majid W, Majorradi M, Nolet G, O'Rourke J, Rolland L, Schubert G, Simons M, Sotin C, Spilker T, Tsai V (2015) Probing the interior structure of Venus. Keck Institute of Space Studies, California Institute of Technology, Pasadena. <https://doi.org/10.26206/CICX-EV12>
- Stoddard PR, Jurdy DM (2012) Topographic comparisons of uplift features on Venus and Earth: implications for Venus tectonics. *Icarus* 217(2):524–533. <https://doi.org/10.1016/j.icarus.2011.09.003>
- Stofan ER, Saunders RS (1990) Geologic evidence of hotspot activity on Venus: predictions for Magellan. *Geophys Res Lett* 17(9):1377–1380. <https://doi.org/10.1029/GL017i009p01377>
- Stofan ER, Smrekar SE (2005) Large topographic rises, coronae, large flow fields, and large volcanoes on Venus: evidence for mantle plumes? In: Foulger GR, Natland JH, Presnall DC, Anderson DL (eds) Plates, plumes and paradigms. Geological Society of America
- Stofan ER, Bindschadler D, Parmentier EM, Head J (1991) Corona structures on Venus: models of origin. *J Geophys Res* 96:20933–20946. <https://doi.org/10.1029/91JE02218>
- Stofan ER, Sharpton VL, Schubert G, Baer G, Bindschadler DL, Janes DM, Squyres SW (1992) Global distribution and characteristics of coronae and related features on Venus: implications for origin and relation to mantle processes. *J Geophys Res, Planets* 97(E8):13347–13378. <https://doi.org/10.1029/92JE01314>
- Stofan ER, Saunders RS, Senske D et al (1993) Venus interior structure mission (VISM): establishing a seismic network on Venus. In: Workshop on Advanced Technologies for Planetary Instruments, Part 1, SEE N93-28764 11-91. Lunar and Planetary Institute, Houston, pp 23–24
- Stofan ER, Smrekar SE, Bindschadler DL, Senske DA (1995) Large topographic rises on Venus: implications for mantle upwelling. *J Geophys Res, Planets* 100(E11):23317–23327. <https://doi.org/10.1029/95JE01834>
- Stofan ER, Hamilton VE, Janes DM, Smrekar SE (1997) Coronae on Venus: morphology and origin, Venus II: geology, geophysics, atmosphere, and solar wind environment. In Bougher SW, Hunten DM, Phillips RJ (eds) University of Arizona Press, Tucson, p 931
- Stofan ER, Anderson SW, Crown DA, Plaut JJ (2000) Emplacement and composition of steep-sided domes on Venus. *J Geophys Res* 105(E11):26,757–26,771. <https://doi.org/10.1029/1999JE001206>
- Stofan ER, Smrekar SE, Tapper SW, Guest JE, Grindrod PM (2001) Preliminary analysis of an expanded corona database for Venus. *Geophys Res Lett* 28(22):4267–4270. <https://doi.org/10.1029/2001GL013307>
- Stofan ER, Smrekar SE, Mueller N, Helbert J (2016) Themis regio, Venus: evidence for recent (?) volcanism from VIRTIS data. *Icarus* 271:375–386. <https://doi.org/10.1016/j.icarus.2016.01.034>
- Strom RG, Schaber GG, Dawson DD (1994) The global resurfacing of Venus. *J Geophys Res, Planets* 99(E5):10899–10926. <https://doi.org/10.1029/94JE00388>
- Suppe J, Connors C (1992) Critical taper wedge mechanics of fold-and-thrust belts on Venus: initial results from Magellan. *J Geophys Res, Planets* 97(E8):13545–13561. <https://doi.org/10.1029/92JE01164>
- Surkov YA, Barsukov VL, Moskalyeva LP, Kharyukova VP, Kemurdzhian AL (1984) New data on the composition, structure, and properties of Venus rock obtained by Venera 13 and Venera 14. *J Geophys Res, Solid Earth* 89(S02):B393–B402. <https://doi.org/10.1029/JB089iS02p0B393>
- Surkov YA, Moskalyova LP, Kharyukova VP, Dudin AD, Smirnov GG, Zaitseva SY (1986) Venus rock composition at the Vega 2 Landing Site. *J Geophys Res, Solid Earth* 91(B13):E215–E218. <https://doi.org/10.1029/JB091iB13p0E215>
- Tackley PJ, Stevenson DJ (1991) The production of small Venusian coronae by Rayleigh-Taylor instabilities in the uppermost mantle. *Eos, Trans Am Geophys Union* 72:287–287
- Taylor SR, McLennan SM (1995) The geochemical evolution of the continental crust. *Rev Geophys* 33(2):241–265. <https://doi.org/10.1029/95RG00262>
- Taylor FW, Svedhem H, Head JW (2018) Venus: the atmosphere, climate, surface, interior and near-space environment of an Earth-like planet. *Space Sci Rev* 214. <https://doi.org/10.1007/s11214-018-0467-8>
- Therriault AM, Fowler AD, Grieve RA (2002) The Sudbury Igneous Complex: a differentiated impact melt sheet. *Econ Geol* 97(7):1521–1540. <https://doi.org/10.2113/gsecongeo.97.7.1521>
- Thordarson T, Garcia MO (2018) Variance of the Flexure Model Predictions with Rejuvenated Volcanism at Kilauea Point, Kaua'i, Hawai'i. *Front Earth Sci* 6. <https://doi.org/10.3389/feart.2018.00121>
- Thurston PC (2015) Greenstone belts and granite-greenstone terranes: constraints on the nature of the Archean world. *Geosci Can* 42(4):437–484. <https://doi.org/10.12789/geocanj.2015.42.081>

- Torsvik TH, van der Voo R, Doubrovine PV, Burke K, Steinberger B, Ashwal LD, Trønnes RG, Webb SJ, Bull AL (2014) Deep mantle structure as a reference frame for movements in and on the Earth. *Proc Natl Acad Sci* 111(24):8735–8740. <https://doi.org/10.1073/pnas.1318135111>
- Treiman AH (2007) Geochemistry of Venus' surface: current limitations as future opportunities. In: Esposito LW, Stofan ER, Cravens TE (eds) *Exploring Venus as a Terrestrial Planet*. Geophysical monograph series, vol 176. <https://doi.org/10.1029/176GM03>
- Treiman A, Harrington E, Sharpton V (2016) Venus' radar-bright highlands: different signatures and materials on Ovda Regio and on Maxwell Montes. *Icarus* 280:172–182. <https://doi.org/10.1016/j.icarus.2016.07.001>
- Tucker WS, Dombard AJ (2023) Evidence of Topographic Change Recorded by Lava Flows at Atete and Aruru Coronae on Venus. *Journ Geophys Res Planets* 128(11):e2023JE007971. <https://doi.org/10.1029/2023JE007971>
- Tuckwell GW, Ghail RC (2003) A 400-km-scale strike-slip zone near the boundary of Thetis Regio. *Venus Earth Planet Sci Lett* 211(1–2):45–55. [https://doi.org/10.1016/S0012-821X\(03\)00128-6](https://doi.org/10.1016/S0012-821X(03)00128-6)
- Turcotte DL (1993) An episodic hypothesis for Venusian tectonics. *J Geophys Res, Planets* 98(E9):17061–17068. <https://doi.org/10.1029/93JE01775>
- Turcotte DL, Morein G, Roberts D, Malamud BD (1999) Catastrophic resurfacing and episodic subduction on Venus. *Icarus* 139(1):49–54. <https://doi.org/10.1006/icar.1999.6084>
- Turner S, Rushmer T, Reagan M, Moyer J-F (2014) Heading down early on? Start of subduction on Earth. *Geology* 42(2):139–142. <https://doi.org/10.1130/G34886.1>
- Ueda K, Gerya T, Sobolev SV (2008) Subduction initiation by thermal-chemical plumes: numerical studies. *Phys Earth Planet Inter* 171(1–4):296–312. <https://doi.org/10.1016/j.pepi.2008.06.032>
- Van Kranendonk MJ (2010) Two types of Archean continental crust: plume and plate tectonics on early Earth. *Am J Sci* 310(10):1187–1209
- Wang YJ, Shellnutt JG, Kung J, Iizuka Y, Lai Y-M (2022) The formation of tonalitic and granodioritic melt from Venusian basalt. *Sci Rep* 12:1652. <https://doi.org/10.1038/s41598-022-05745-3>
- Warren AO, Kite ES (2023) Narrow range of early habitable Venus scenarios permitted by modeling of oxygen loss and radiogenic argon degassing. *Proc Natl Acad Sci* 120(11):e2209751120. <https://doi.org/10.1073/pnas.2209751120>
- Way MJ, Del Genio AD (2020) Venusian habitable climate scenarios: modeling Venus through time and applications to slowly rotating Venus-like exoplanets. *J Geophys Res, Planets* 125(5):e2019JE006276. <https://doi.org/10.1029/2019JE006276>
- Way MJ, Del Genio AD, Kiang NY, Sohl LE, Grinspoon DH, Aleinov I, Kelley M, Clune T (2016) Was Venus the first habitable world of our solar system? *Geophys Res Lett* 43(16):8376–8383. <https://doi.org/10.1002/2016GL069790>
- Wei DY, Yang A, Huang JS (2014) The gravity field and crustal thickness of Venus. *Sci China Earth Sci* 57(9):2025–2035. <https://doi.org/10.1007/s11430-014-4824-5>
- Wei SS, Shearer PM, Lithgow-Bertelloni C, Stixrude L, Tian D (2020) Oceanic Plateau of the Hawaiian mantle plume head subducted to the uppermost lower mantle. *Science* 370(6519):983–987. <https://doi.org/10.1126/science.abd0312>
- Weller MB, Duncan MS (2015) Insight into terrestrial planetary evolution via mantle potential temperatures. 46th Lunar Planetary Science Conference. Abstract #2749
- Weller MB, Lenardic A, O'Neill C (2015) The effects of internal heating and large-scale climate variations on tectonic bi-stability in terrestrial planets. *Earth Planet Sci Lett* 420:85–94. <https://doi.org/10.1016/j.epsl.2015.03.021>
- Westall F, Höning D, Avicé G, Gentry D, Gerya T, Gillmann C, Izenberg N, Way MJ, Wilson C (2023) The habitability of Venus. *Space Sci Rev* 219:17. <https://doi.org/10.1007/s11214-023-00960-4>
- Whattam SA, Stern RJ (2015) Late Cretaceous plume-induced subduction initiation along the southern margin of the Caribbean and NW South America: The first documented example with implications for the onset of plate tectonics. *Gondwana Research* 27(1):38–63. <https://doi.org/10.1016/j.gr.2014.07.011>
- White RS, McKenzie D (1995) Mantle plumes and flood basalts. *J Geophys Res, Solid Earth* 100(B9):17543–17585. <https://doi.org/10.1029/95JB01585>
- Whitten JL, Campbell BA (2016) Recent volcanic resurfacing of Venusian craters. *Geology* 44(7):519–522. <https://doi.org/10.1130/G37681.1>
- Widemann T, Smrekar S, Garvin J, Straume-Lindner AG, Ocampo A, Schulte M, Voirin T, Hensley S, Dyar MD, Whitten J, Nunes D, Getty S, Arney G, Johnson N, Kohler E, Spohn T, O'Rourke JG, Wilson C, Way M, Ostberg C, Westall F, Höning D, Jacobson S, Salvador A, Avicé G, Breuer D, Carter L, Gilmore M, Ghail R, Helbert J, Byrne P, Santos A, Herrick R, Izenberg N, Marcq E, Rolf T, Weller M, Gillmann C, Korabely O, Zelenyi L, Zasova L, Gorinov D, Seth G, Narasimha Rao CV, Desai N (2023) Venus evolution through time: key science questions, selected mission concepts and future investigations. *Space Sci Rev* 219:56. <https://doi.org/10.1007/s11214-023-00992-w>

- Wiens RC, Maurice S, Barraclough B et al (2012) The ChemCam instrument suite on the Mars Science Laboratory (MSL) rover: body unit and combined system tests. *Space Sci Rev* 170:167–227. <https://doi.org/10.1007/s11214-012-9902-4>
- Williams DA, Kerr RC, Leshner CM, Barnes SJ (2001) Analytical/numerical modeling of komatiite lava emplacement and thermal erosion at Perseverance, Western Australia. *J Volcanol Geotherm Res* 110(1–2):27–55. [https://doi.org/10.1016/S0377-0273\(01\)00206-2](https://doi.org/10.1016/S0377-0273(01)00206-2)
- Williams-Jones G, Williams-Jones AE, Stix J (1998) The nature and origin of Venusian canali. *J Geophys Res, Planets* 103(E4):8545–8555. <https://doi.org/10.1029/98JE00243>
- Wilson CF, Chassefière E, Hinglais E et al (2012) The 2010 European Venus Explorer (EVE) mission proposal. *Exp Astron* 33:305–335. <https://doi.org/10.1007/s10686-011-9259-9>
- Wilson CF, Marcq E, Gillmann C, Widemann T, Korablev O, Mueller N, Lefevre M, Rimmer P, Robert S, Zolotov M (2024) Magmatic volatiles and effects on the modern atmosphere of Venus. *Space Sci Rev* this collection, in revision
- Windely BF, Kusky T, Polat A (2021) Onset of plate tectonics by the Eoarchean. *Precambrian Res* 352:105980. <https://doi.org/10.1016/j.precamres.2020.105980>
- Windley BF, Kusky T, Polat A (2021) Onset of plate tectonics by the Eoarchean. *Precambrian Res* 352:105980. <https://doi.org/10.1016/j.precamres.2020.105980>
- Wroblewski FB, Treiman AH, Bhiravarasu S, Gregg TKP (2019) Ovda Fluctus, the festoon lava flow on Ovda Region, Venus: not silica-rich. *J Geophys Res, Planets* 124:2233–2245. <https://doi.org/10.1029/2019JE006039>
- Wyman DA, Kerrich R, Polat A (2002) Assembly of Archean cratonic mantle lithosphere and crust: plume-arc interaction in the Abitibi-Wawa subduction-accretion complex. *Precambrian Res* 115:37–62. [https://doi.org/10.1016/S0301-9268\(02\)00005-0](https://doi.org/10.1016/S0301-9268(02)00005-0)
- Zahnle KJ (1992) Airburst origin of dark shadows on Venus. *J Geophys Res, Planets* 97(E6):10243–10255. <https://doi.org/10.1029/92JE00787>
- Zegers TE, van Keken PE (2001) Middle Archean continent formation by crustal delamination. *Geology* 29(12):1083–1086. [https://doi.org/10.1130/0091-7613\(2001\)029<1083:MACFBC>2.0.CO;2](https://doi.org/10.1130/0091-7613(2001)029<1083:MACFBC>2.0.CO;2)
- Zuber MT (1990) Ridge belts: evidence for regional- and local-scale deformation on the surface of Venus. *Geophys Res Lett* 17(9):1369–1372. <https://doi.org/10.1029/GL017i009p01369>

Publisher's Note Springer Nature remains neutral with regard to jurisdictional claims in published maps and institutional affiliations.

Authors and Affiliations

Richard C. Ghail¹  · Suzanne E. Smrekar²  · Thomas Widemann^{3,4}  · Paul K. Byrne⁵  · Anna J.P. Gülcher²  · Joseph G. O'Rourke⁶  · Madison E. Borrelli⁶  · Martha S. Gilmore⁷  · Robert R. Herrick⁸  · Mikhail A. Ivanov⁹  · Ana-Catalina Plesa¹⁰  · Tobias Rolf¹¹  · Leah Sabbeth²  · Joe W. Schools¹²  · J. Gregory Shellnutt¹³ 

✉ R.C. Ghail
richard.ghail@rhul.ac.uk

S.E. Smrekar
suzanne.e.smrekar@jpl.nasa.gov

T. Widemann
thomas.widemann@obspm.fr

P.K. Byrne
paul.byrne@wustl.edu

A.J.P. Gülcher
anna.gulcher@caltech.edu

J.G. O'Rourke
jgorourke@asu.edu

M.E. Borrelli
meborrel@asu.edu

M.S. Gilmore
mgilmore@wesleyan.edu

R.R. Herrick
rrherrick@alaska.edu

M.A. Ivanov
mikhail_ivanov@brown.edu

A.-C. Plesa
ana.plesa@dlr.de

T. Rolf
tobias.rolf@geo.uio.no

L. Sabbeth
leah.sabbeth@jpl.nasa.gov

J.W. Schools
jschools@arizona.edu

J. Gregory Shellnutt
jgshelln@ntnu.edu.tw

- ¹ Department of Earth Sciences, Royal Holloway, University of London, Egham, Surrey, TW20 0EX, UK
- ² Jet Propulsion Laboratory, California Institute of Technology, 4800 Oak Grove Drive, Pasadena, CA 91109, USA
- ³ LESIA, Observatoire de Paris, Université PSL, CNRS, Sorbonne Université, Université Paris Cité, 5 place Jules Janssen, 92195 Meudon, France
- ⁴ Université Paris-Saclay, UVSQ, DYPAC, 78000 Versailles, France
- ⁵ Department of Earth, Environmental, and Planetary Sciences, Washington University, St. Louis, MO 63130, USA
- ⁶ Arizona State University, School of Earth and Space Exploration, Tempe, AZ 85287, USA
- ⁷ Department of Earth and Environmental Sciences, Wesleyan University, 265 Church Street, Middletown, CT 06457, USA
- ⁸ Institute of Northern Engineering, University of Alaska Fairbanks, Fairbanks, AK 99775-5910, USA
- ⁹ Vernadsky Institute of Geochemistry and Analytical Chemistry, RAS, 119991, Moscow, Russia
- ¹⁰ Institute of Planetary Research, Deutsches Zentrum für Luft- und Raumfahrt, Rutherfordstraße 2, 12489 Berlin, Germany
- ¹¹ Centre for Earth Evolution and Dynamics, Dept. of Geosciences, University of Oslo, PO Box 1028 Blindern, 0315 Oslo, Norway
- ¹² Lunar and Planetary Laboratory, The University of Arizona, PO Box 210092, Tucson, AZ 85721, USA
- ¹³ Department of Earth Sciences, National Taiwan Normal University, 88 Tingzhou Road Sect. 4, Taipei 11677, Taiwan